Supplementary Information

for

Synthesis and anion binding properties of (thio)urea functionalized Ni(II)-salen complexes

Jae Elise L. Payong [a], Nadia G. Léonard[b], Lauren M. Anderson-Sanchez[a], Joseph W. Ziller[a] and Jenny Y. Yang[a†]

[a] *Department of Chemistry, University of California, Irvine, Irvine, California 92697, USA*

[b] *Department of Chemistry and Biochemistry, University of California, Santa Barbara, Santa Barbara, California 93106, United States.*

† Corresponding Author.

Table of Contents

Experimental Methods

Synthetic reactions were performed in air unless stated otherwise. Commercially sourced chemicals were used as received unless stated otherwise. Deuterated solvents were purchased from Cambridge Isotope Laboratories. Tetrabutylammonium salts for titration experiments were stored in a desiccator. Air- and moisture-sensitive manipulations were performed using Schlenk line techniques under N_2 atmosphere. Glassware and stir bars used in air- and moisture-sensitive manipulations were dried in a Quincy Lab Inc. Model 40GC Lab Oven for at least 1 hour at 350 °F (177 °C). Dry and degassed solvents were obtained from an Ar-pressurized solvent purification system (JC Meyer Solvent Systems) equipped with an alumina drying column and stored over activated 3 Å molecular sieves (3 - 4 mm (0.04 - 0.08 in), ThermoFisher) inside a Vacuum Atmospheres Company (VAC) N_2 atmosphere glovebox. High-Resolution Mass Spectrometry (HRMS) data were obtained in the UCI Mass Spectrometry Facility using a Waters LCT Premier equipped with a TOF detector on positive mode.

NMR measurements were taken using a 500 MHz Bruker DRX500 spectrometer with a BBO probe at 298.1 K (^{1}H = 498.557 MHz) or a 600 MHz Bruker Avance 600 spectrometer with a CBBFO probe at 298.0 K (^{1}H = 600.124 MHz; ^{13}C{^{1}H} = 150.919 MHz; ^{19}F = 564.505 MHz). All ^{1}H and ^{13}C{^{1}H} chemical shifts are reported in ppm relative to $SiMe_4$ using the chemical shift of the solvent as the standard (^{1}H: DMSO-*d*$_6$ = 2.50 ppm, chloroform-*d* ($CDCl_3$) = 7.26 ppm; ^{13}C{^{1}H}: DMSO-*d*$_6$ = 39.52 ppm, $CDCl_3$ = 77.16 ppm). ^{19}F chemical shifts were referenced to 1-fluorobenzene (δ = –112.83 ppm in DMSO-*d*$_6$ relative to neat $CFCl_3$) as the internal standard.[1] ^{1}H and ^{13}C{^{1}H} data are reported as follows: chemical shift, (multiplicity (s = singlet, d = doublet, t = triplet, m = multiplet, br = broad), coupling constant(s), integration, assignment).

Titration experiments were performed with the 600 MHz Bruker Avance 600 spectrometer by obtaining a ^{1}H NMR spectra of the host complex (5 mM in DMSO-*d*$_6$, 500 μL) with the desired equivalent amount of the tetrabutylammonium (TBA) salt (200 mM in DMSO-*d*$_6$) added using a Hamilton microsyringe. Up to 20 mole equivalents (250 μL total volume) of TBACl, $TBAH_2PO_4$, or $TBACH_3COO$ were titrated over 8 ^{1}H NMR spectra or 12 mole equivalents (150 μL total volume) of TBAF•$3H_2O$ over 15 ^{1}H NMR spectra were measured.

To calculate the binding constant of F^- in the slow exchange regime, **Eqn. 1** was used assuming that 1 – [**Ni(II)**] = [**Ni(II)•F**$^-$], that the integration of the C(Ar)–H signal at 8.13 ppm of **NiL$^{3,3'\text{-O}}$** is proportional to [**Ni(II)**] + [**Ni(II)•F**$^-$]. ^{1}H NMR spectra were obtained with the relaxation delay time (d1) set to 10 s. [F^-] was calculated from the integration of the terminal CH_3 signal of the tetrabutylammonium counterion.

$$K = \frac{[Ni(II) \cdot F^-]}{[Ni(II)][F^-]} = \frac{[Ni(II)]_0 \times \left(1 - \frac{\frac{I_{Na-H} + I_{Nb-H}}{2}}{I_{CH}}\right)}{\left([Ni(II)]_0 \times \left(\frac{\frac{I_{Na-H} + I_{Nb-H}}{2}}{I_{CH}}\right)\right) \times \left(\frac{I_{CH3}}{12} \times [Ni(II)]_0\right)}$$

(Equation 1)

Where $I_{Na–H}$ = integration of the N_a–H peak, $I_{Nb–H}$ = integration of the N_b–H peak, I_{CH} = integration of the CH peak at 8.13 ppm and I_{CH3} = integration of the CH_3 peak of tetrabutylammonium at 0.93 ppm.

Diffusion Ordered Spectroscopy (DOSY) experiments were performed using a 600 MHz Bruker Avance 600 spectrometer at 298.0 K, measuring 8 scans over 16 spectra using the following parameters: gradient strength, gpz6 = 2-95%; relaxation delay time, d1 = 5.000 s; diffusion time, d20 (Δ) = 0.1000 s; diffusion gradient length, p30 (δ) = 1000 μs.

X-ray diffraction studies were performed at the UCI Department of Chemistry X-ray Crystallography Facility using a Bruker SMART APEX II (Mo Kα, λ = 0.71073 Å) or a Bruker X8 Prospector APEX III (Cu Kα, λ = 1.54178 Å) x-ray diffractometer. ORTEP representations were generated through ORTEP-3.[2] Bond metrics were measured from the CIF file through Olex2.[3]

Synthetic Procedures

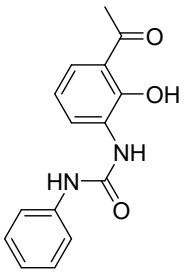

Synthesis of ***HL$^{3\text{-}O}$***. To a round bottom flask equipped with a stir bar, 1-(3-amino-2-hydroxyphenyl)ethanone (1.512 g, 10.0 mmol) was dissolved in dichloromethane (DCM) (20.0 mL) forming a brownish black solution. Phenyl isocyanate (1.09 mL, 10.0 mmol) was added dropwise *via* syringe, and the reaction was stirred vigorously. Precipitation of the product occurred gradually throughout the reaction. After 2 hours, the reaction was quenched with deionized water and the crude product was collected *via* vacuum filtration and triturated in DCM. The final product was collected once more *via* vacuum filtration as an off-white powder. Yield = 68% (1.836 g, 6.8 mmol). **^{1}H NMR (DMSO-*d*$_6$):** δ 12.87 (s, 1H, Ar–OH), 9.41 (s, 1H, Ar–NH), 8.39 (m, 2H, Ar–H and Ar–NH), 7.57 (d, *J* = 7.9 Hz, 1H, Ar–H), 7.46 (d, *J* = 7.7 Hz, 2H, Ar–H), 7.29 (t, *J* = 6.7 Hz, 2H, Ar–H), 6.96 (dd, *J* = 19.3, 8.2 Hz, 2H Ar–H), 2.67 (s, 3H, Ar–C(=O)). **^{13}C NMR (DMSO-*d*$_6$):** δ 206.0 (s, Ar–C=O), 152.4 (s, Ar–OH), 150.3 (s, HN–C(=O)–NH), 139.6 (s, Ar–NH), 128.8 (s, Ar–NH), 128.7 (s, Ar), 124.3 (s, Ar), 123.6 (s, Ar), 121.9 (s, Ar), 118.8 (s, Ar), 118.7 (s, Ar), 118.0 (s, Ar), 26.9 (s, ArC–CH_3). **HRMS (ESI-MS):** calculated $C_{15}H_{14}N_2O_3Na^+$ = 293.0902 *m/z*, found 293.0915 *m/z*.

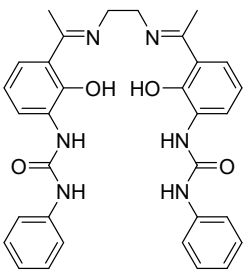

Synthesis of ***H$_2$L$^{3,3'\text{-}O}$***. To a round bottom flask equipped with a stir bar, addition funnel, and a reflux condenser, **HL$^{3\text{-}O}$** (0.511 g, 3.0 mmol) was heated

to reflux in methanol (MeOH) (60.0 mL), appearing as a murky brown solution. Ethylenediamine (0.10 mL, 1.5 mmol) was dissolved in MeOH (90.0 mL) in a beaker, then poured into the addition funnel. The ethylenediamine solution was added dropwise into the refluxing solution of **$HL^{3\text{-}O}$** for over 1 hour, at which point the solution turned dark orange. The flask was taken off heat after 2 hours and allowed to stand overnight at room temperature. The product was collected as a yellow orange powder *via* vacuum filtration and washed with MeOH. The mother liquor was concentrated under vacuum and stored in a –5 °C freezer overnight to collect the second crop of product. Yield = 89% (0.750 g, 1.3 mmol). **^{1}H NMR (DMSO-d_6):** δ 9.38 (s, 2H, Ar–NH), 8.42 (s, 2H, Ar–NH), 8.14 (d, J = 7.7 Hz, 2H, Ar–H), 7.41 (d, J = 7.7 Hz, 4H, Ar–H), 7.27 (d, J = 8.4 Hz, 2H, Ar–H), 7.23 (t, J = 7.3 Hz, 4H, Ar–H), 6.92 (t, J = 7.3 Hz, 2H, Ar–H), 6.58 (t, J = 8.0 Hz, 2H, Ar–H), 4.06 (s, 4H, $N(CH_3)_2N$), 2.53 (s, 6H, Ar–C(=N)CH_3). **^{13}C NMR (DMSO-d_6):** δ 175.3 (s, Ar–C(=N)), 158.9 (s, Ar–OH), 152.5 (s, HN–C(=O)–NH), 140.0 (s, Ar–NH), 130.7 (s, Ar–NH), 128.7 (s, Ar), 121.5 (s, Ar), 121.0 (s, Ar), 119.4 (s, Ar), 117.8 (s, Ar), 115.1 (s, Ar), 114.2 (s, Ar), 46.7 (s, $N(CH_3)_2N$), 14.8 (s, ArC–CH_3). **HRMS (ESI-MS):** calculated $C_{32}H_{32}N_6O_4H^+$ = 565.2563 *m/z*, found 565.2549 *m/z*.

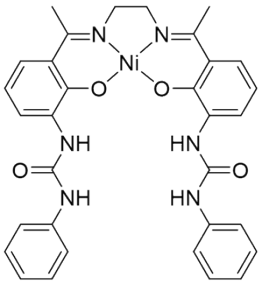

Synthesis of ***$NiL^{3,3'\text{-}O}$***. To a round bottom flask equipped with a stir bar and reflux condenser, **$H_2L^{3,3'\text{-}O}$** (0.392 g, 0.695 mmol) was heated to reflux in MeOH (15.0 mL). $Ni(CH_3COO)_2$•$4H_2O$ (0.173 g, 0.695 mmol) was quickly added to the refluxing solution, and a gradual color change to orange brown was observed. The solution was allowed to reflux for 1 hour, then cooled to room temperature. The product was collected as an orange powder *via* vacuum filtration. Yield = 95% (0.408 g, 0.66 mmol). **^{1}H NMR (DMSO-d_6):** δ 9.03 (s, 2H, Ar–NH), 8.37 (s, 2H, Ar–NH), 8.13 (dd, J = 7.8, 1.5 Hz, 2H, Ar–H), 7.27 (d, J = 7.5 Hz, 4H, Ar–H), 7.21 (dd, J = 8.5, 1.5 Hz, 2H, Ar–H), 7.03 (t, J = 8.0 Hz, 4H, Ar–H), 6.87 (t, J = 7.3 Hz, 2H, Ar–H), 6.52 (t, J = 8.0 Hz, 2H, Ar–H), 3.49 (s, 4H, $N(CH_3)_2N$), 2.43 (s, 6H, Ar–C(=N)CH_3). **^{13}C NMR (DMSO-d_6):** δ 169.6 (s, Ar–C(=N)), 152.7 (s, Ar–O), 152.4 (s, HN–C(=O)–NH), 139.3 (s, Ar–NH), 131.0 (s, Ar–NH), 128.4 (s, Ar), 121.8 (s, Ar), 121.7 (s, Ar), 121.0 (s, Ar), 118.9 (s, Ar), 118.3 (s, Ar), 114.1 (s, Ar), 54.1 (s, $N(CH_3)_2N$), 18.4 (s, ArC–CH_3). **HRMS (ESI-MS):** calculated $NiC_{32}H_{30}N_6O_4H^+$ = 621.1760 *m/z*, found 621.1758 *m/z*.

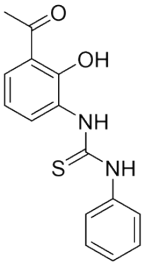

Synthesis of ***$HL^{3\text{-}S}$***. To a round bottom flask equipped with a stir bar, 1-(3-amino-2-hydroxyphenyl)ethanone (0.605 g, 4.0 mmol) was dissolved in MeOH (20.0 mL), forming a dark brown solution. Phenyl isothiocyanate (0.50 mL, 4.2 mmol) was added dropwise *via* syringe, and the reaction was stirred vigorously. After 6 hours, the reaction was quenched with deionized water, then extracted thrice with DCM and dried over anhydrous magnesium sulfate. The filtrate was obtained *via* vacuum filtration and dried under vacuum. The crude product was triturated in MeOH, and the final product was obtained as a brown powder *via* vacuum filtration. Yield = 73% (0.837 g, 2.9 mmol). **^{1}H NMR (DMSO-d_6):** δ 12.71 (s,

1H, Ar–OH), 10.08 (s, 1H, Ar–NH), 9.24 (m, 2H, Ar–H and Ar–NH), 8.20 (d, J = 8.1 Hz, 1H, Ar–H), 7.79 (d, J = 8.1 Hz, 1H, Ar–H), 7.54 (d, J = 8.0 Hz, 2H, Ar–H), 7.35 (t, J = 7.6 Hz, 2H, Ar–H), 7.15 Hz (t, J = 7.3 Hz, 1H, Ar–H), 6.98 (t, J = 7.8 Hz, 1H, Ar–H), 2.68 (s, 3H, Ar–C(=O)CH_3). **^{13}C NMR (DMSO-d_6):** δ 205.8 (s, Ar–C=O), 179.6 (s, HN–C(=S)–NH), 154.6 (s, Ar–OH), 139.2 (s, Ar–NH), 132.6 (s, Ar–NH), 128.5 (s, Ar), 128.0 (s, Ar), 127.8 (s, Ar), 124.7 (s, Ar), 123.7 (s, Ar), 119.7 (s, Ar), 118.0 (s, Ar), 27.1 (s, ArC–CH_3). **HRMS (ESI-MS):** calculated $C_{15}H_{14}N_2O_2SNa^+$ = 309.0674 *m/z*, found 309.0672 *m/z*.

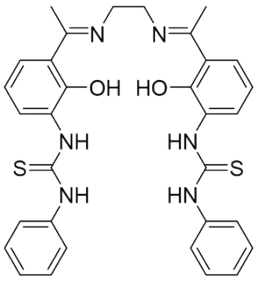

Synthesis of ***$H_2L^{3,3'\text{-}S}$***. To a round bottom flask equipped with a stir bar, addition funnel, and a reflux condenser, **$HL^{3\text{-}S}$** (0.286 g, 1.0 mmol) was heated to reflux in methanol (MeOH) (20.0 mL), appearing as a clear yellow solution. Ethylenediamine (0.030 g, 0.5 mmol) was dissolved in MeOH (30.0 mL) in a beaker, then poured into the addition funnel. The ethylenediamine solution was added dropwise into the refluxing solution of **$HL^{3\text{-}S}$** for over 1 hour, at which point the solution turned dark orange. The flask was taken off heat after 2 hours and allowed to stand overnight at room temperature. The product was collected as a yellow orange powder *via* vacuum filtration and washed with MeOH. The mother liquor was concentrated under vacuum and stored in a –5 °C freezer overnight to collect the second crop of product. Yield = 72% (0.215 g, 0.36 mmol). **^{1}H NMR (DMSO-d_6):** δ 10.27 (s, 2H, Ar–NH), 9.40 (s, 2H, Ar–NH), 8.57 (d, J = 7.2 Hz, 2H, Ar–H), 7.48 (d, J = 8.1 Hz, 4H, Ar–H), 7.40 (d, J = 8.5 Hz, 2H, Ar–H), 7.31 (t, J = 7.8 Hz, 4H, Ar–H), 7.12 (t, J = 7.2 Hz, 2H, Ar–H), 6.57 (t, J = 8.1 Hz, 2H, Ar–H), 4.06 (s, 4H, N(CH_3)$_2$N), 2.53 (s, 6H, Ar–C(=N)CH_3). **^{13}C NMR (DMSO-d_6):** δ 177.8 (s, HN–C(=S)–NH), 175.7 (s, Ar–C(=N)), 162.1 (s, Ar–OH), 139.0 (s, Ar–NH), 130.3 (s, Ar–NH), 128.6 (s, Ar), 124.6 (s, Ar), 124.5 (s, Ar), 124.2 (s, Ar), 123.6 (s, Ar), 115.3 (s, Ar), 112.9 (s, Ar), 46.3 (s, N(CH_3)$_2$N), 14.8 (s, ArC–CH_3). **HRMS (ESI-MS):** calculated $C_{32}H_{32}N_6O_2S_2Na^+$ = 619.1926 *m/z*, found 619.1920 *m/z*.

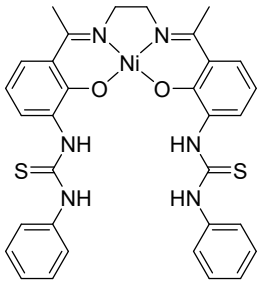

Synthesis of ***$NiL^{3,3'\text{-}S}$***. To a round bottom flask equipped with a stir bar and reflux condenser, **$H_2L^{3,3'\text{-}S}$** (0.060 g, 0.10 mmol) was heated to reflux in MeCN (5 mL). Ni(CH_3COO)$_2$•4H_2O (0.025 g, 0.10 mmol) was quickly added to the refluxing solution, and a gradual color change to orange brown was observed. The solution was allowed to reflux for 2 hours, then cooled to room temperature. The product was collected as shiny orange crystals powder *via* vacuum filtration. Yield = 75% (0.049 g, 0.75 mmol). **^{1}H NMR (DMSO-d_6):** δ 9.74 (s, 2H, Ar–NH), 9.24 (s, 2H, Ar–NH), 8.33 (d, J = 7.0 Hz, 2H, Ar–H), 7.37 (d, J = 8.4 Hz, 2H, Ar–H), 7.26 (d, J = 7.9 Hz, 4H, Ar–H), 7.10 (t, J = 7.5 Hz, 4H, Ar–H), 6.99 (t, J = 6.8 Hz, 2H, Ar–H), 6.54 (t, J = 7.9 Hz, 2H, Ar–H), 3.49 (s, 4H, N(CH_3)$_2$N), 2.44 (s, 6H, Ar–C(=N)CH_3). **^{13}C NMR (DMSO-d_6):** δ 178.4 (s, HN–C(=S)–NH), 169.5 (s, Ar–C(=N)), 154.3 (s, Ar–O), 139.0 (s, Ar–NH), 130.0 (s, Ar–NH), 127.9 (s, Ar), 124.9 (s, Ar), 124.7 (s, Ar), 124.4 (s, Ar), 123.8 (s, Ar), 121.5 (s, Ar), 113.2 (s, Ar), 54.5 (s,

$N(CH_3)_2N$), 18.5 (s, ArC–CH_3). **HRMS (ESI-MS):** calculated $NiC_{32}H_{30}N_6O_2S_2Na^+$ = 675.1123 *m/z*, found 675.1143 *m/z*.

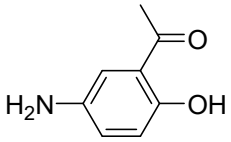

Synthesis of ***5-NH$_2$.*** The synthesis was adapted from a previously reported procedure.[4] 1-(2-hydroxy-5-nitrophenyl)ethanone (0.906 g, 5.0 mmol), 10 wt.% Pd/C (0.025 g), and anhydrous tetrahydrofuran (THF) (25.0 mL) was added to an oven-dried Schlenk flask equipped with a stir bar and a septum cap. The Schlenk flask was opened to vacuum and N_2 intermittently, then the stopcock was closed before an H_2 balloon equipped with an 18G needle was inserted into the septum cap. The solution was stirred under H_2 atmosphere at room temperature for 1 day. The solution was filtered through celite, then filtered again through a 0.45 μm PTFE syringe filter before drying under vacuum. The product was collected as yellow solids. *Note: the product decomposes over time under ambient conditions, and therefore must be made fresh before using in the next step*. Yield = 94% (0.710 g, 4.7 mmol). **^{1}H NMR (CDCl$_3$):** δ 11.71 (s, 1H, Ar–OH), 7.03 (d, *J* = 2.8 Hz, 1H, Ar–H), 6.91 (dd, *J* = 8.8, 2.8 Hz, 1H, Ar–H), 6.83 (d, *J* = 8.8 Hz, 1H, Ar–H), 3.46 (s, 2H, Ar–NH_2), 2.58 (s, 3H, Ar–C(=O)CH_3). **^{13}C NMR (CDCl$_3$):** δ 204.3 (s, Ar–C=O), 155.6 (s, Ar–OH), 138.2 (s, Ar–NH_2), 125.4 (s, Ar), 119.5 (s, Ar), 119.0 (s, Ar), 115.4 (s, Ar), 26.8 (s, ArC–CH_3). **HRMS (ESI-MS):** calculated $C_8H_9NO_2H^+$ = 152.0712 *m/z*, found 152.0714 *m/z*.

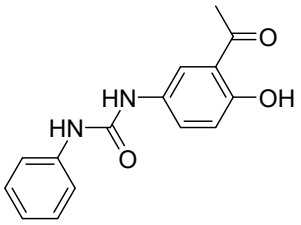

Synthesis of ***HL$^{5\text{-}O}$.*** To a round bottom flask equipped with a stir bar, **5-NH$_2$** (0.30 g, 2.0 mmol) was dissolved in DCM (10 mL), forming a golden yellow solution. Phenyl isothiocyanate (0.50 mL, 4.2 mmol) was added dropwise *via* syringe, and the reaction was stirred vigorously. Precipitation of the product occurred gradually throughout the reaction. After 1.5 hours, the product was obtained *via* vacuum filtration as a beige powder. Yield = 84% (0.451 g, 1.7 mmol). **^{1}H NMR (DMSO-*d*$_6$):** δ 11.54 (s, 1H, Ar–OH), 8.64 (s, 1H, Ar–NH_2), 8.58 (s, 1H, Ar–NH_2), 7.97 (d, *J* = 2.7 Hz, 1H, Ar–H), 7.53 (dd, *J* = 8.9, 2.7 Hz, 1H, Ar–H), 7.45 (dd, *J* = 8.6, 1.1 Hz, 2H, Ar–H), 7.30 – 7.23 (m, 2H, Ar–H), 6.96 (tt, *J* = 7.4, 1.1 Hz, 1H, Ar–H), 6.92 (d, *J* = 8.9 Hz, 1H), Ar–H, 2.62 (s, 3H, Ar–C(=O)CH_3). **^{13}C NMR (DMSO-*d*$_6$):** δ 203.8 (s, Ar–C=O), 155.9 (s, Ar–OH), 152.9 (s, HN–C(=O)–NH), 139.7 (s, Ar–NH), 131.3 (s, Ar–NH), 128.7 (s, Ar), 127.9 (s, Ar), 121.8 (s, Ar), 120.5 (s, Ar), 120.1 (s, Ar), 118.3 (s, Ar), 117.7 (s, Ar), 27.8 (s, ArC–CH_3). **HRMS (ESI-MS):** calculated $C_{15}H_{14}N_2O_3Na^+$ = 293.0902 *m/z*, found 293.0914 *m/z*.

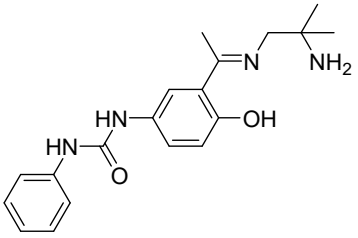

Synthesis of ***HL$^{5\text{-}O}$NH$_2$.*** To a round bottom flask equipped with a stir bar, addition funnel, and a reflux condenser, **HL$^{5\text{-}O}$** (0.135 g, 0.50 mmol) was heated to reflux in MeOH (10.0 mL), appearing as a clear yellow solution. 2-methylpropane-1,2-diamine (0.2645 g, 1.5 mmol) was dissolved in MeOH (10.0 mL) in a scintillation vial, then poured

into the addition funnel. The diamine solution was added dropwise into the refluxing solution of **$HL^{5\text{-}O}$** for over 30 minutes, which maintained a clear yellow color. The reaction was taken off the heat after 3 hours. The product was collected as a golden yellow oil. Excess diamine was removed by heating the scintillation vial of the product to 55 °C for 3 hours under vacuum. The crude product was obtained as yellow-orange solids without further purification. Yield = 82% by ^{1}H NMR. **^{1}H NMR (DMSO-d_6):** δ 8.83 (s, 1H, Ar–NH), 8.65 (s, 1H, Ar–NH), 7.79 (d, J = 2.5 Hz, 1H, Ar–H), 7.45 (d, J = 7.7 Hz, 2H, Ar–H), 7.29 (dd, J = 8.8, 2.5 Hz, 1H, Ar–H), 7.25 (t, J = 8.0 Hz, 2H, Ar–H), 6.93 (t, J = 7.3 Hz, 1H, Ar–H), 6.73 (d, J = 8.8 Hz, 1H, Ar–H), 3.41 (s, 2H, N–CH_2), 2.33 (s, 3H, Ar–C(=N)CH_3), 1.11 (s, 6H, N–C(CH_3)$_2$). **^{13}C NMR (DMSO-d_6):** δ 171.9 (s, Ar–C(=N)), 159.2 (s, Ar–OH), 153.0 (s, HN–C(=O)–NH) 140.0 (s, Ar–NH), 129.0 (s, Ar–NH), 128.7 (s, Ar), 124.7 (s, Ar), 121.5 (s, Ar), 119.1 (s, Ar), 118.4 (s, Ar), 118.1 (s, Ar), 117.9 (s, Ar), 61.7 (s, N–CH_2), 50.0 (s, H_2N–C(CH_3)$_2$), 28.4 (s, NC–(CH_3)$_2$), 14.5 (s, ArC–CH_3). **HRMS (ESI-MS):** calculated $C_{19}H_{24}N_4O_2H^+$ 341.1978 *m/z*, found 341.1965 *m/z*.

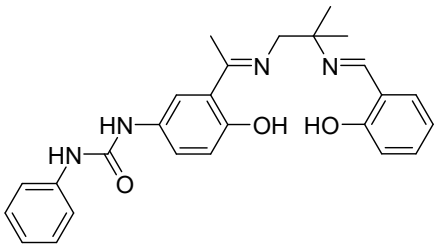

Synthesis of ***$H_2L^{5\text{-}O}$***. To a round bottom flask equipped with a stir bar, addition funnel, and a reflux condenser, **$HL^{5\text{-}O}NH_2$** (0.212 g, 82% purity, 0.51 mmol) was heated to reflux in MeOH (10.0 mL), appearing as a clear yellow solution. Salicylaldehyde (0.075 g, 0.61 mmol) was dissolved in MeOH (10.0 mL) in a scintillation vial, then poured into the addition funnel. The salicylaldehyde solution was added dropwise into the refluxing solution of **$HL^{5\text{-}O}NH_2$** over 30 minutes. The solution was allowed to reflux for 2 hours before cooling to room temperature. The solution was dried under vacuum, then redissolved in minimal MeOH. Sonication of the solution for 2 minutes precipitated a yellow powder that was obtained upon filtration. Yield = 65%. **^{1}H NMR (DMSO-d_6):** δ 13.92 (s, 1H, Ar–C(=N)H), 8.62 (s, 1H, Ar–NH), 8.58 (s, 1H, Ar–NH), 8.40 (s, 1H, Ar–OH), 7.78 (d, J = 2.3 Hz, 1H, Ar–H), 7.49 (dd, J = 7.7, 1.5 Hz, 1H, Ar–H), 7.43 (d, J = 7.9 Hz, 2H, Ar–H), 7.31 (t, J = 8.0 Hz, 1H, Ar–H), 7.28 – 7.23 (m, 3H, Ar–H), 6.94 (t, J = 7.4 Hz, 1H, Ar–H), 6.88 (t, J = 7.6 Hz, 1H, Ar–H), 6.83 (d, J = 8.6 Hz, 1H, Ar–H), 6.72 (d, J = 8.8 Hz, 1H, Ar–H), 3.75 (s, 2H, N–CH_2), 2.34 (s, 3H, Ar–C(=N)CH_3), 1.40 (s, 6H, NC(CH_3)$_2$). **^{13}C NMR (DMSO-d_6):** δ 172.4 (s, Ar–C(=N)), 162.6 (s, Ar–C(=N)), 160.9 (s, Ar–OH), 158.1 (s, Ar–OH), 153.0 (s, HN–C(=O)–NH), 139.9 (s, Ar–NH), 132.2 (s, Ar–NH), 132.0 (s, Ar), 129.5 (s, Ar), 128.7 (s, Ar), 124.4 (s, Ar), 121.6 (s, Ar), 119.0 (s, Ar), 118.7 (s, Ar), 118.7 (s, Ar), 118.3(s, Ar), 118.14 (s, Ar), 117.6 (s, Ar), 116.5 (s, Ar), 60.2 (s, N–C(CH_3)$_2$), 59.9 (s, N–CH_2), 25.2 (s, NC–(CH_3)$_2$), 14.8 (s, ArC–CH_3). **HRMS (ESI-MS):** calculated $C_{26}H_{28}N_4O_3H^+$ = 445.2240 *m/z*, found 445.2252 *m/z*.

Synthesis of ***NiL$^{5\text{-}O}$***. To a round bottom flask equipped with a stir bar and reflux condenser, **$H_2L^{5\text{-}O}$** (0.089 g, 0.20 mmol) was heated to reflux in MeCN (5.0 mL). $Ni(CH_3COO)_2$•$4H_2O$ (0.055 g, 0.22 mmol) was dissolved in MeCN (5.0 mL) in a scintillation vial under sonication before it was added to the refluxing solution. A gradual color change from bright yellow to dark orange was observed. The solution was allowed to reflux for 1 hour, then cooled to room temperature before storing in a –5 °C freezer overnight. The solution was sonicated to precipitate the product. The crude product was obtained by vacuum filtration, then redissolved in minimal MeOH before adding excess Et_2O. The precipitate was obtained by vacuum filtration as tan-brown flakes. Yield = 53% (0.054 g, 0.11 mmol). **^{1}H NMR (DMSO-*d*$_6$):** 8.55 (s, 1H, Ar–NH), 8.22 (s, 1H, Ar–NH), 7.78 (s, 1H, Ar–H), 7.68 (d, *J* = 3.2 Hz, 1H, Ar–H), 7.43 (d, *J* = 8.0 Hz, 2H, Ar–H), 7.35 (dd, *J* = 7.8, 2.0 Hz, 1H, Ar–H), 7.25 (t, *J* = 7.9 Hz, 2H, Ar–H), 7.15 (ddd, *J* = 9.0, 7.0, 1.8 Hz, 1H, Ar–H), 7.10 (dd, *J* = 8.7, 2.8 Hz, 1H, Ar–H), 6.93 (t, *J* = 7.3 Hz, 1H, Ar–H), 6.67 (d, *J* = 8.7, Hz, 1H, Ar–H), 6.66 (d, *J* = 8.4, Hz, 1H, Ar–H), 6.50 (t, *J* = 7.4 Hz, 1H, Ar–H), 3.37 (s, 2H*, N–CH_2), 2.37 (s, 3H, Ar–C(=N)CH_3), 1.43 (s, 6H, NC$(CH_3)_2$). *Partially overlaps with residual H_2O peak. **^{13}C NMR (DMSO-*d*$_6$):** δ 168.7 (s, Ar–C(=N)), 163.4 (s, Ar–C(=N)), 160.1 (s, Ar–O), 159.0 (s, Ar–O), 153.1 (s, HN–C(=O)–NH), 140.1 (s, Ar–NH), 133.5 (s, Ar–NH), 133.2 (s, Ar), 128.7 (s, Ar), 126.4 (s, Ar), 126.2 (s, Ar), 121.4 (s, Ar), 120.9 (s, Ar), 120.5 (s, Ar), 120.5 (s, Ar), 119.6 (s, Ar), 119.5 (s, Ar), 118.0 (s, Ar), 114.0 (s, Ar), 66.3 (s, N–C$(CH_3)_2$), 65.5 (s, N–CH_2), 25.6 (s, NC–$(CH_3)_2$), 18.3 (s, ArC–CH_3). **HRMS (ESI-MS):** calculated $NiC_{26}H_{26}N_4O_3Na^+$ = 523.1256 *m/z*, found 523.1268 *m/z*.

Crystallographic Information

X-ray Data Collection, Structure Solution and Refinement for NiL$^{3,3'\text{-}O}$•DMSO-d$_6$.

An orange crystal of approximate dimensions 0.190 x 0.415 x 0.429 mm was mounted on a glass fiber and transferred to a Bruker SMART APEX II diffractometer system. The APEX2[5] program package was used to determine the unit-cell parameters and for data collection 20 sec/frame scan time). The raw frame data was processed using SAINT[6] and SADABS[7] to yield the reflection data file. Subsequent calculations were carried out using the SHELXTL[8] program package. The diffraction symmetry was 2/*m* and the systematic absences were consistent with the monoclinic space group $P2_1/n$ that was later determined to be correct.

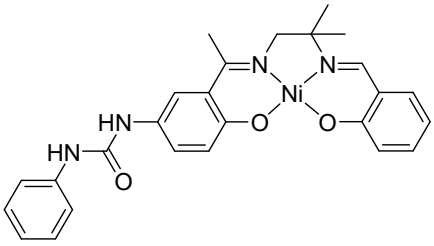

The structure was solved by direct methods and refined on F^2 by full-matrix least-squares techniques. The analytical scattering factors[9] for neutral atoms were used throughout the analysis. Hydrogen atoms were either located from a difference-Fourier map and refined (x,y,z and U_{iso}) or were included using a riding model. There was one molecule of dimethyl sulfoxide-d$_6$ solvent present.

Least-squares analysis yielded wR2 = 0.0701 and Goof = 1.034 for 466 variables refined against 10013 data (0.68 Å), R1 = 0.0248 for those 9302 data with I > 2.0σ(I).

X-ray Data Collection, Structure Solution and Refinement for $NiL^{3,3'\text{-}O}\bullet(H_2O)_2(THF)_2$.

A yellow crystal of approximate dimensions 0.119 x 0.121 x 0.286 mm was mounted in a cryoloop and transferred to a Bruker SMART APEX II diffractometer system. The APEX2[5] program package was used to determine the unit-cell parameters and for data collection (120 sec/frame scan time). The raw frame data was processed using SAINT[6] and SADABS[7] to yield the reflection data file. Subsequent calculations were carried out using the SHELXTL[8] program package. The diffraction symmetry was 2/*m* and the systematic absences were consistent with the monoclinic space group $P2_1/n$ that was later determined to be correct.

The structure was solved by direct methods and refined on F^2 by full-matrix least-squares techniques. The analytical scattering factors[9] for neutral atoms were used throughout the analysis. Hydrogen atoms were either located from a difference-Fourier map and refined (x,y,z and U_{iso}) or were included using a riding model. There were two molecules of tetrahydrofuran solvent and two water molecules present.

Least-squares analysis yielded wR2 = 0.1154 and Goof = 1.054 for 526 variables refined against 9623 data (0.75 Å), R1 = 0.0488 for those 7289 data with I > 2.0σ(I).

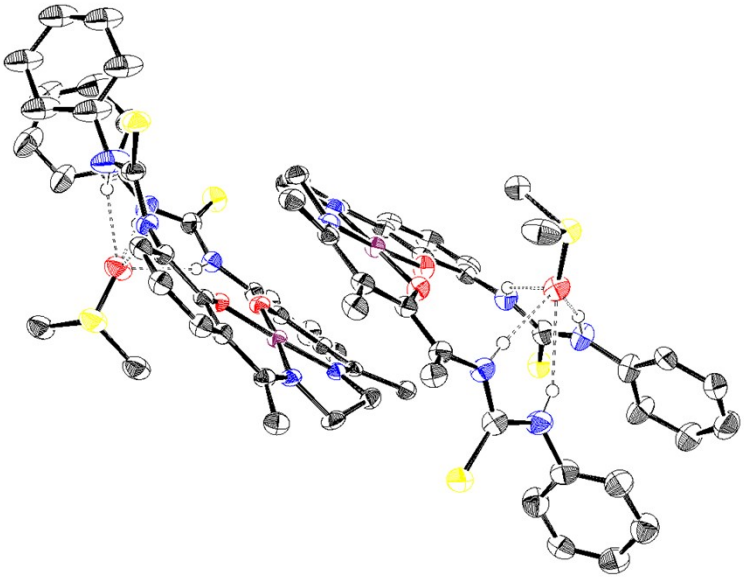

Figure S1. Solid-state structure of the full asymmetric unit of **NiL$^{3,3'\text{-S}}$•DMSO**. Hydrogen atoms that do not participate in hydrogen bonding have been omitted for clarity. Thermal ellipsoids are represented at 50% probability. Ellipsoids are labeled as follows: maroon = Ni, black = C, red = O, blue = N, yellow = S. Hydrogen atoms are represented as black spheres.

X-ray Data Collection, Structure Solution and Refinement for NiL$^{3,3'\text{-S}}$•DMSO.

An orange crystal of approximate dimensions 0.088 x 0.323 x 0.431 mm was mounted in a cryoloop and transferred to a Bruker X8 Prospector diffractometer system. The APEX3[10] program package was used to determine the unit-cell parameters and for data collection (10 sec/frame scan time). The raw frame data was processed using SAINT[6] and SADABS[7] to yield the reflection data file. Subsequent calculations were carried out using the SHELXTL[8] program package. There were no systematic absences. The centrosymmetric triclinic space group $P\bar{1}$ was assigned and later determined to be correct.

The structure was solved by direct methods and refined on F^2 by full-matrix least-squares techniques[4]. The analytical scattering factors[9] for neutral atoms were used throughout the analysis. Hydrogen atoms were included using a riding model. There are two symmetry unique Ni molecules in the asymmetric unit, and each Ni complex participates in hydrogen bonding interactions with a DMSO molecule. There were several high residuals present in the final difference-Fourier map. It was not possible to determine the nature of the residuals although it was probable that DMSO solvent was present. The SQUEEZE[11] routine in the PLATON[12] program package was used to account for the electrons in the solvent accessible voids. Disordered atoms were included using multiple components, partial-site occupancies, and geometric (SADI), and displacement (SIMU, ISOR, EADP) constraints.

Least-squares analysis yielded wR2 = 0.2016 and Goof = 1.024 for 855 variables refined against 13642 data (0.81 Å), R1 = 0.0742 for those 10805 data with I > 2.0σ(I).

X-ray Data Collection, Structure Solution and Refinement for $NiL^{5\text{-}O}$.

An orange crystal of approximate dimensions 0.171 x 0.171 x 0.367 mm was mounted on a glass fiber and transferred to a Bruker SMART APEX II diffractometer system. The APEX2[5] program package was used to determine the unit-cell parameters and for data collection (180 sec/frame scan time). The raw frame data was processed using SAINT[6] and SADABS[7] to yield the reflection data file. Subsequent calculations were carried out using the SHELXTL[8] program package. There were no systematic absences nor any diffraction symmetry other than the Friedel condition. The centrosymmetric triclinic space group $P\bar{1}$ was assigned and later determined to be correct.

The structure was solved by direct methods and refined on F^2 by full-matrix least-squares techniques. The analytical scattering factors[9] for neutral atoms were used throughout the analysis. Hydrogen atoms were located from a difference-Fourier map and refined (x,y,z and U_{iso}). There are three symmetry unique Ni molecules locked in place through several hydrogen bonding interactions. Two carbon atoms were disordered and included multiple components, partial-site occupancies, geometric (SADI), and displacement (SIMU, EADP) constraints. There is also one molecule of ethanol and half a molecule of methanol present in the asymmetric unit.

Least-squares analysis yielded wR2 = 0.1397 and Goof = 1.021 for 983 variables refined against 20850 data (0.70 Å), R1 = 0.0501 for those 15415 data with I > 2.0σ(I).

X-ray Data Collection, Structure Solution and Refinement for $[NiL^{3,3'\text{-}O}]_2 \bullet Cl^-$.

An orange crystal of approximate dimensions 0.172 x 0.236 x 0.265 mm was mounted in a cryoloop and transferred to a Bruker SMART APEX II diffractometer system. The APEX2[5] program package and the CELL_NOW[13] were used to determine the unit-cell parameters. Data was collected using a 120 sec/frame scan time. The raw frame data was processed using SAINT[6] and TWINABS[14] to yield the reflection data file (HKLF5 format)[14]. Subsequent calculations were carried out using the SHELXTL[8] program package. There were no systematic absences nor any diffraction symmetry other than the Friedel condition. The centrosymmetric triclinic space group $P\bar{1}$ was assigned and later determined to be correct.

The structure was solved by direct methods and refined on F^2 by full-matrix least-squares techniques. The analytical scattering factors[8] for neutral atoms were used throughout the analysis. Hydrogen atoms H(3), H(4), H(5), H(6), H(9), H(10), H(11) and H(12) were located from a difference-Fourier map and refined (x,y,z and riding U_{iso}). The remaining hydrogen atoms were included using a riding

model. There were three molecules of tetrahydrofuran solvent present. Disordered atoms were included using multiple components, partial site-occupancy-factors and restraint/constraints.

Least-squares analysis yielded wR2 = 0.1368 and Goof = 1.063 for 1132 variables refined against 17549 data (0.80 Å), R1 = 0.0519 for those 15615 with I > 2.0σ(I). The structure was refined as a two-component twin, BASF[8] = 0.3687.

Definitions:

$wR2 = [\Sigma[w(F_o^2-F_c^2)^2] / \Sigma[w(F_o^2)^2]]^{1/2}$

$R1 = \Sigma||F_o|-|F_c|| / \Sigma|F_o|$

$Goof = S = [\Sigma[w(F_o^2-F_c^2)^2] / (n-p)]^{1/2}$ where n is the number of reflections and p is the total number of parameters refined.

Table S1. Crystal data and structure refinement for **$NiL^{3,3'\text{-}O}$•DMSO-d_6**.

Deposition Number	2379616	
Empirical formula	$C_{32}H_{30}N_6NiO_4$•C_2D_6SO	
Formula weight	705.49	
Temperature	93(2) K	
Wavelength	0.71073 Å	
Crystal system	Monoclinic	
Space group	$P2_1/n$	
Unit cell dimensions	a = 18.2951(5) Å	α = 90°
	b = 8.7660(3) Å	β = 91.9571(5)°
	c = 19.4810(6) Å	γ = 90°
Volume	3122.44(17) Å^3	
Z	4	
Density (calculated)	1.501 Mg/m^3	
Absorption coefficient	0.742 mm^{-1}	
F(000)	1464	
Crystal color	orange	
Crystal size	0.429 x 0.415 x 0.190 mm^3	
Theta range for data collection	2.092 to 31.652°	
Index ranges	-25<=h<=26, -12<=k<=12, -28<=l<=28	
Reflections collected	80109	
Independent reflections	10013 [R(int) = 0.0216]	
Completeness to theta = 25.242°	99.9 %	
Absorption correction	Semi-empirical from equivalents	
Max. and min. transmission	0.8623 and 0.8092	
Refinement method	Full-matrix least-squares on F^2	
Data / restraints / parameters	10013 / 0 / 466	
Goodness-of-fit on F2	1.034	
Final R indices [I>2sigma(I) = 9302 data]	R1 = 0.0248, wR2 = 0.0687	
R indices (all data, 0.68 Å)	R1 = 0.0270, wR2 = 0.0701	
Largest diff. peak and hole	0.485 and -0.329 e.Å^{-3}	

Table S2. Crystal data and structure refinement for **$NiL^{3,3'-O}\bullet(H_2O)_2(THF)_2$**.

Deposition Number	2379617	
Empirical formula	$C_{32}H_{30}N_6NiO_4\bullet2(H_2O)\bullet2(C_4H_8O)$	
Formula weight	801.57	
Temperature	133(2) K	
Wavelength	0.71073 Å	
Crystal system	Monoclinic	
Space group	$P2_1/n$	
Unit cell dimensions	a = 23.663(3) Å	α = 90°
	b = 7.1548(8) Å	β = 113.9687(17)°
	c = 25.033(3) Å	γ = 90°
Volume	3872.7(8) $Å^3$	
Z	4	
Density (calculated)	1.375 Mg/m^3	
Absorption coefficient	0.562 mm^{-1}	
F(000)	1696	
Crystal color	yellow	
Crystal size	0.286 x 0.121 x 0.119 mm^3	
Theta range for data collection	1.536 to 28.282°	
Index ranges	-30<=h<=31, -9<=k<=9, -33<=l<= 33	
Reflections collected	45957	
Independent reflections	9623 [R(int) = 0.0687]	
Completeness to theta = 25.242°	99.9 %	
Absorption correction	Semi-empirical from equivalents	
Max. and min. transmission	0.8017 and 0.6246	
Refinement method	Full-matrix least-squares on F^2	
Data / restraints / parameters	9623 / 6 / 526	
Goodness-of-fit on F2	1.054	
Final R indices [I>2sigma(I) = 7288 data]	R1 = 0.0488, wR2 = 0.1051	
R indices (all data, 0.75 Å)	R1 = 0.0727, wR2 = 0.1154	
Largest diff. peak and hole	0.716 and -0.653 $e.Å^{-3}$	

Table S3. Crystal data and structure refinement for **NiL$^{3,3'\text{-}S}$•DMSO**.

Deposition Number	2379620	
Empirical formula	$C_{32}H_{30}N_6NiO_2S_2$•1.6(C_2H_6SO)	
Formula weight	778.45	
Temperature	93.15 K	
Wavelength	1.54178 Å	
Crystal system	Triclinic	
Space group	P-1	
Unit cell dimensions	a = 13.4469(4) Å	a= 79.477(2)°
	b = 14.7117(5) Å	b= 86.598(2)°
	c = 18.4767(7) Å	g = 88.997(2)°
Volume	3587.3(2) Å^3	
Z	4	
Density (calculated)	1.441 Mg/m^3	
Absorption coefficient	3.119 mm^{-1}	
F(000)	1629	
Crystal color	orange	
Crystal size	0.431 x 0.323 x 0.088 mm^3	
Theta range for data collection	2.436 to 72.674°	
Index ranges	-16 <= h <= 16, -18 <= k <= 17, -22 <= l <= 22	
Reflections collected	94171	
Independent reflections 1	3642 [R(int) = 0.0871]	
Completeness to theta = 67.679°	96.4 %	
Absorption correction	Semi-empirical from equivalents	
Max. and min. transmission	0.7536 and 0.5254	
Refinement method	Full-matrix least-squares on F^2	
Data / restraints / parameters	13642 / 122 / 855	
Goodness-of-fit on F^2	1.024	
Final R indices [I>2sigma(I) = 10805 data]	R1 = 0.0742, wR2 = 0.1888	
R indices (all data, 0.81 Å)	R1 = 0.0905, wR2 = 0.2016	
Extinction coefficient	n/a	
Largest diff. peak and hole	1.148 and -2.005 e.Å^{-3}	

Table S4. Crystal data and structure refinement for **NiL$^{5\text{-}O}$**.

Deposition Number	2379619	
Empirical formula	$C_{26.83}H_{28}N_4NiO_{3.50}$	
Formula weight	521.24	
Temperature	93(2) K	
Wavelength	0.71073 Å	
Crystal system	Triclinic	
Space group	P-1	
Unit cell dimensions	a = 11.6000(10) Å	α = 72.4119(14)°
	b = 16.4750(15) Å	β = 88.1460(15)°
	c = 21.5479(19) Å	γ = 71.8599(15)°
Volume	3721.7(6) Å^3	
Z	6	
Density (calculated)	1.395 Mg/m^3	
Absorption coefficient	0.820 mm^{-1}	
F(000)	1638	
Crystal color	orange	
Crystal size	0.367 x 0.171 x 0.171 mm^3	
Theta range for data collection	1.922 to 29.574°	
Index ranges	-16<=*h*<=16, -22<=*k*<=22, -29<=*l*<=29	
Reflections collected	73631	
Independent reflections	20850 [R(int) = 0.0588]	
Completeness to theta = 25.242°	99.9 %	
Absorption correction	Semi-empirical from equivalents	
Max. and min. transmission	0.7461 and 0.6621	
Refinement method	Full-matrix least-squares on F^2	
Data / restraints / parameters	20850 / 2 / 983	
Goodness-of-fit on F^2	1.021	
Final R indices [I>2sigma(I) = 15415 data]	R1 = 0.0501, wR2 = 0.1261	
R indices (all data, 0.70 Å)	R1 = 0.0760, wR2 = 0.1397	
Largest diff. peak and hole	1.414 and -1.141 e.Å^{-3}	

Table S5. Crystal data and structure refinement for **[NiL3,3'-O]$_2$•Cl$^-$**.

Deposition Number	2379618	
Empirical formula	$[C_{32}H_{30}N_6O_4Ni]_2[Cl][C_{16}H_{36}N]\bullet(C_4H_8O)_3$	
Formula weight	1736.87	
Temperature	93(2) K	
Wavelength	0.71073 Å	
Crystal system	Triclinic	
Space group	P-1	
Unit cell dimensions	a = 11.4188(9) Å	α = 97.4909(14)°
	b = 15.6518(13) Å	β = 100.7164(14)°
	c = 25.611(2) Å	γ = 104.6492(14)°
Volume	4274.9(6) Å^3	
Z	2	
Density (calculated)	1.349 Mg/m^3	
Absorption coefficient	0.541 mm^{-1}	
F(000)	1848	
Crystal color	orange	
Crystal size	0.265 x 0.236 x 0.172 mm^3	
Theta range for data collection	1.460 to 26.419°	
Index ranges	$-14 \le h \le 13$, $-19 \le k \le 19$, $0 \le l \le 32$	
Reflections collected	17549	
Completeness to theta = 25.242°	100.0 %	
Absorption correction	Semi-empirical from equivalents	
Max. and min. transmission	0.7454 and 0.6744	
Refinement method	Full-matrix least-squares on F^2	
Data / restraints / parameters	17549 / 90 / 1132	
Goodness-of-fit on F2	1.063	
Final R indices [I>2sigma(I) = 15615 data]	R1 = 0.0519, wR2 = 0.1310	
R indices (all data, 0.80 Å)	R1 = 0.0616, wR2 = 0.1368	
Largest diff. peak and hole	2.139 and -1.628 e.Å^{-3}	

Table S6. Relevant bond metrics for **NiL$^{3,3'\text{-O}}$•DMSO-d$_6$**.

Atom 1	Atom 2		Bond length (Å)
N3	O5		2.9082(11)
N4	O5		3.1416(11)
N5	O5		3.3966(11)
N6	O5		2.7956(10)
Atom 1	**Atom 2**	**Atom 3**	**Bond angle (°)**
N3	H3	O5	145.963
N4	H4	O5	148.641
N5	H5	O5	140.793
N6	H6	O5	169.447

Table S7. Relevant bond metrics for **NiL$^{3,3'\text{-S}}$•DMSO**.

Atom 1	Atom 2		Bond length (Å)
N3	O3		2.971(5)
N4	O3		3.006(15)
N5	O3		3.157(5)
N6	O3		2.785(5)
N9	O6		2.984(5)
N10	O6		3.278(5)
N11	O6		3.277(5)
N12	O6		2.835(9)
Atom 1	**Atom 2**	**Atom 3**	**Bond angle (°)**
N3	H3	O3	158.646
N4	H4	O3	157.419
N5	H5	O3	148.989
N6	H6	O3	173.156
N9	H9	O6	172.648
N10	H10	O6	150.475
N11	H11	O6	149.309
N12	H12	O6	161.470

Table S8. Relevant bond metrics for **NiL$^{3,3'-O}$•$(H_2O)_2(THF)_2$**.

Atom 1	Atom 2	Bond length (Å)
N3	O8	3.324(3)
N4	O8	2.871(3)
N5	O7	3.020(3)
N6	O7	3.036(3)
O7	O1	2.927(2)
O7	O5	2.708(2)
O8	O6	2.733(3)

Atom 1	Atom 2	Atom 3	Bond angle (°)
N3	H3	O8	130.308
N4	H4	O8	168.216
N5	H5	O7	155.270
N6	H6	O7	152.506
O7	H72	O1	173.513
O7	H71	O5	173.532
O8	H81	O6	162.226

Table S9. Relevant bond metrics for **NiL^{5-O}**.

Atom 1	Atom 2	Bond length (Å)
N3	O8	2.754(3)
N4	O7	3.150(3)
N11	O5	2.906(3)
N12	O4	2.986(3)

Atom 1	Atom 2	Atom 3	Bond angle (°)
N3	H3	O8	165.548
N4	H4	O7	160.484
N11	H11	O5	159.769
N12	H12	O4	161.248

Table S10. Relevant bond metrics for $[NiL^{3,3'-O}]_2 \bullet Cl^-$.

Atom 1	Atom 2		Bond length (Å)
N3	Cl1		3.588(3)
N4	Cl1		3.202(3)
N5	Cl1		3.444(3)
N6	Cl1		3.284(3)
N9	Cl1		3.599(3)
N10	Cl1		3.228(3)
N11	Cl1		3.541(3)
N12	Cl1		3.235(3)
Atom 1	**Atom 2**	**Atom 3**	**Bond angle (°)**
Ni1	Cl1	Ni2	89.022
N3	H3	Cl1	148.869
N4	H4	Cl1	170.324
N5	H5	Cl1	149.175
N6	H6	Cl1	166.221
N9	H9	Cl1	146.884
N10	H10	Cl1	173.632
N11	H11	Cl1	158.215
N12	H12	Cl1	178.275

Titration Curves and Relevant NMR Spectra

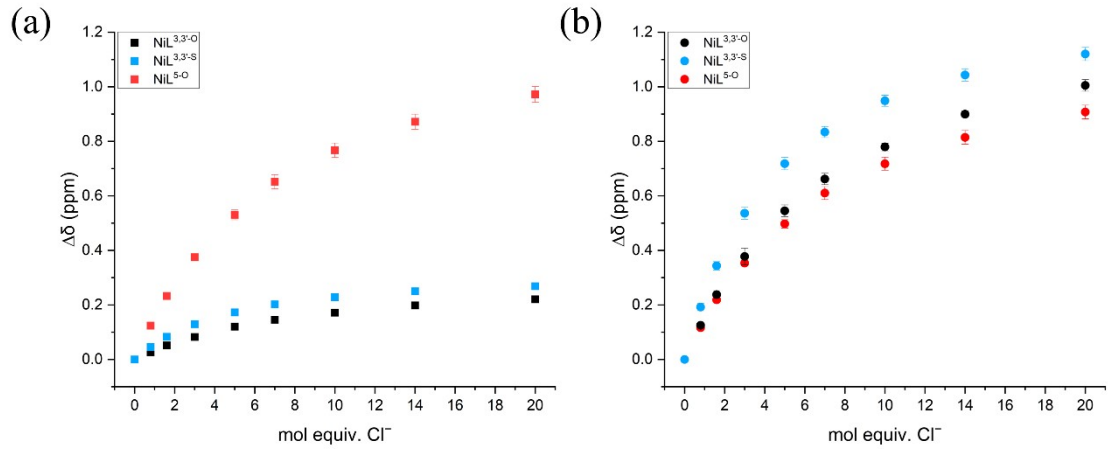

Figure S2. (a) Titration curve of the change in chemical shift (Δδ)of N_a–H upon titration of Cl^-. **(b)** Titration curve of the change in chemical shift (Δδ)of N_b–H upon titration of Cl^-.

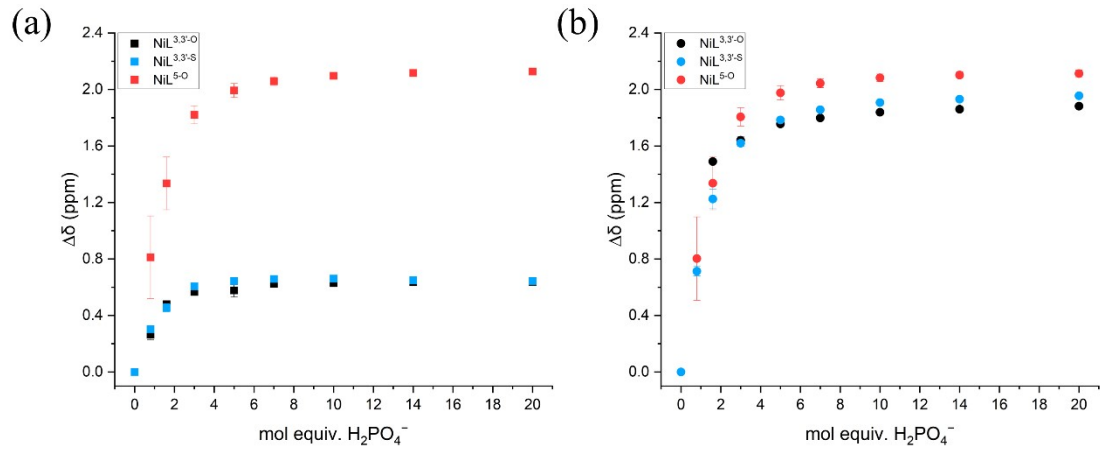

Figure S3. (a) Titration curve of the change in chemical shift (Δδ)of N_a–H upon titration of $H_2PO_4^-$. **(b)** Titration curve of the change in chemical shift (Δδ)of N_b–H upon titration of $H_2PO_4^-$.

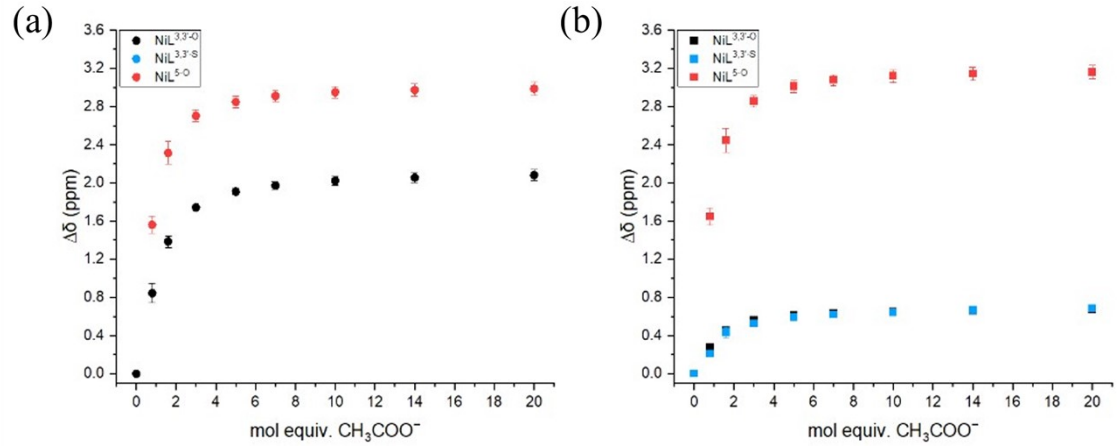

Figure S4. (a) Titration curve of the change in chemical shift (Δδ)of N_a–H upon titration of CH_3COO^-. **(b)** Titration curve of the change in chemical shift (Δδ)of N_b–H upon titration of CH_3COO^-.

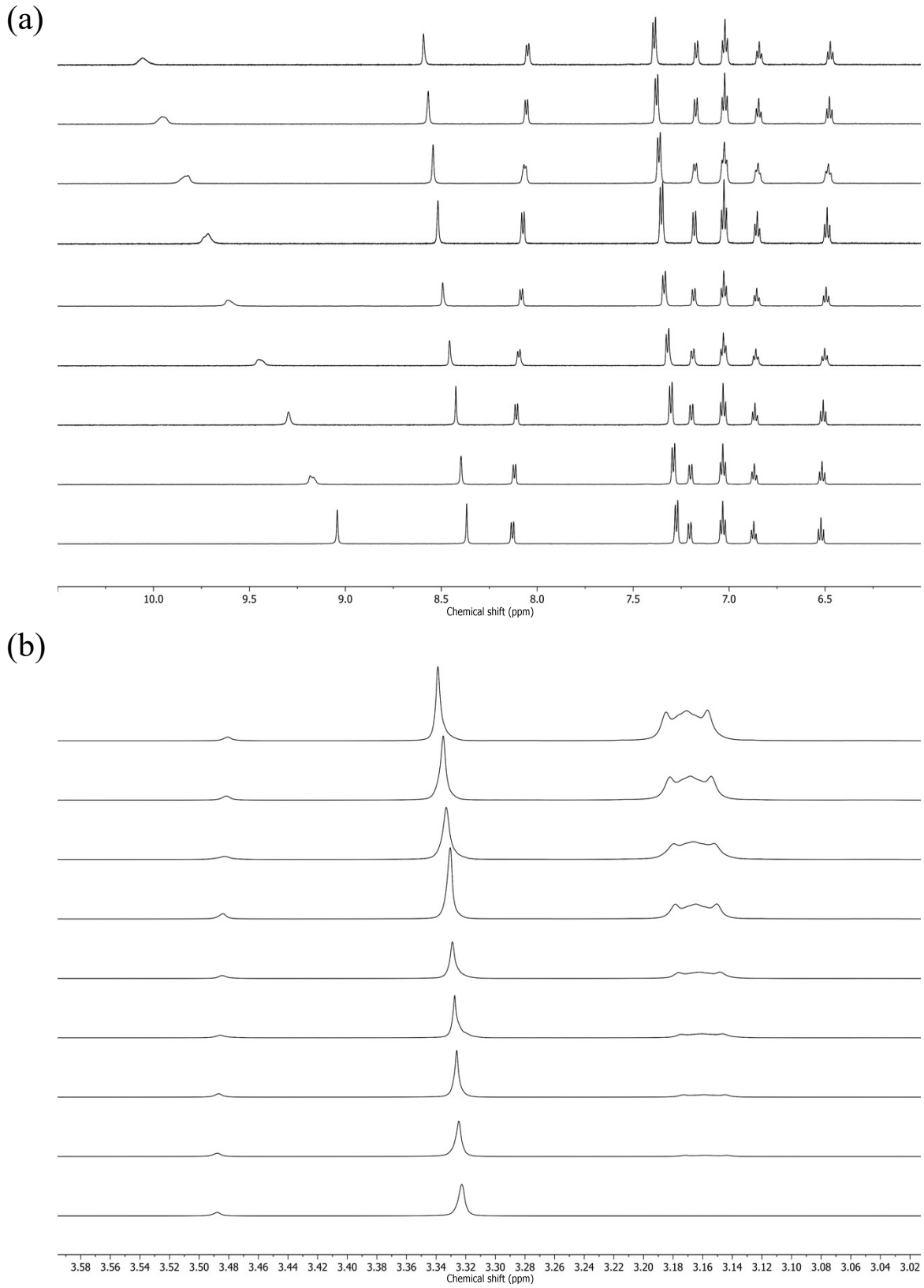

Figure S5. ^{1}H NMR spectra observing the titration of Cl^{-} into **NiL$^{3,3'\text{-}O}$ (a)** in the aromatic region, where N_a–H starts from 9.04 ppm and N_b–H starts from 8.37 ppm. **(b)** following the water signal beginning at 3.32 ppm. From the bottom up: 0, 0.8, 1.6, 3, 5, 7, 10, 14, 20 mole equivalents of Cl^{-} titrated.

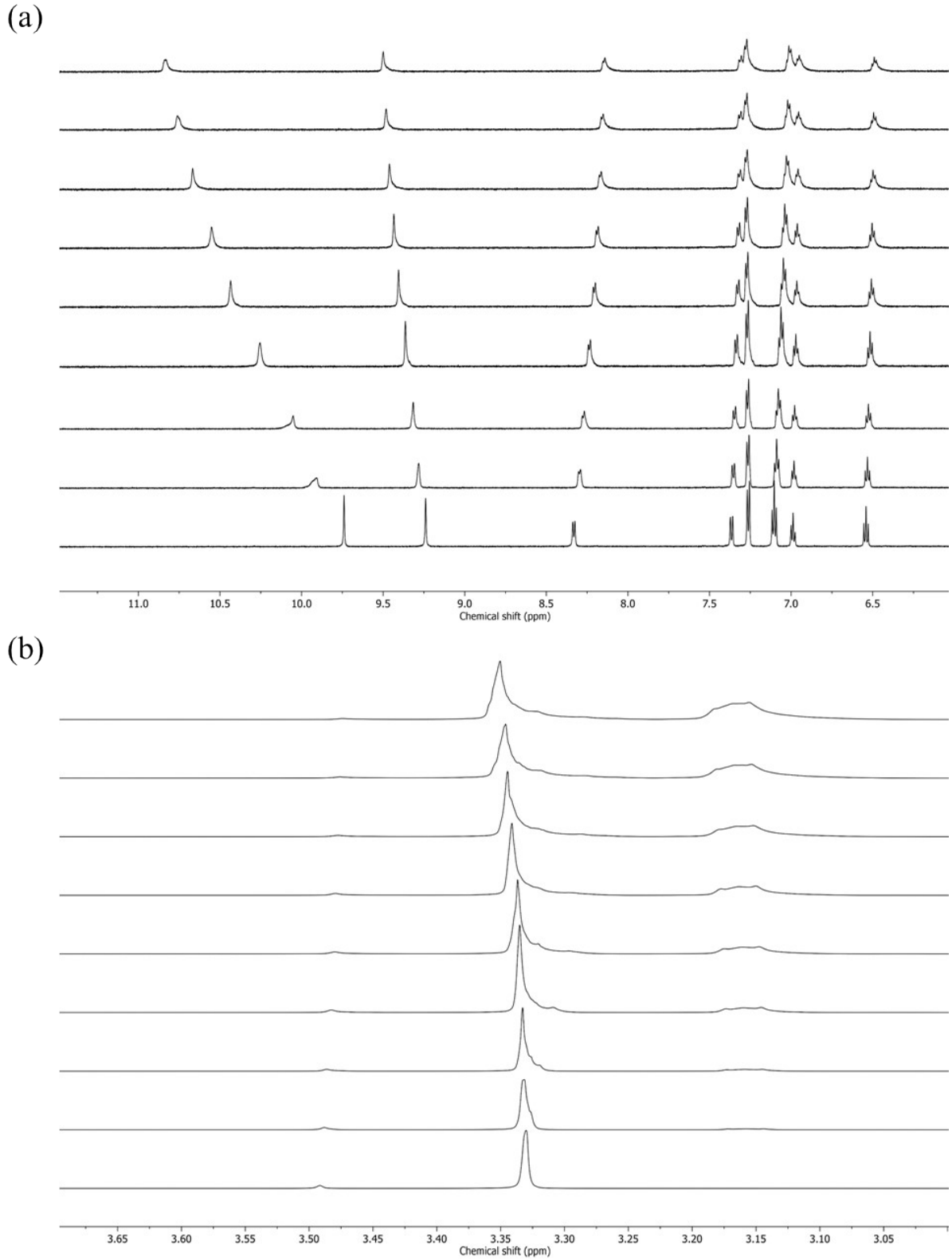

Figure S6. ^{1}H NMR spectra observing the titration of Cl^- into **NiL$^{3,3'\text{-}S}$ (a)** in the aromatic region, where N_a–H starts from 9.74 ppm and N_b–H starts from 9.24 ppm. **(b)** following the water signal beginning at 3.32 ppm. From the bottom up: 0, 0.8, 1.6, 3, 5, 7, 10, 14, 20 mole equivalents of Cl^- titrated.

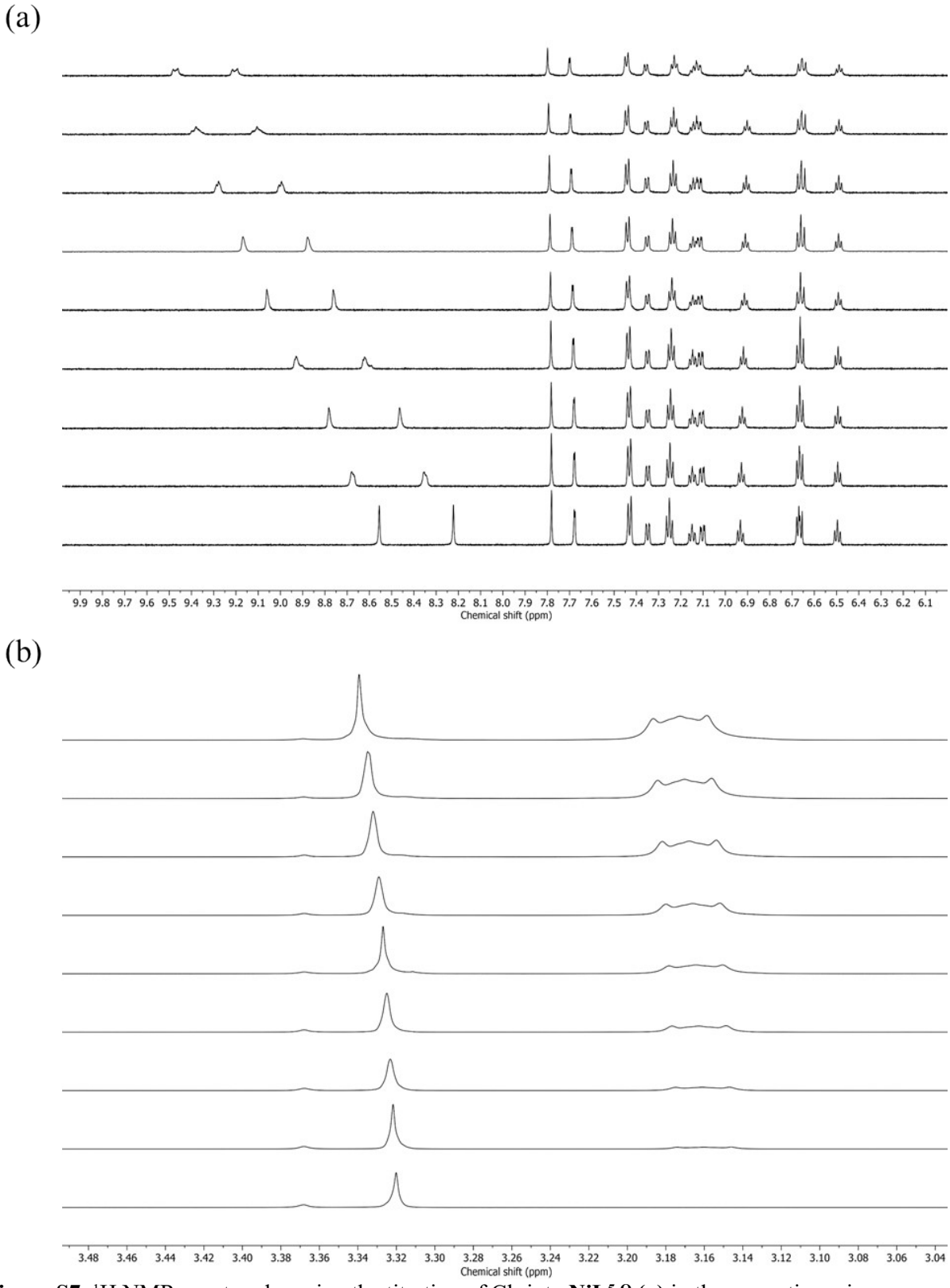

Figure S7. ^{1}H NMR spectra observing the titration of Cl^- into **NiL$^{5\text{-}O}$ (a)** in the aromatic region, where N_a–H starts from 8.55 ppm and N_b–H starts from 8.22 ppm. **(b)** following the water signal beginning at 3.32 ppm. From the bottom up: 0, 0.8, 1.6, 3, 5, 7, 10, 14, 20 mole equivalents of Cl^- titrated.

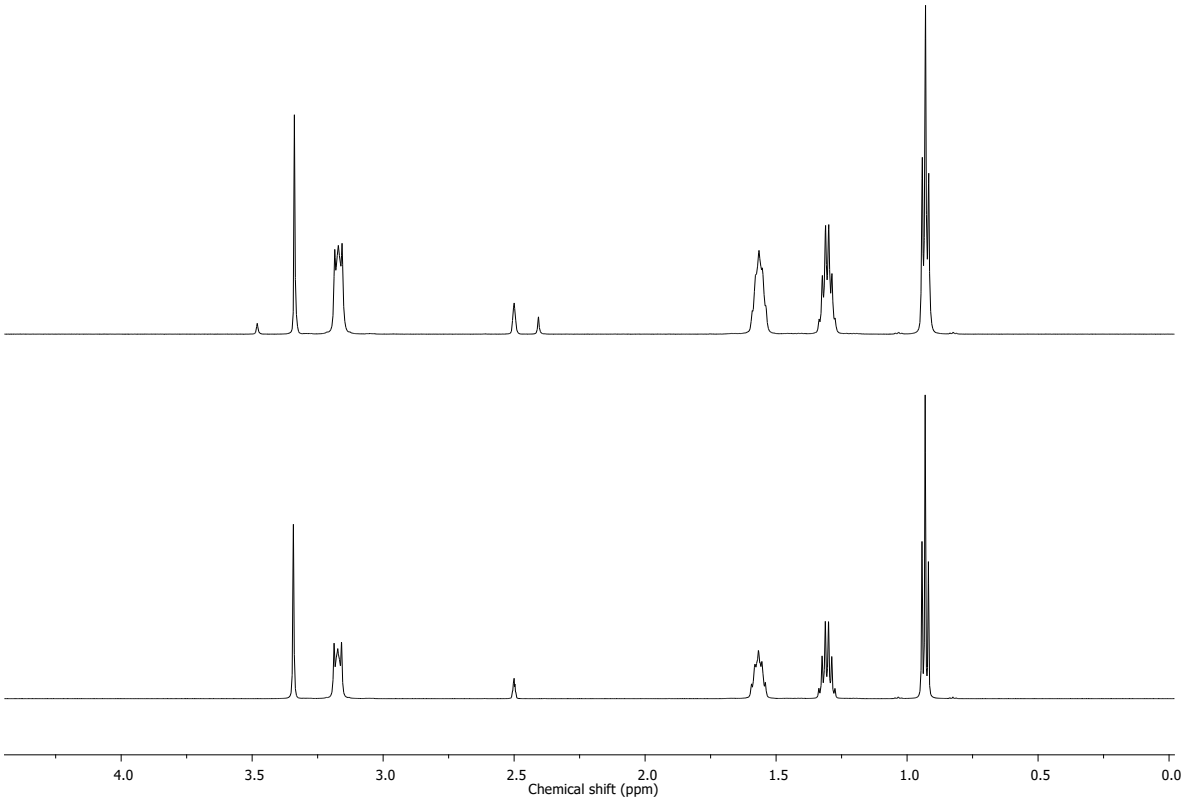

Figure S8. ^{1}H NMR spectra observing the addition of 250 µL TBACl into **NiL$^{3,3'\text{-O}}$** (500 µL; top) and plain DMSO-d_6 (500 µL; bottom).

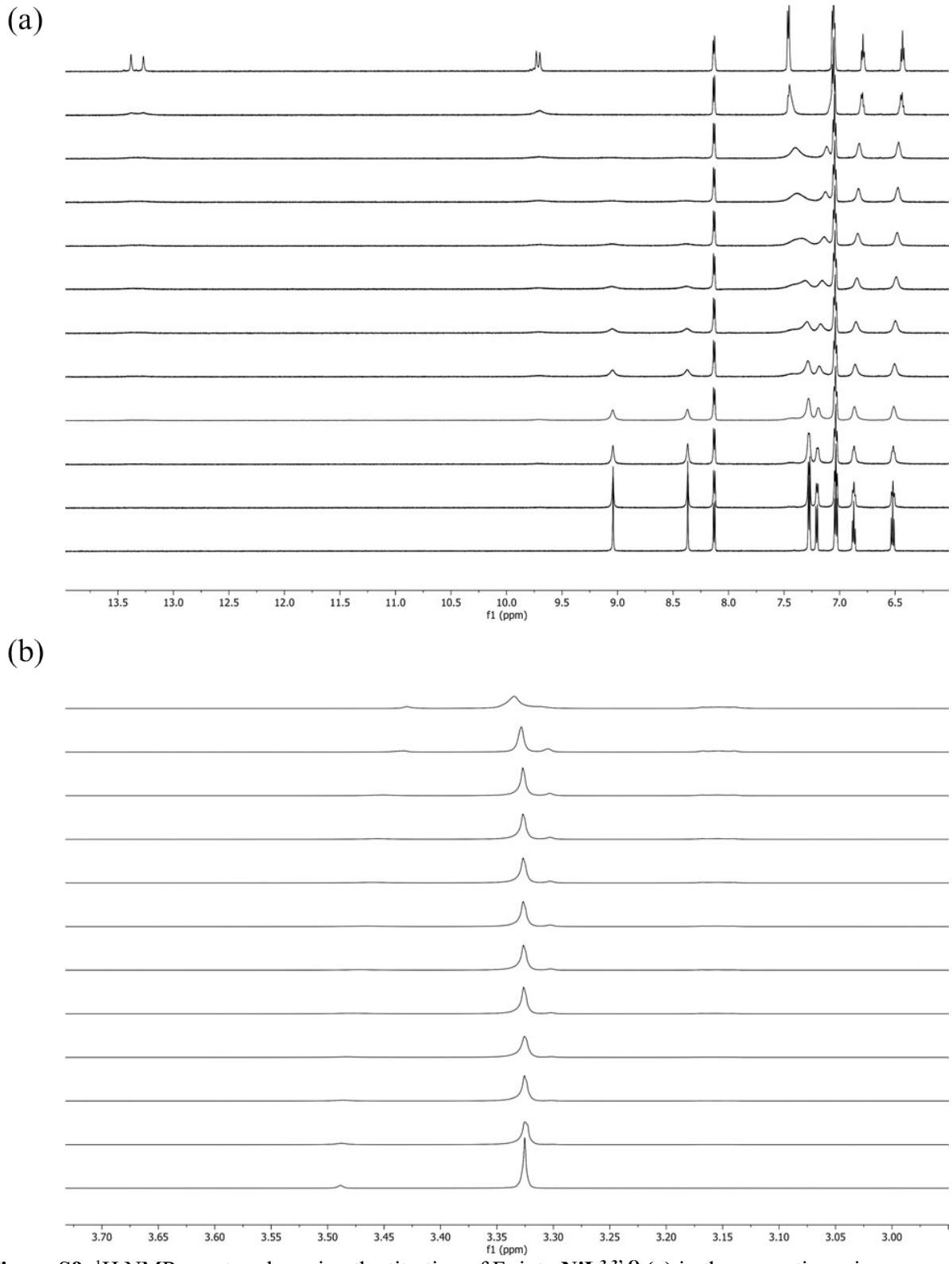

Figure S9. ^{1}H NMR spectra observing the titration of F^- into **NiL$^{3,3'\text{-}O}$ (a)** in the aromatic region, where N_a–H starts from 9.04 ppm and N_b–H starts from 8.37 ppm. **(b)** following the water signal beginning at 3.32 ppm. From the bottom up: 0, 0.08, 0.16, 0.24, 0.32, 0.40, 0.48, 0.56, 0.64, 0.72, 1.12, 1.52 mole equivalents of F^- titrated.

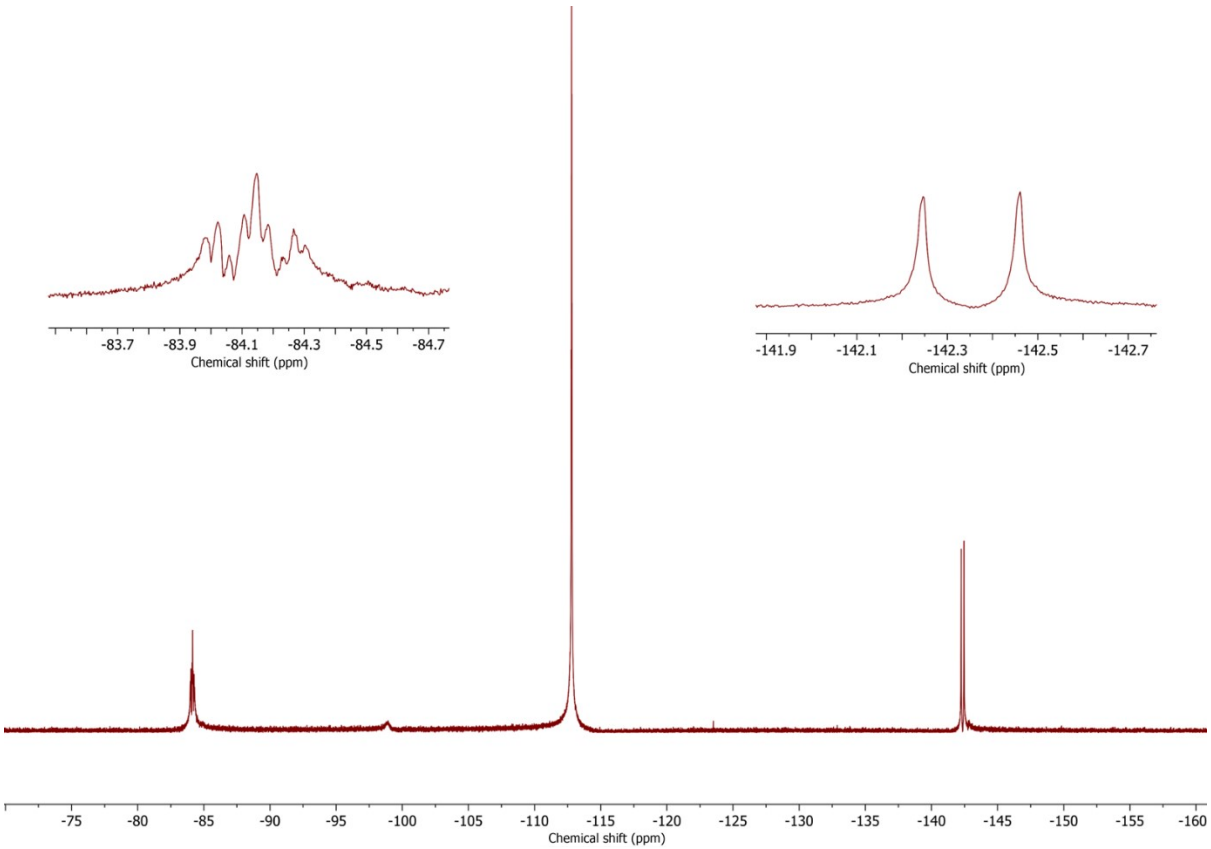

Figure S10. ^{19}F NMR spectra of **NiL$^{3,3'\text{-}O}$** with 2 mole equivalents of F^-. Inset: zoomed in spectrum of the signal at -84 ppm corresponding to the bound F^- (left), zoomed in spectrum of the signal at -142 ppm corresponding to HF_2^- (right). The signal at -112.8 ppm corresponds to 1-fluorobenzene, added as an internal standard.

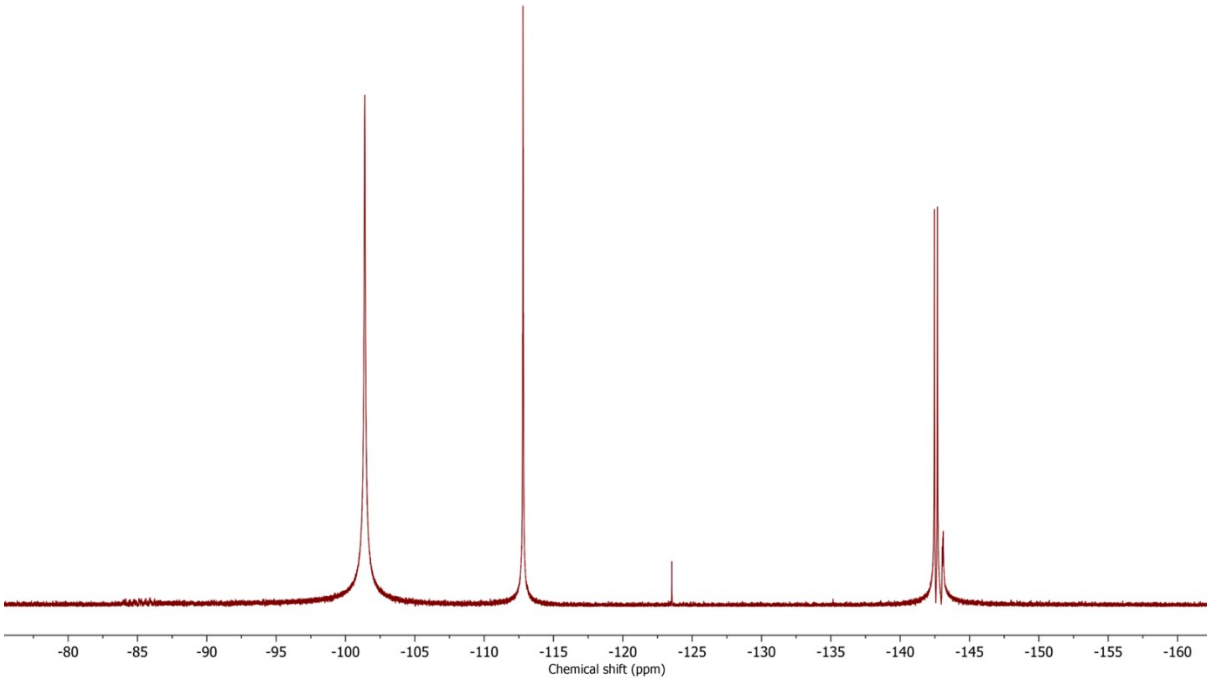

Figure S11. ^{19}F NMR spectrum of **NiL$^{3,3'\text{-}O}$** with 10 mole equivalents of F^-. The signal at -112.8 ppm corresponds to 1-fluorobenzene, added as an internal standard.

(a)

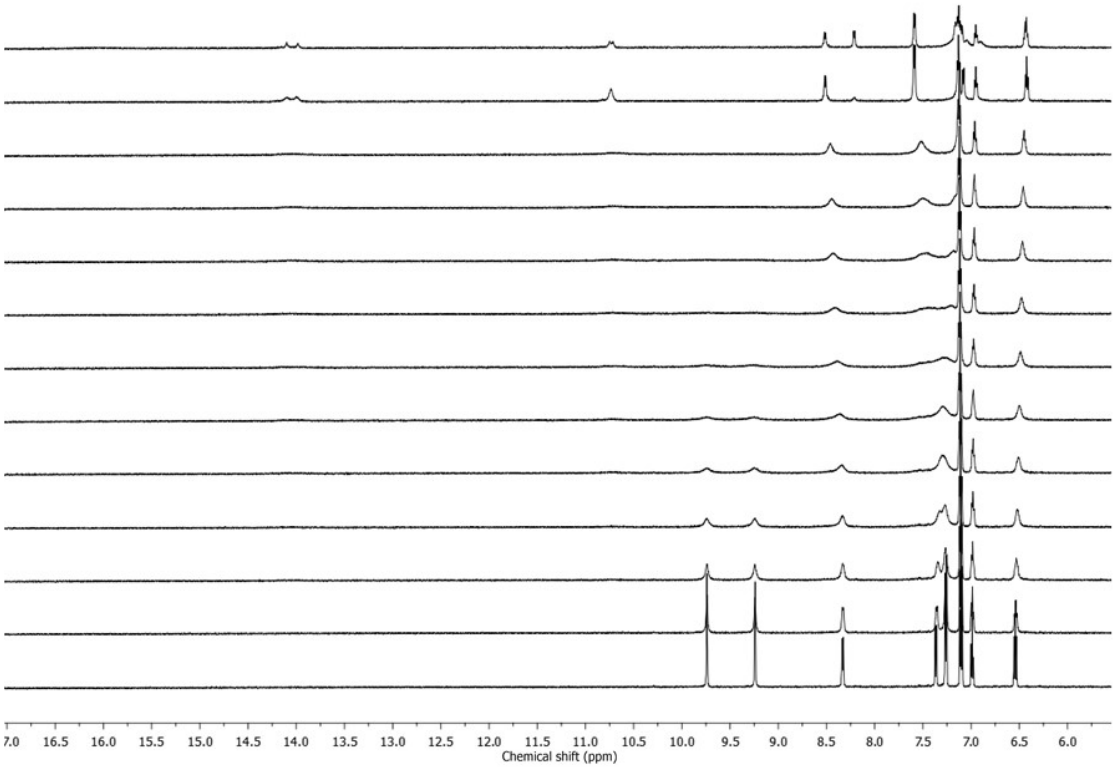

(b)

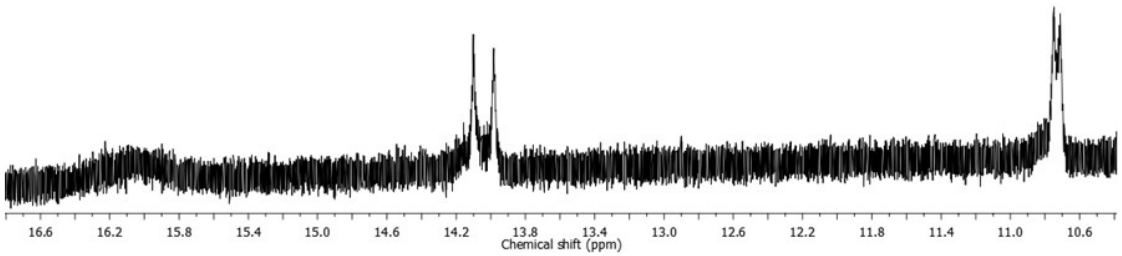

Figure S12. ^{1}H NMR spectra observing the titration of F^- into **NiL$^{3,3'\text{-}S}$ (a)** in the aromatic region, where N_a–H starts from 9.74 ppm and N_b–H starts from 9.24 ppm. From the bottom up: 0, 0.08, 0.16, 0.24, 0.32, 0.40, 0.48, 0.56, 0.64, 0.72, 0.80, 1.60, 2.40 mole equivalents of F^- titrated. **(b)** The ^{1}H NMR spectrum at 2.40 mole equivalents of F^- titrated, to emphasize the doublets formed at 14.04 ($^{1}J_{H-F}$ = 71 Hz) and 10.73 ($^{1}J_{H-F}$ = 22 Hz) ppm, and the beginning of the growth of the HF^- signal at 16.1 ppm.

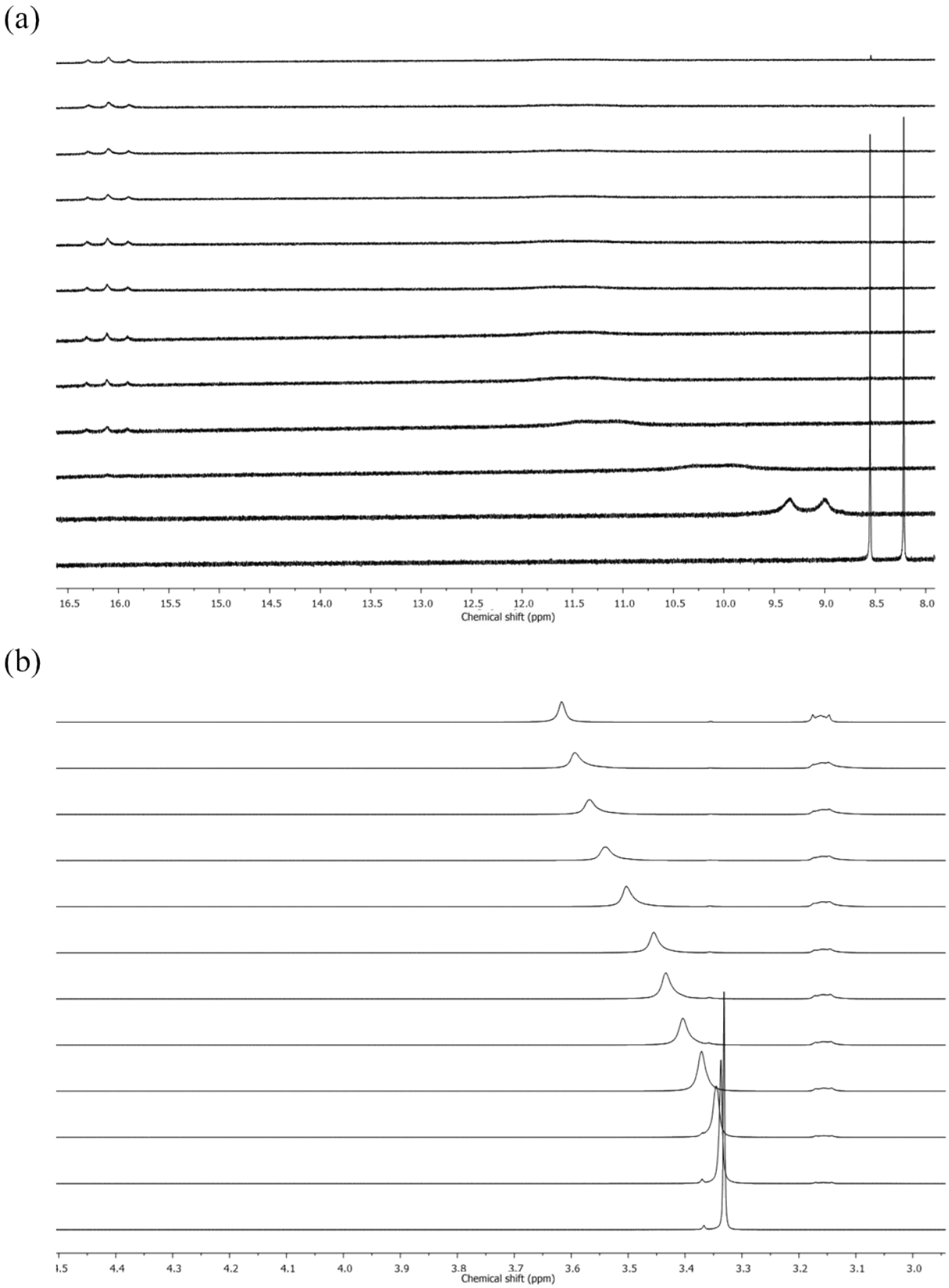

Figure S13. ^{1}H NMR spectra observing the titration of F^- into **NiL$^{5\text{-O}}$ (a)** in the aromatic region, where N_a–H starts from 8.55 ppm and N_b–H starts from 8.22 ppm. **(b)** following the water signal beginning at 3.33 ppm. From the bottom up: 0.8, 1.6, 2.4, 3.2, 4.0, 4.8, 5.6, 6.4, 7.2, 8.0, 8.8, 9.6, 10.4, 11.2, 12.0 mole equivalents of F^- titrated.

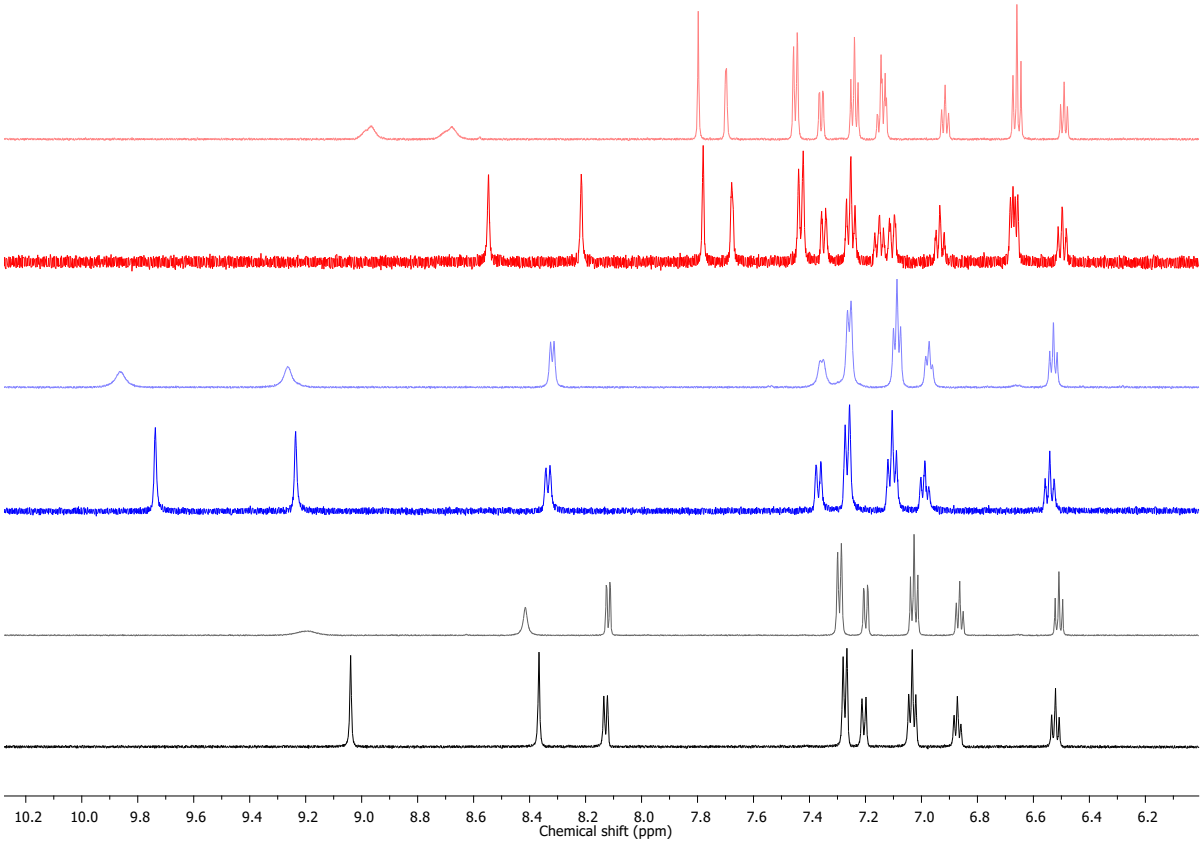

Figure S14. ^{1}H NMR spectra displaying 0 equiv (dark) and 20 equiv (light) TBABr added to **NiL$^{3,3'\text{-}O}$** (black), **NiL$^{3,3'\text{-}S}$** (blue), and **NiL$^{5\text{-}O}$** (red).

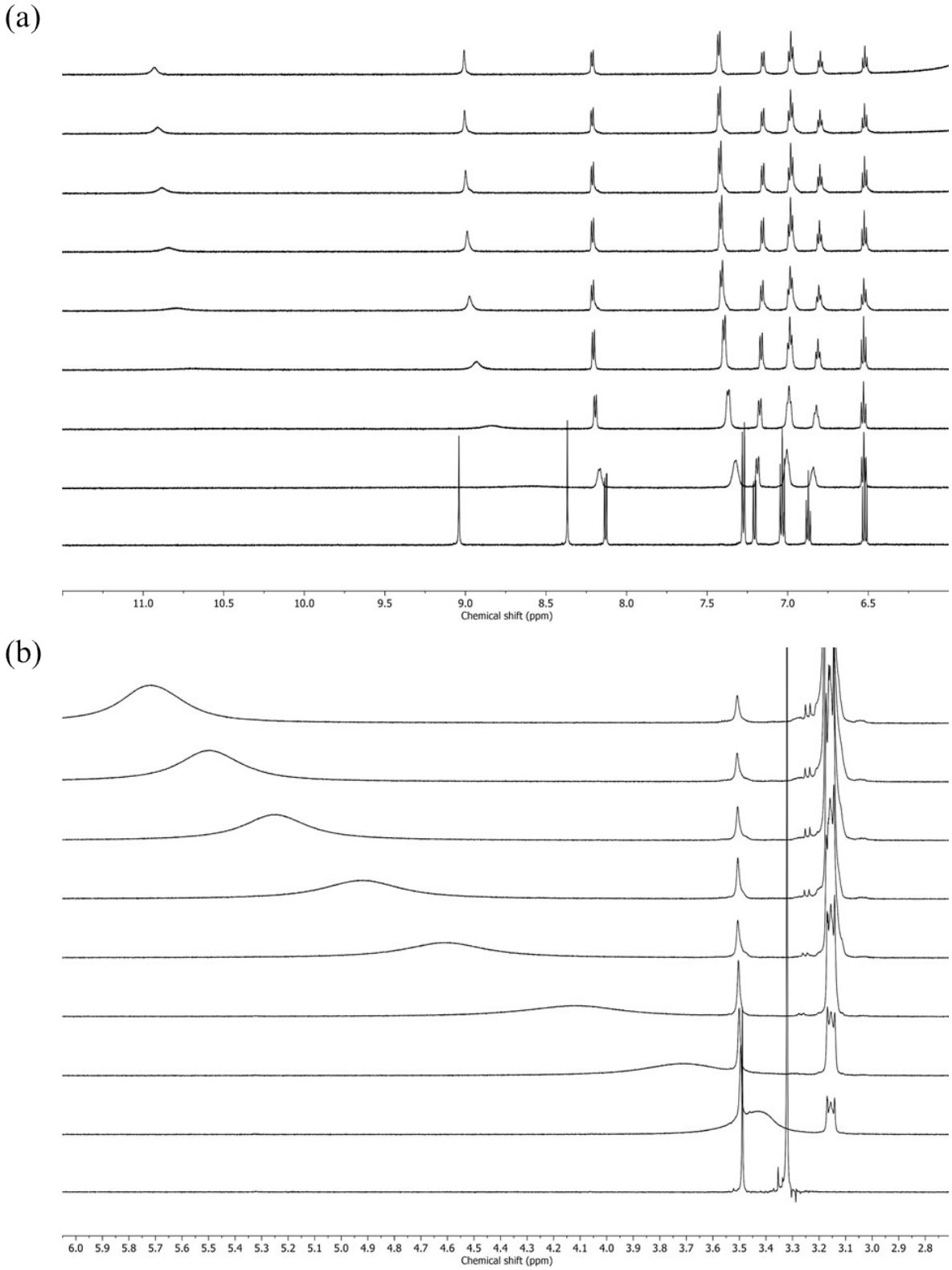

Figure S15. ^{1}H NMR spectra observing the titration of $H_2PO_4^-$ into **NiL$^{3,3'\text{-}O}$ (a)** in the aromatic region, where N_a–H starts from 9.04 ppm and N_b–H starts from 8.37 ppm. **(b)** following the water signal beginning at 3.33 ppm. From the bottom up: 0, 0.8, 1.6, 3, 5, 7, 10, 14, 20 mole equivalents of $H_2PO_4^-$ titrated.

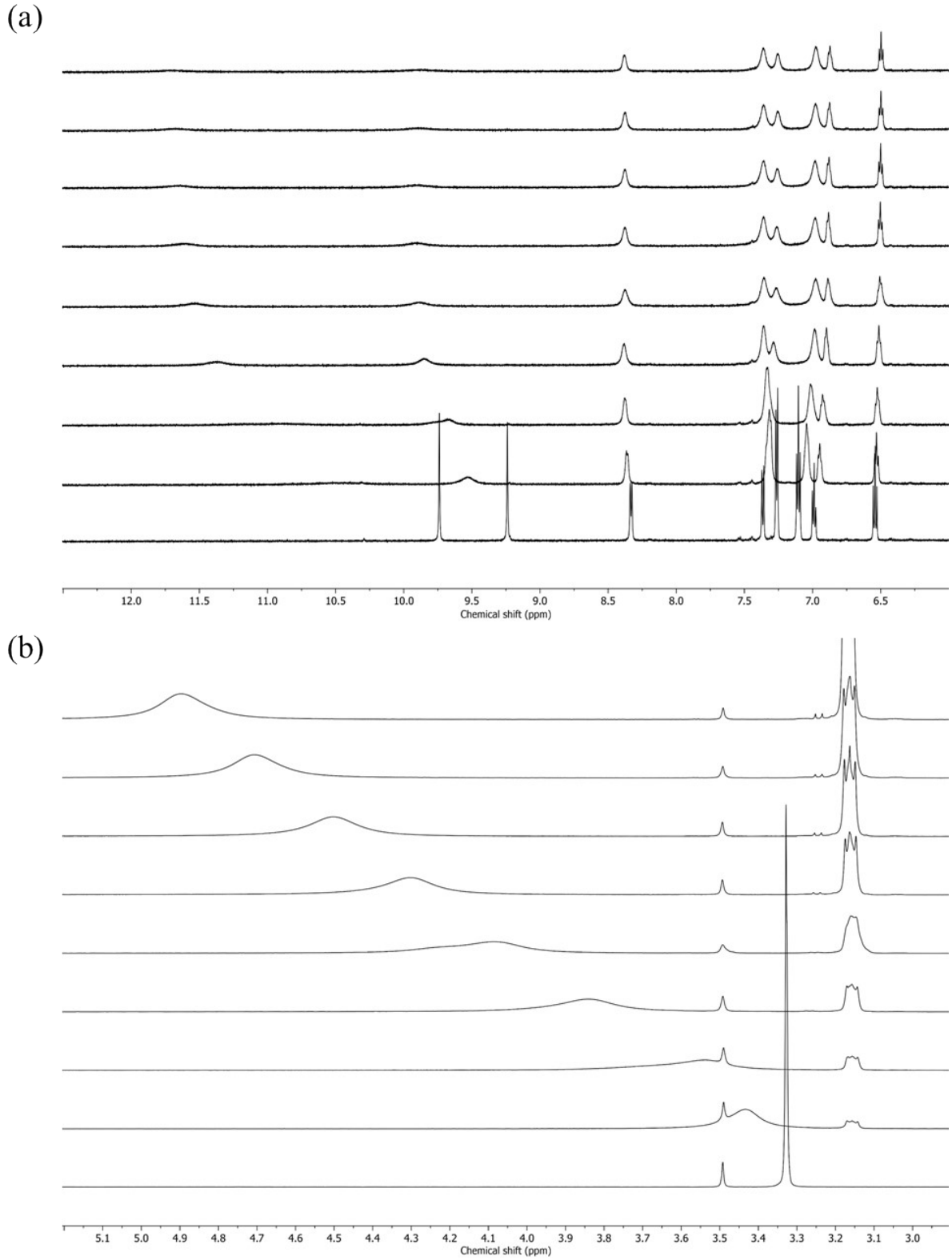

Figure S16. ^{1}H NMR spectra observing the titration of $H_2PO_4^-$ into **NiL$^{3,3'\text{-}S}$ (a)** in the aromatic region, where N_a–H starts from 9.74 ppm and N_b–H starts from 9.24 ppm. **(b)** following the water signal beginning at 3.32 ppm. From the bottom up: 0, 0.8, 1.6, 3, 5, 7, 10, 14, 20 mole equivalents of $H_2PO_4^-$ titrated.

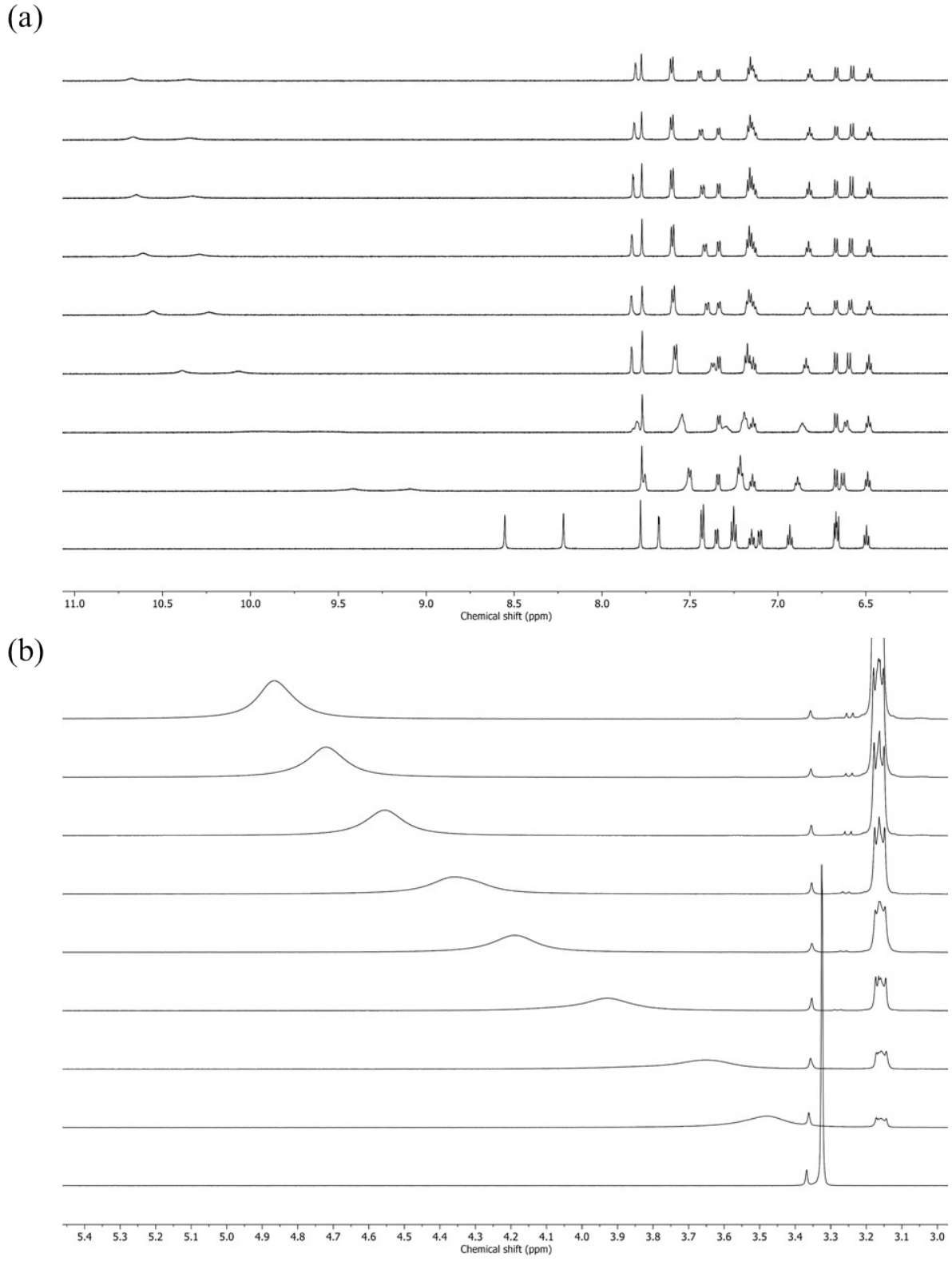

Figure S17. ^{1}H NMR spectra observing the titration of $H_2PO_4^-$ into **NiL$^{5\text{-}O}$ (a)** in the aromatic region, where N_a–H starts from 8.55 ppm and N_b–H starts from 8.22 ppm. **(b)** following the water signal beginning at 3.32 ppm. From the bottom up: 0, 0.8, 1.6, 3, 5, 7, 10, 14, 20 mole equivalents of $H_2PO_4^-$ titrated.

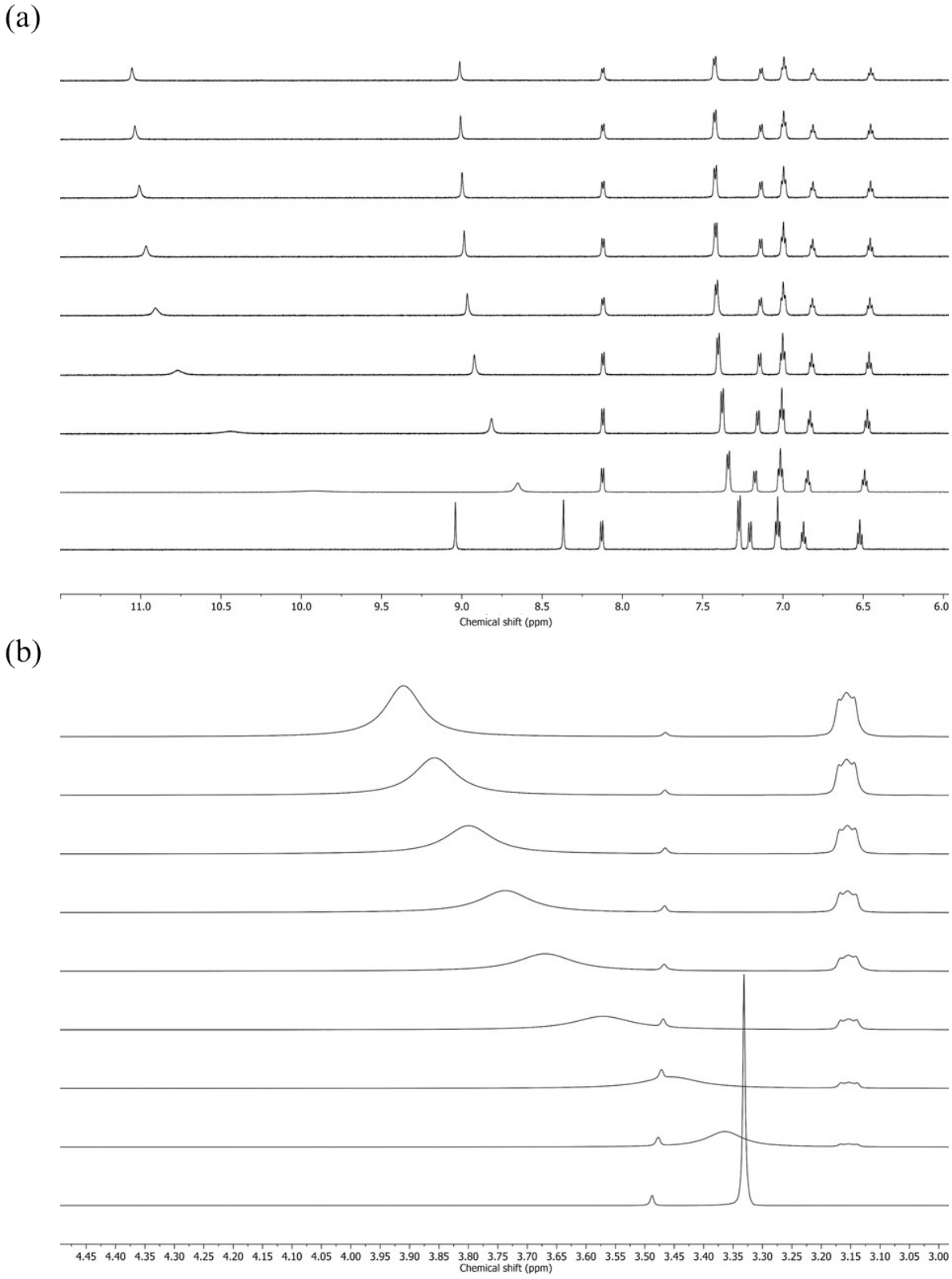

Figure S18. ^{1}H NMR spectra observing the titration of CH_3COO^- into **NiL$^{3,3'\text{-}O}$ (a)** in the aromatic region, where N_a–H starts from 9.04 ppm and N_b–H starts from 8.37 ppm. **(b)** following the water signal beginning at 3.32 ppm. From the bottom up: 0, 0.8, 1.6, 3, 5, 7, 10, 14, 20 mole equivalents of CH_3COO^- titrated.

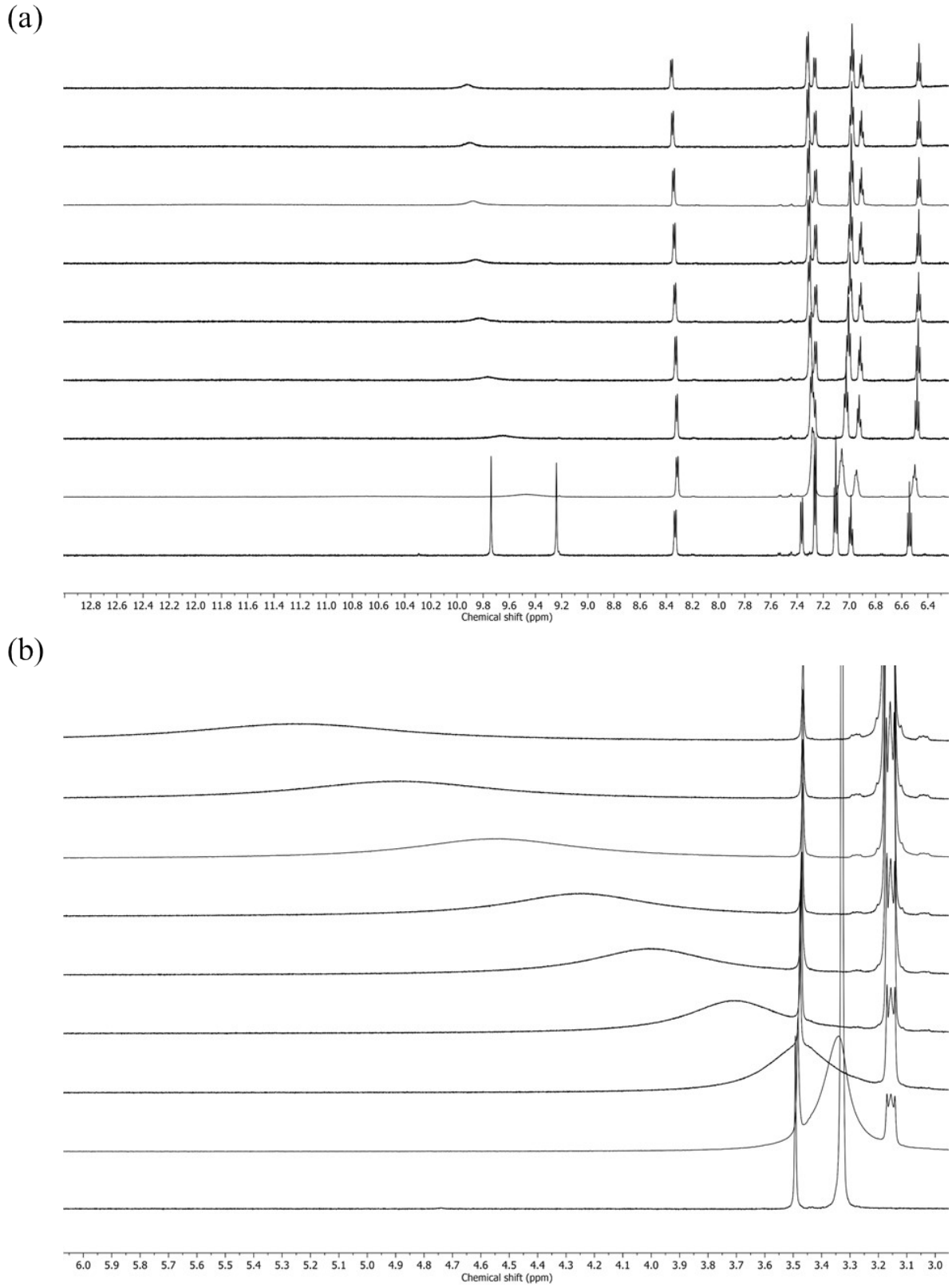

Figure S19. ^{1}H NMR spectra observing the titration of CH_3COO^- into **NiL$^{3,3'\text{-}S}$ (a)** in the aromatic region, where N_a–H starts from 9.74 ppm and N_b–H starts from 9.24 ppm. **(b)** following the water signal beginning at 3.32 ppm. From the bottom up: 0, 0.8, 1.6, 3, 5, 7, 10, 14, 20 mole equivalents of CH_3COO^- titrated.

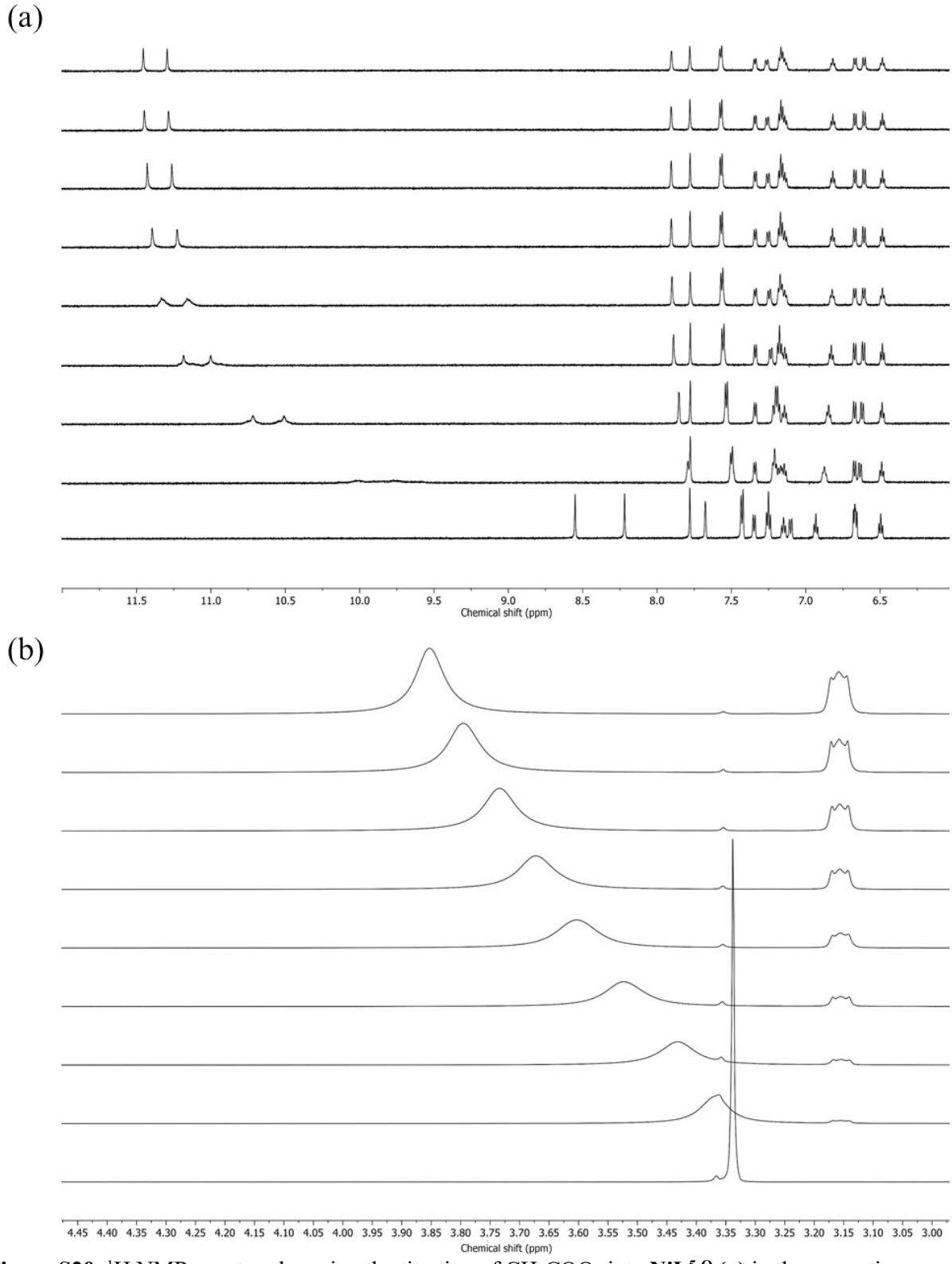

Figure S20. ^{1}H NMR spectra observing the titration of CH_3COO^- into **NiL$^{5\text{-}O}$** **(a)** in the aromatic region, where N_a–H starts from 8.55 ppm and N_b–H starts from 8.22 ppm. **(b)** following the water signal beginning at 3.32 ppm. From the bottom up: 0, 0.8, 1.6, 3, 5, 7, 10, 14, 20 mole equivalents of CH_3COO^- titrated.

Job Plots

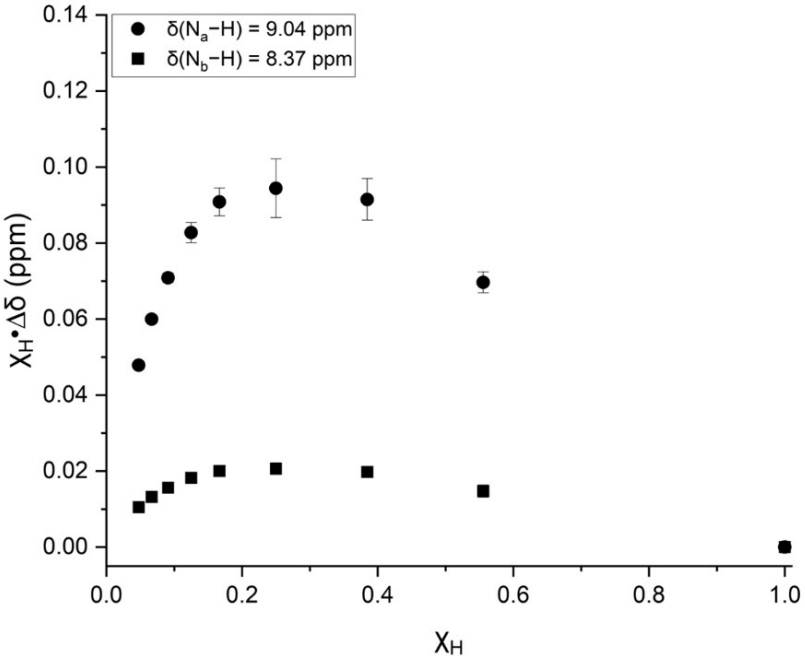

Figure S21. Job Plot of the titration of Cl^- into **NiL$^{3,3'\text{-O}}$** following the downfield shift of the urea protons in the ^{1}H NMR spectra.

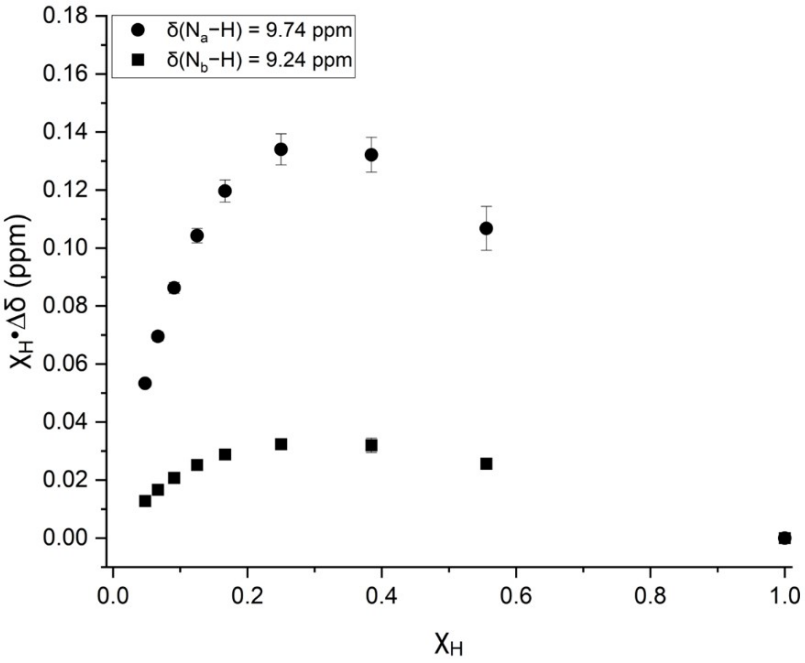

Figure S22. Job Plot of the titration of Cl^- into **NiL$^{3,3'\text{-S}}$** following the downfield shift of the thiourea protons in the ^{1}H NMR spectra.

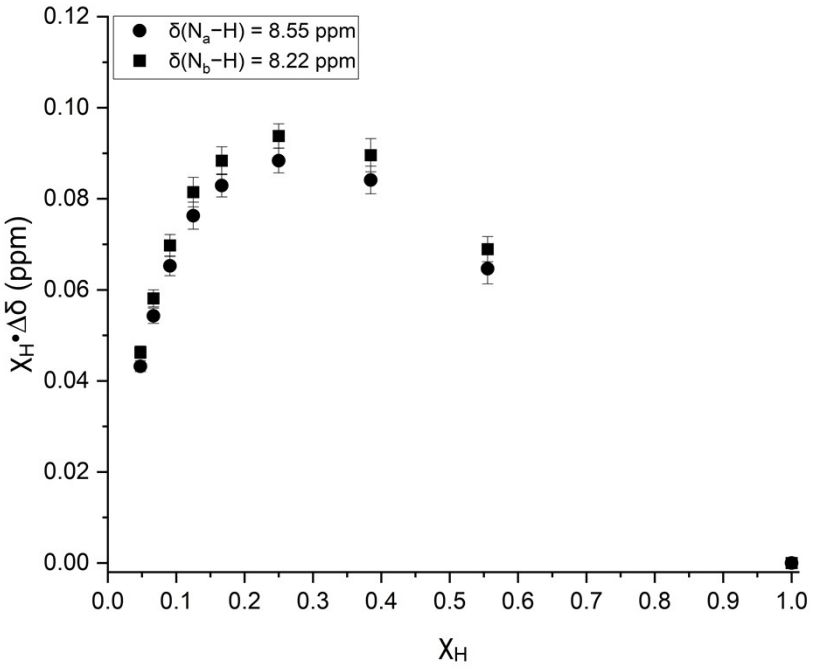

Figure S23. Job Plot of the titration of Cl^- into **NiL$^{5\text{-}O}$** following the downfield shift of the urea protons in the ^{1}H NMR spectra.

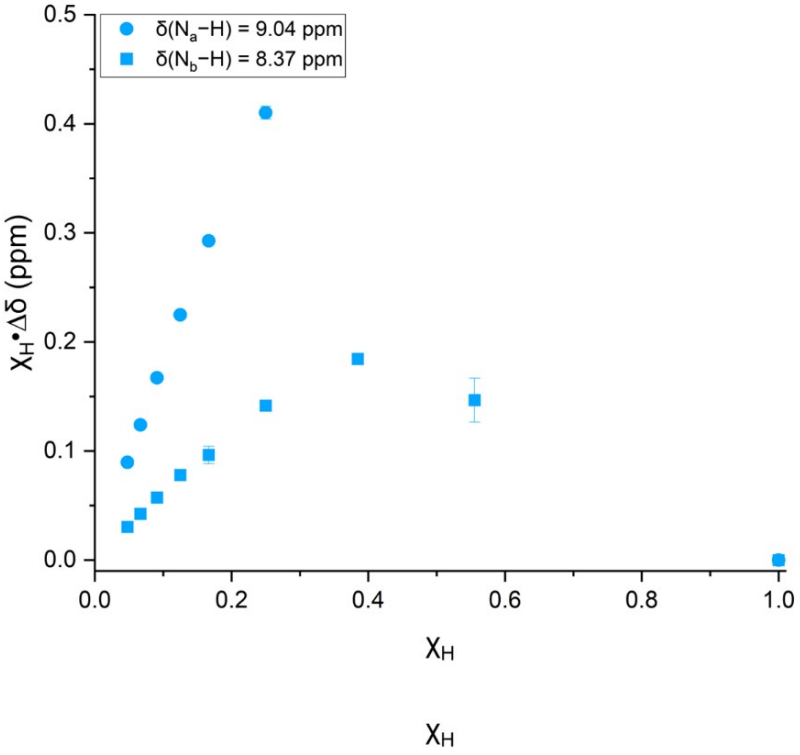

Figure S24. Job Plot of the titration of $H_2PO_4^-$ into **NiL$^{3,3'\text{-O}}$** following the downfield shift of the urea protons in the ^{1}H NMR spectra.

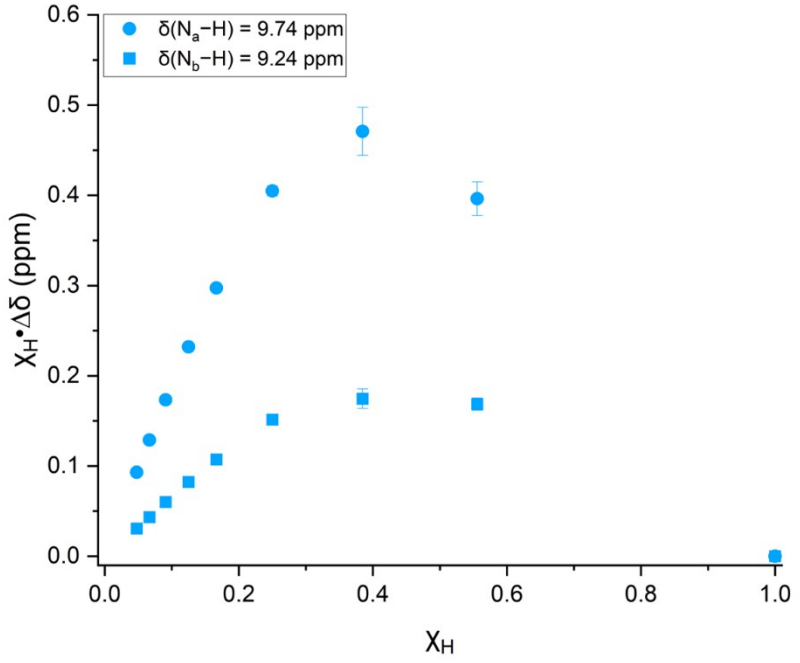

Figure S25. Job Plot of the titration of $H_2PO_4^-$ into **NiL$^{3,3'\text{-S}}$** following the downfield shift of the thiourea protons in the ^{1}H NMR spectra.

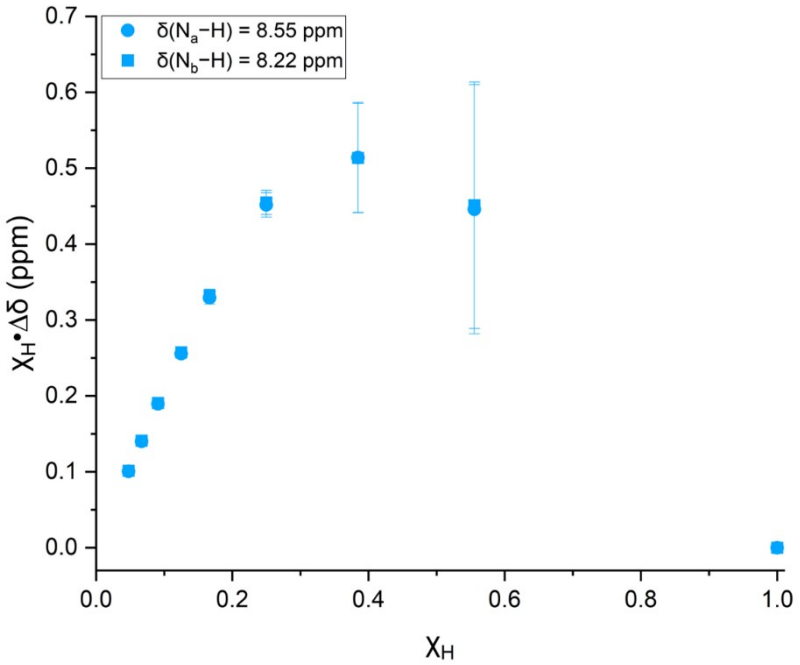

Figure S26. Job Plot of the titration of $H_2PO_4^-$ into **NiL$^{5\text{-}O}$** following the downfield shift of the urea protons in the ^{1}H NMR spectra.

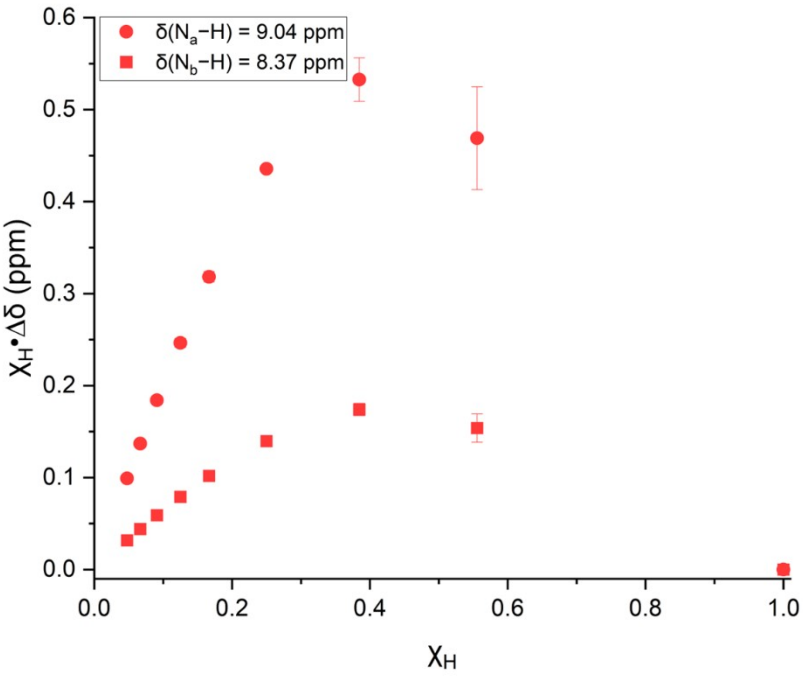

Figure S27. Job Plot of the titration of CH_3COO^- into **NiL$^{3,3'\text{-}O}$** following the downfield shift of the urea protons in the ^{1}H NMR spectra.

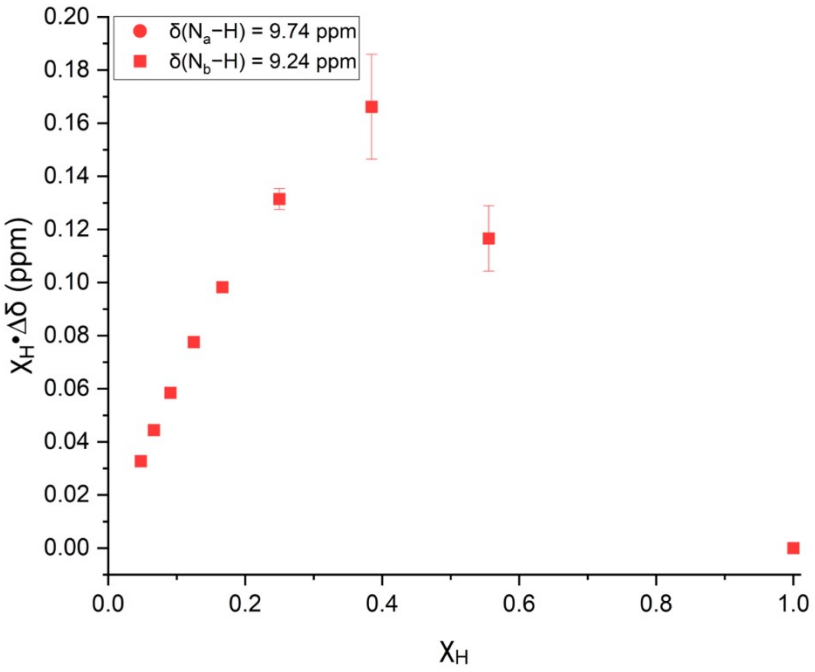

Figure S28. Job Plot of the titration of CH_3COO^- into **NiL$^{3,3'\text{-}S}$** following the downfield shift of the thiourea protons in the ^{1}H NMR spectra.

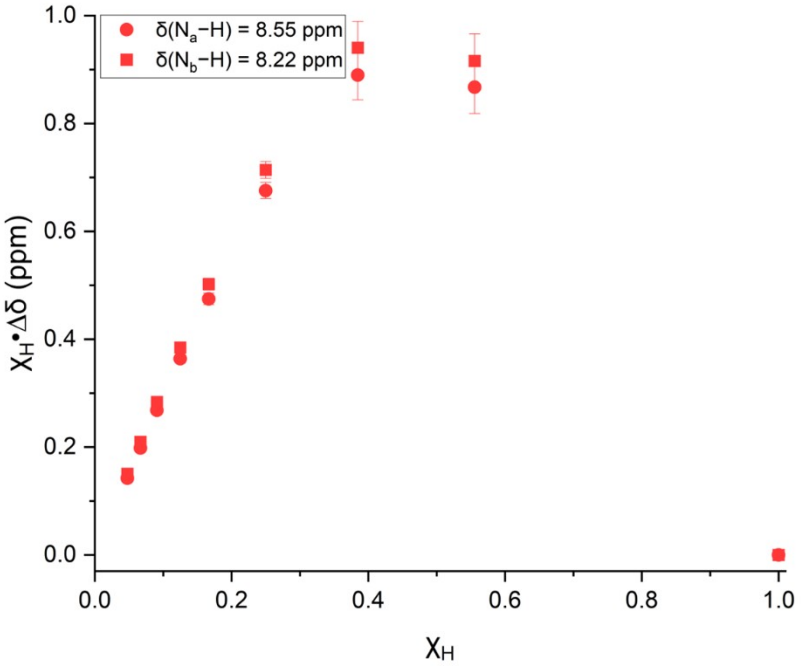

Figure S29. Job Plot of the titration of CH_3COO^- into **NiL$^{3,3'\text{-}S}$** following the downfield shift of the thiourea protons in the ^{1}H NMR spectra.

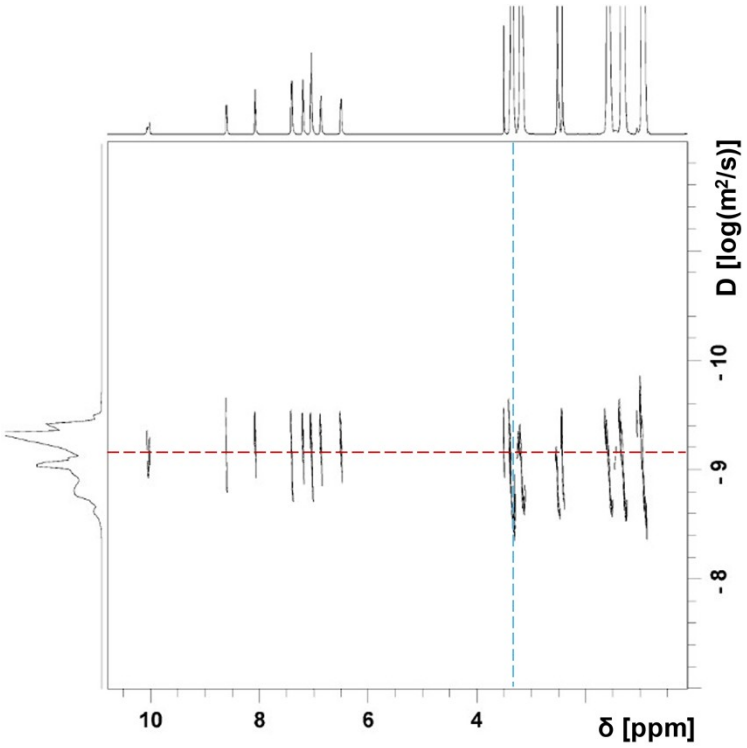

Diffusion Ordered Spectroscopy (DOSY) Plots

Figure S30. DOSY spectrum of **NiL$^{3,3'\text{-O}}$** in the presence of 20 mole equivalents of Cl^-. The dashed red line indicates the diffusion signal for the nickel(II) complex and the dashed blue line traces the diffusion signal for H_2O.

Figure S31. DOSY spectrum of **NiL$^{3,3'\text{-S}}$** in the presence of 20 mole equivalents of Cl^-. The dashed red line indicates the diffusion signal for the nickel(II) complex and the dashed blue line traces the diffusion signal for H_2O.

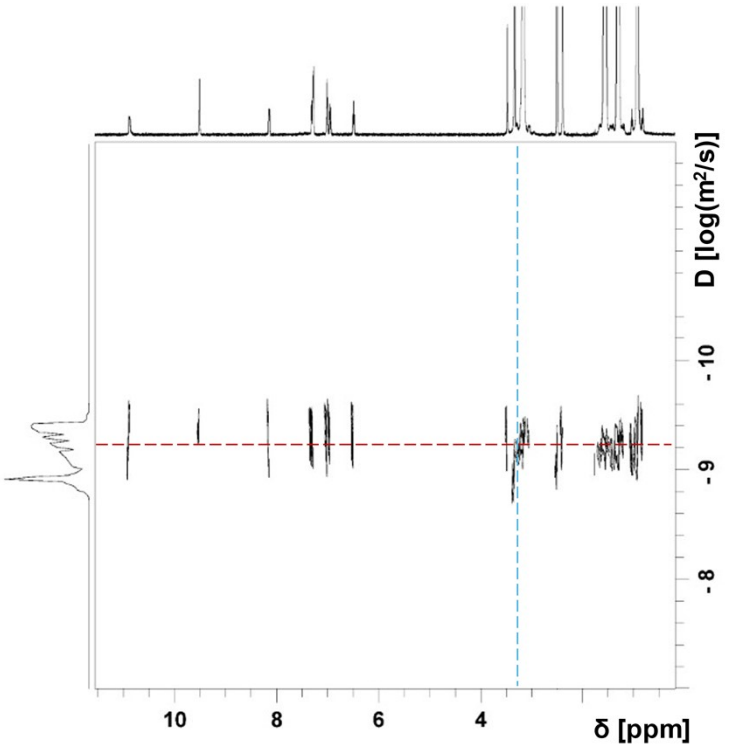

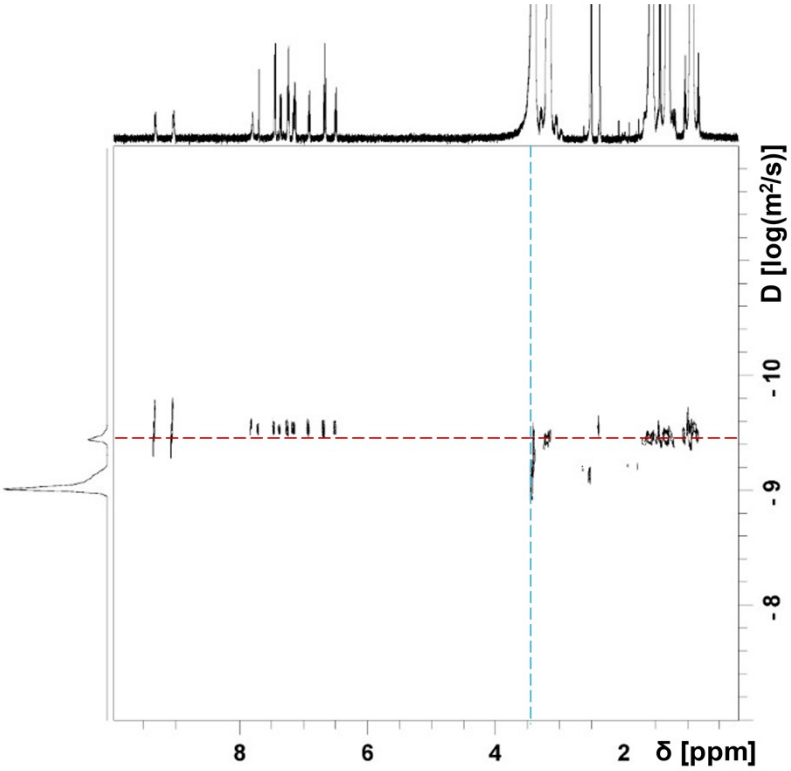

Figure S32. DOSY spectrum of **NiL$^{5\text{-}O}$** in the presence of 20 mole equivalents of Cl^-. The dashed red line indicates the diffusion signal for the nickel(II) complex and the dashed blue line traces the

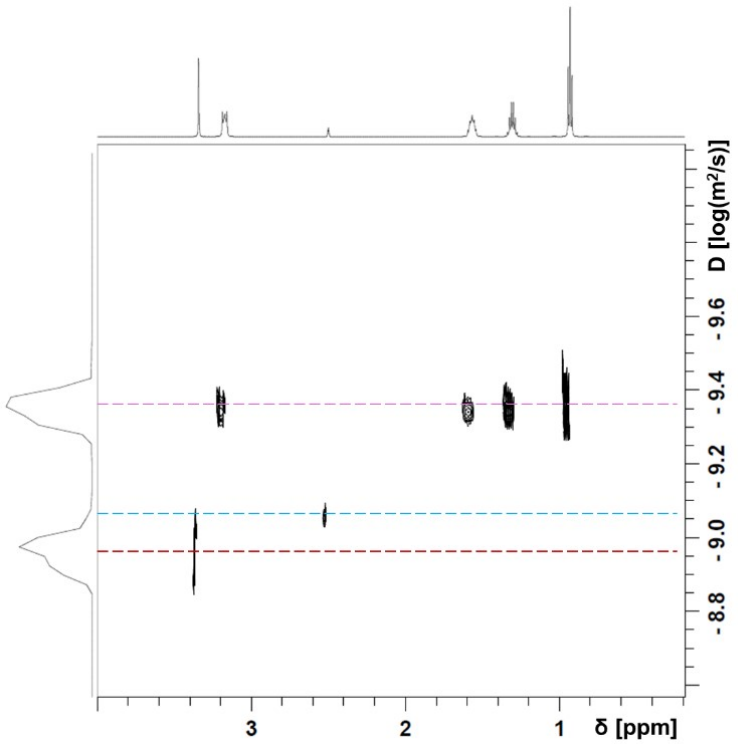

diffusion signal for H_2O.

Figure S33. DOSY spectrum of TBACl (250 µL) in DMSO-d_6 (500 µL). The diffusion signals of H_2O (red), DMSO-d_6 (blue), and the tetrabutylammonium cation (pink) are indicated by dashed lines.

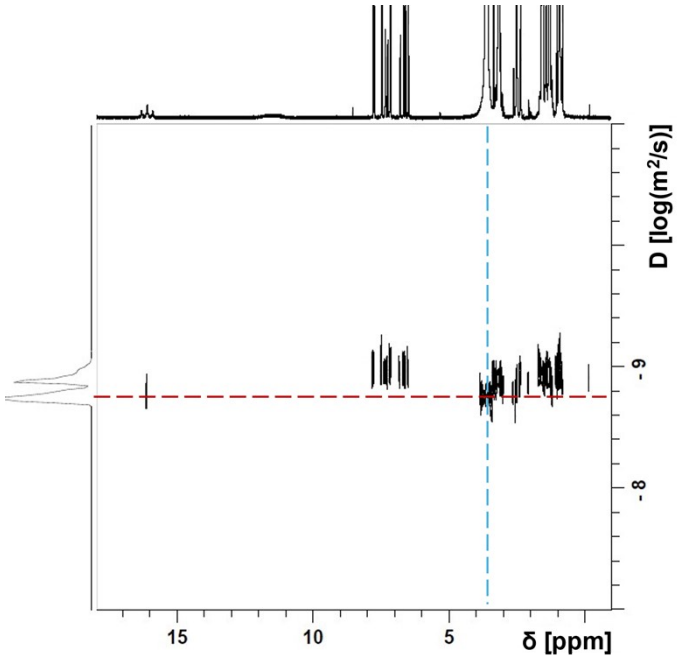

Figure S34. DOSY spectrum of **NiL$^{5\text{-}O}$** in the presence of 12 mole equivalents of F^-. The dashed red line indicates the diffusion signal for HF_2^- and the dashed blue line traces the diffusion signal for H_2O.

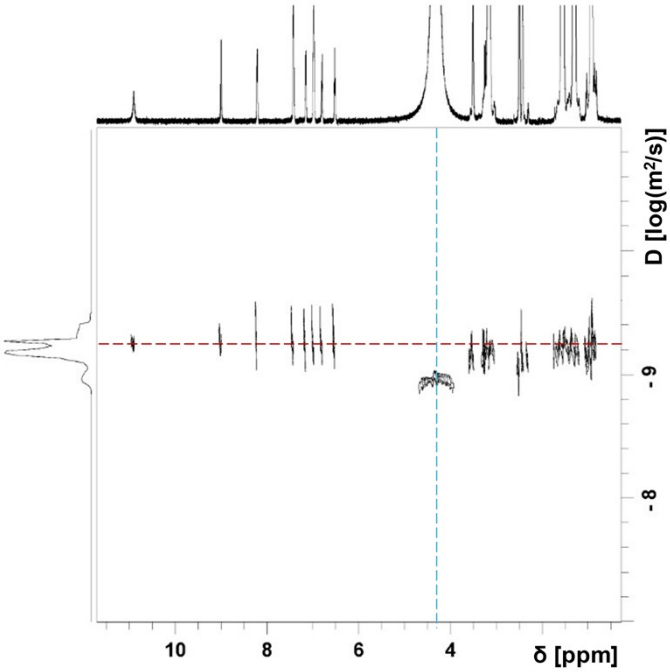

Figure S35. DOSY spectrum of **NiL$^{3,3'\text{-O}}$** in the presence of 20 mole equivalents of $H_2PO_4^-$. The dashed red line indicates the diffusion signal for the nickel(II) complex and the dashed blue line traces the diffusion signal for H_2O.

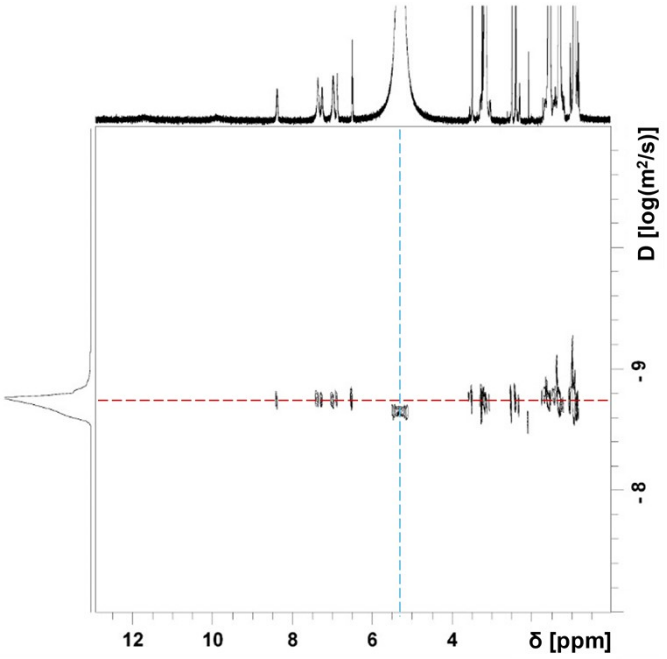

Figure S36. DOSY spectrum of **NiL$^{3,3'\text{-S}}$** in the presence of 20 mole equivalents of $H_2PO_4^-$. The dashed red line indicates the diffusion signal for the nickel(II) complex and the dashed blue line traces the diffusion signal for H_2O.

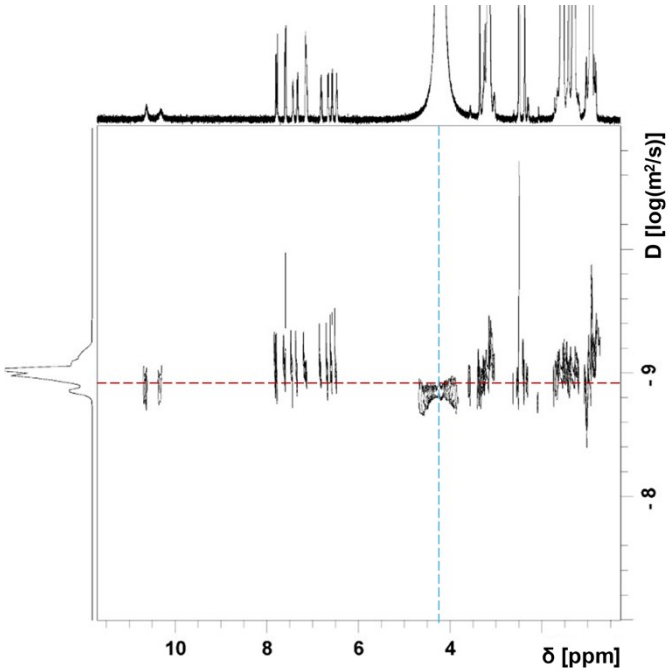

Figure S37. DOSY spectrum of **NiL$^{5\text{-}O}$** in the presence of 20 mole equivalents of $H_2PO_4^-$. The dashed red line indicates the diffusion signal for the nickel(II) complex and the dashed blue line traces the diffusion signal for H_2O.

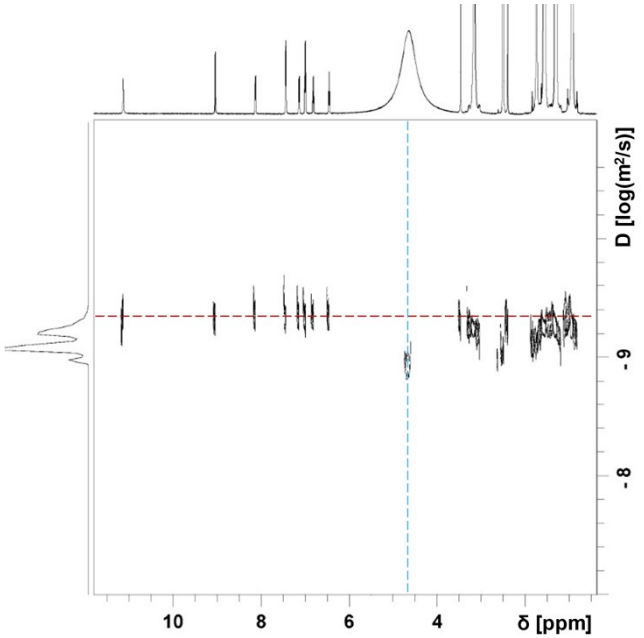

Figure S38. DOSY spectrum of **NiL$^{3,3'\text{-}O}$** in the presence of 20 mole equivalents of CH_3COO^-. The dashed red line indicates the diffusion signal for the nickel(II) complex and the dashed blue line traces the diffusion signal for H_2O.

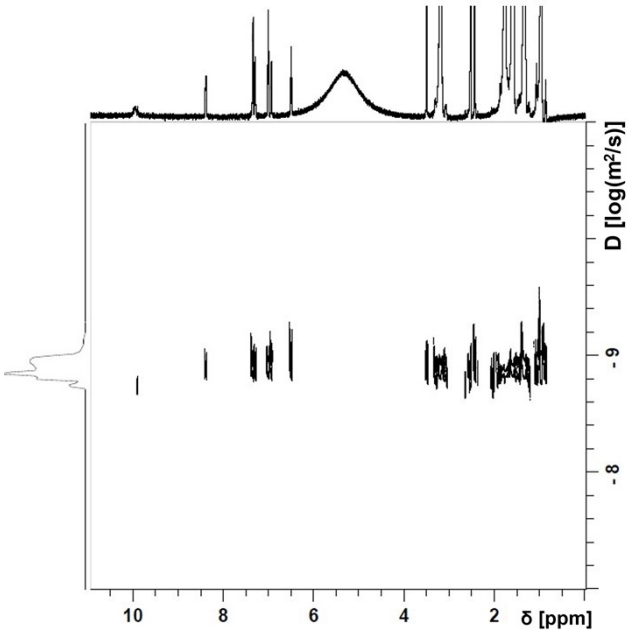

Figure S39. DOSY spectrum of **NiL$^{3,3'\text{-S}}$** in the presence of 20 mole equivalents of CH_3COO^-.

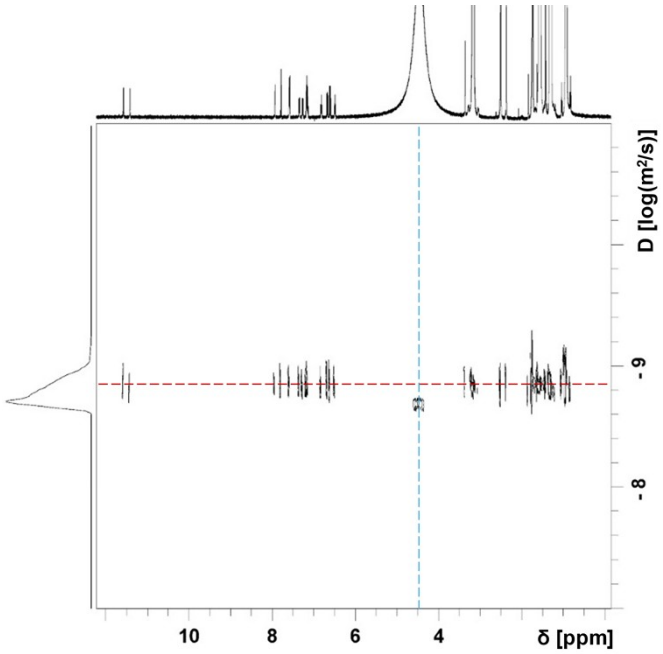

Figure S40. DOSY spectrum of **NiL$^{5\text{-O}}$** in the presence of 20 mole equivalents of CH_3COO^-. The dashed red line indicates the diffusion signal for the nickel(II) complex and the dashed blue line traces the diffusion signal for H_2O.

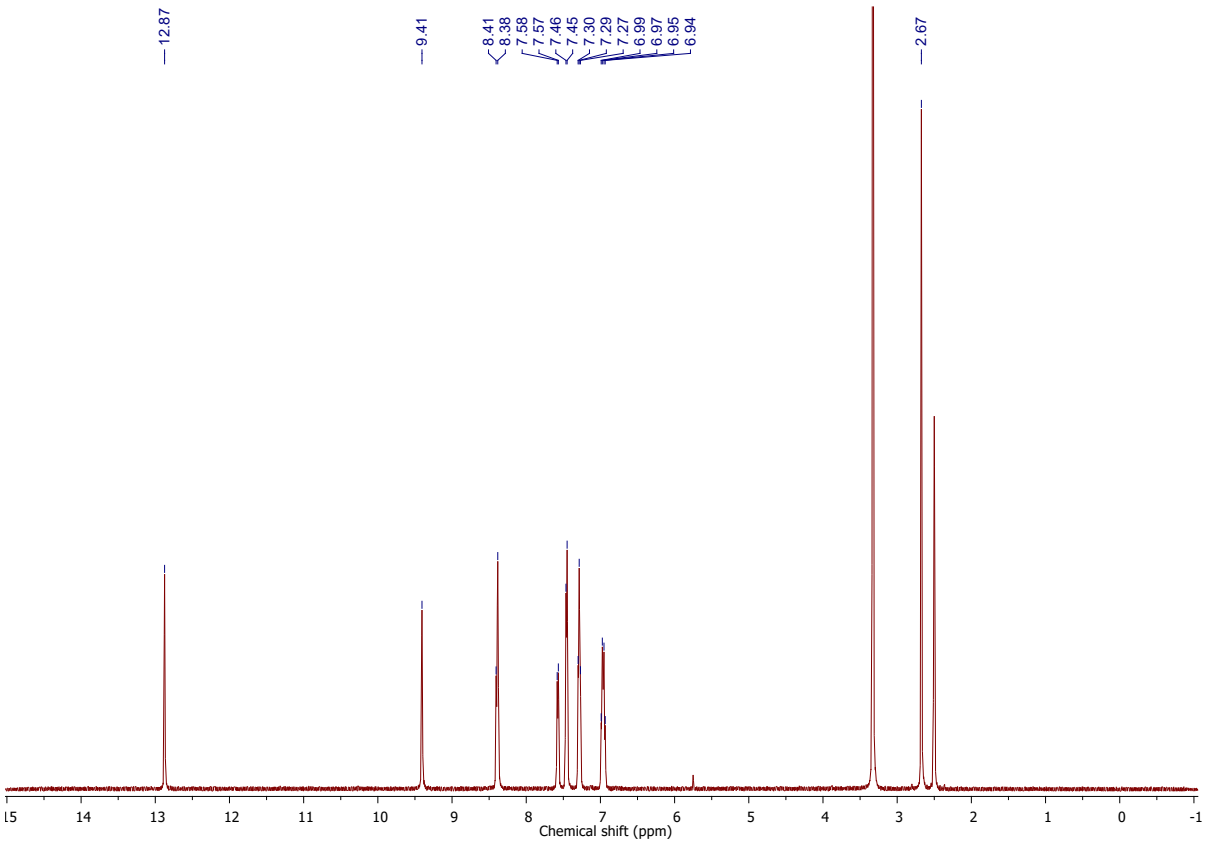

Copies of NMR Spectra

Figure S41. ^{1}H NMR (^{1}H = 498.557 MHz, 298.1 K, DMSO-d_6) spectrum of **HL$^{3\text{-O}}$**.

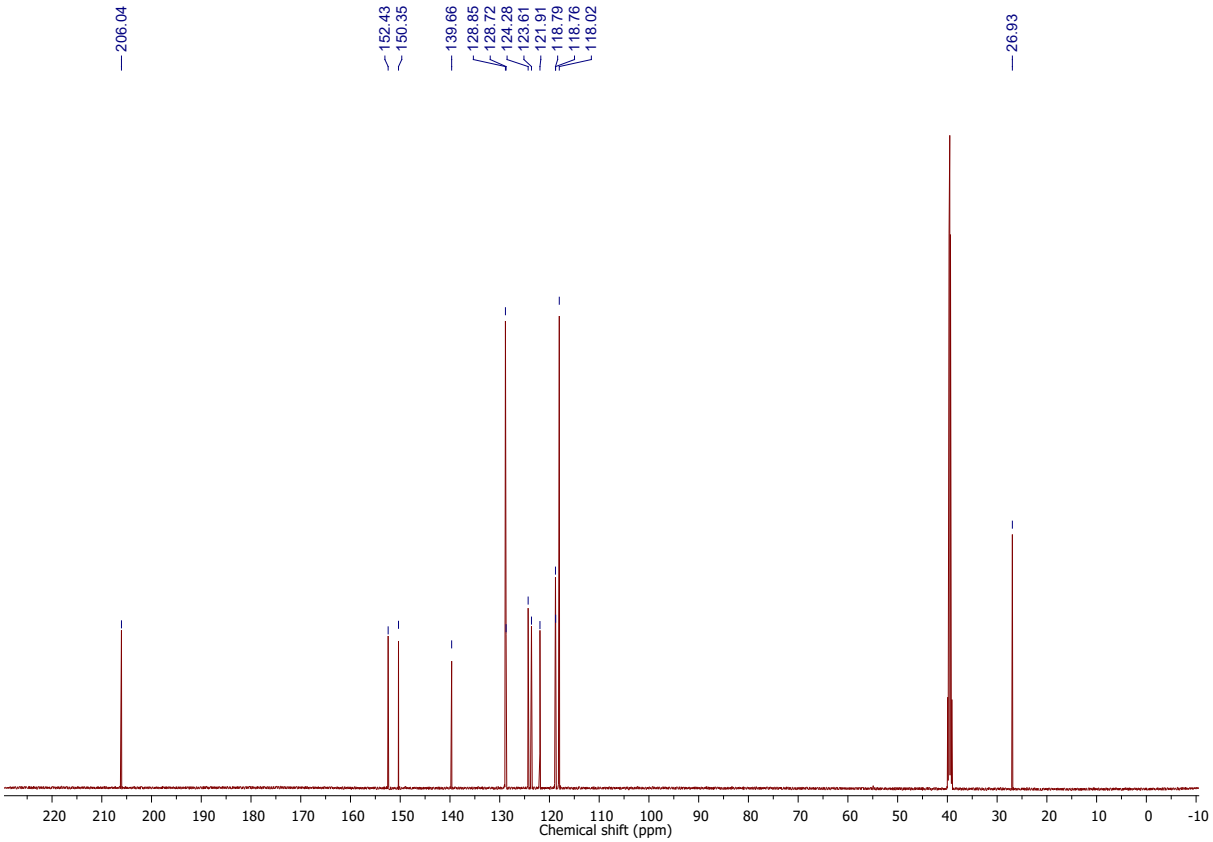

Figure S42. ^{13}C NMR ($^{13}C\{^{1}H\}$ = 150.919 MHz, 298.0 K, DMSO-d_6) spectrum of $\mathbf{HL^{3\text{-}O}}$.

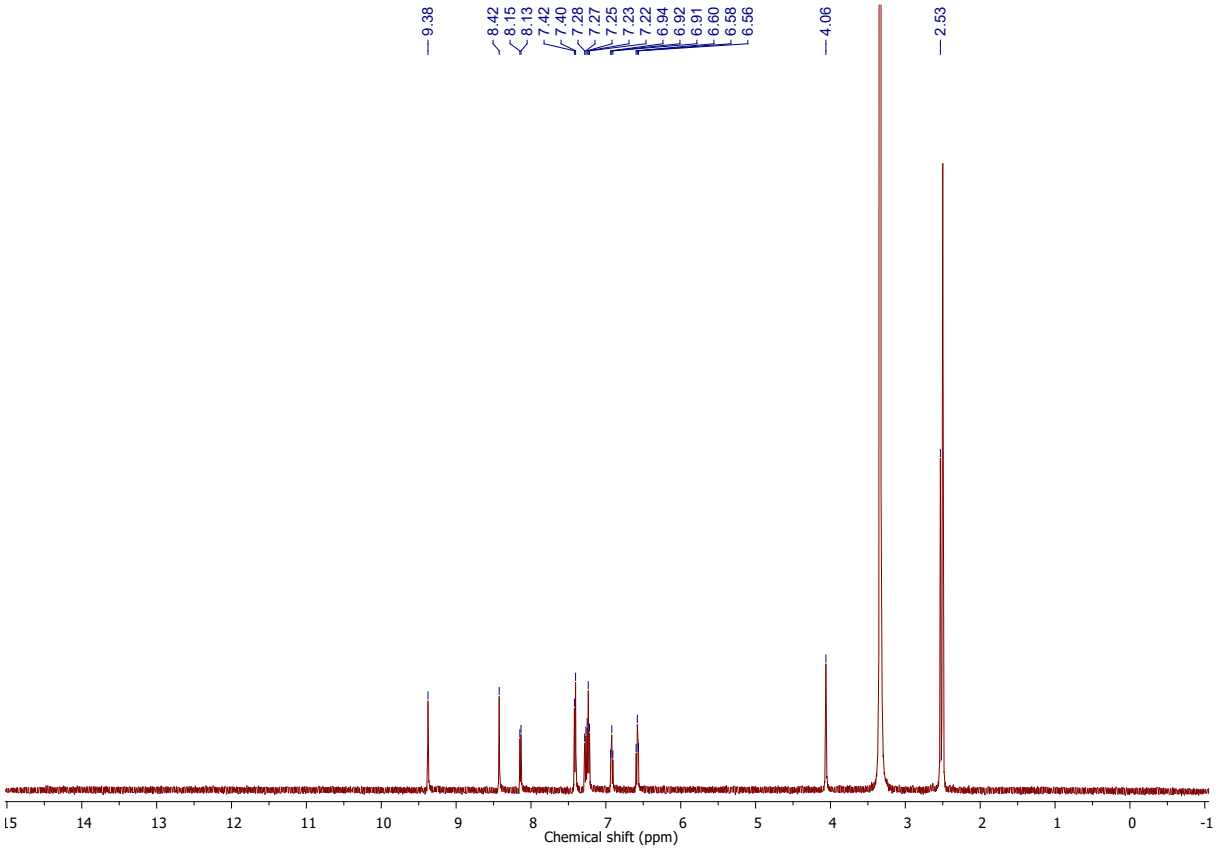

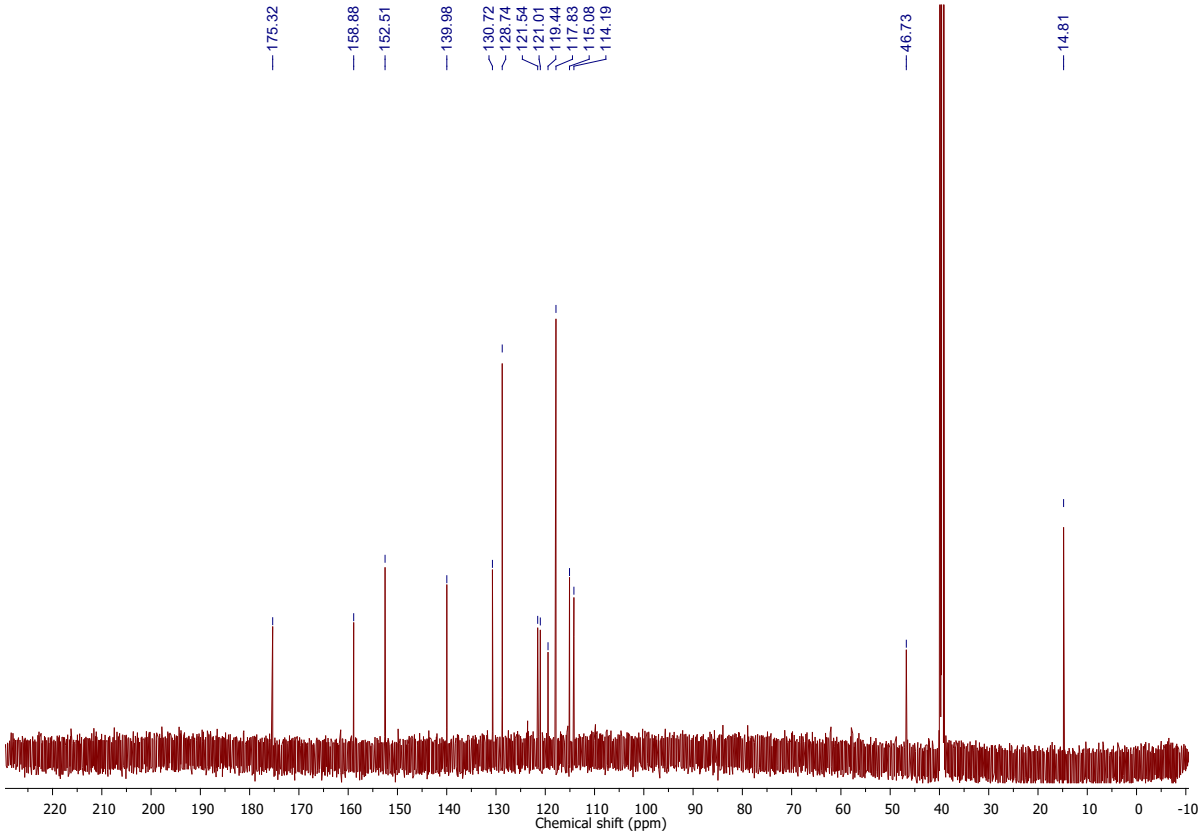

Figure S43. ^{1}H NMR (^{1}H = 498.557 MHz, 298.1 K, DMSO-d_6) spectrum of $\mathbf{H_2L^{3,3'\text{-}O}}$.

Figure S44. ^{13}C NMR (^{13}C{^{1}H} = 150.919 MHz, 298.0 K, DMSO-d_6) spectrum of $\mathbf{H_2L^{3,3'\text{-}O}}$.

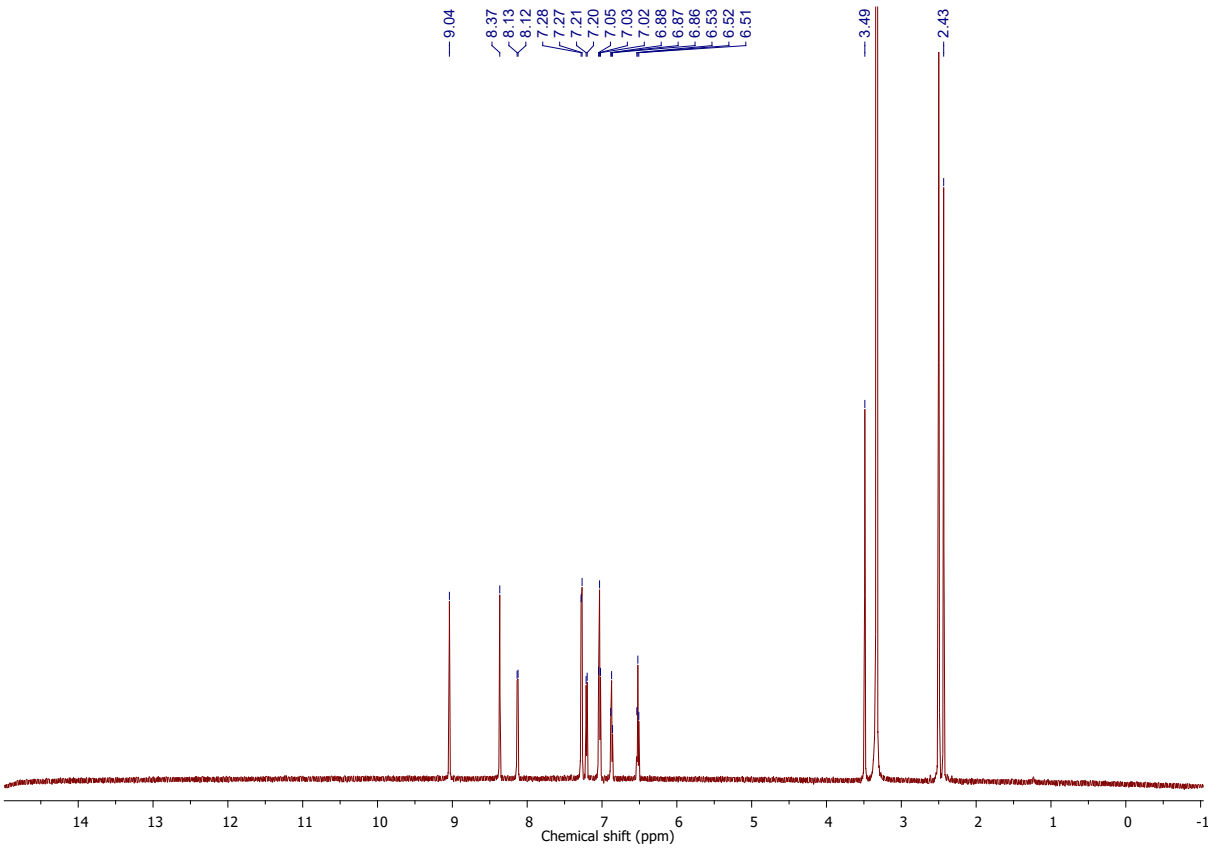

Figure S45. ^{1}H NMR (^{1}H = 600.124 MHz, 298.0 K, DMSO-d_6) spectrum of **NiL$^{3,3'\text{-O}}$**.

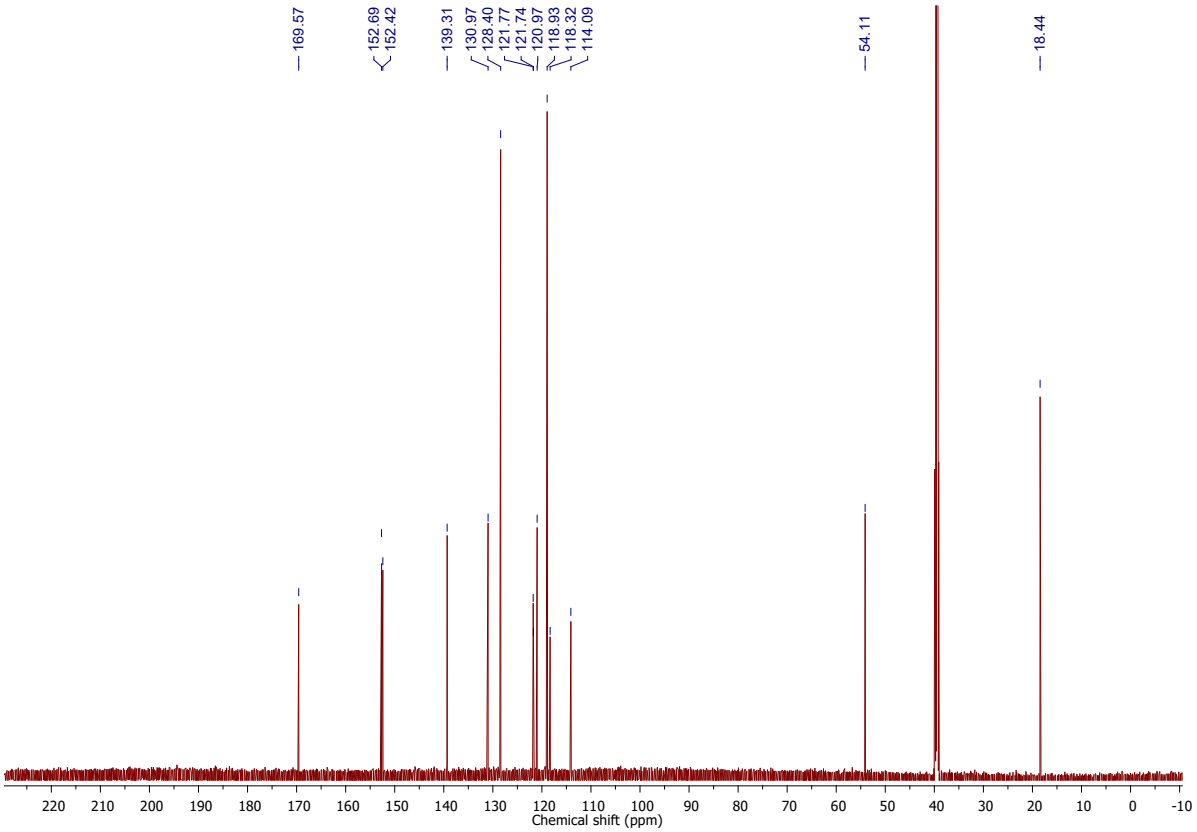

Figure S46. ^{13}C NMR (^{13}C{^{1}H} = 150.919 MHz, 298.0 K, DMSO-d_6) spectrum of **NiL$^{3,3'\text{-O}}$**.

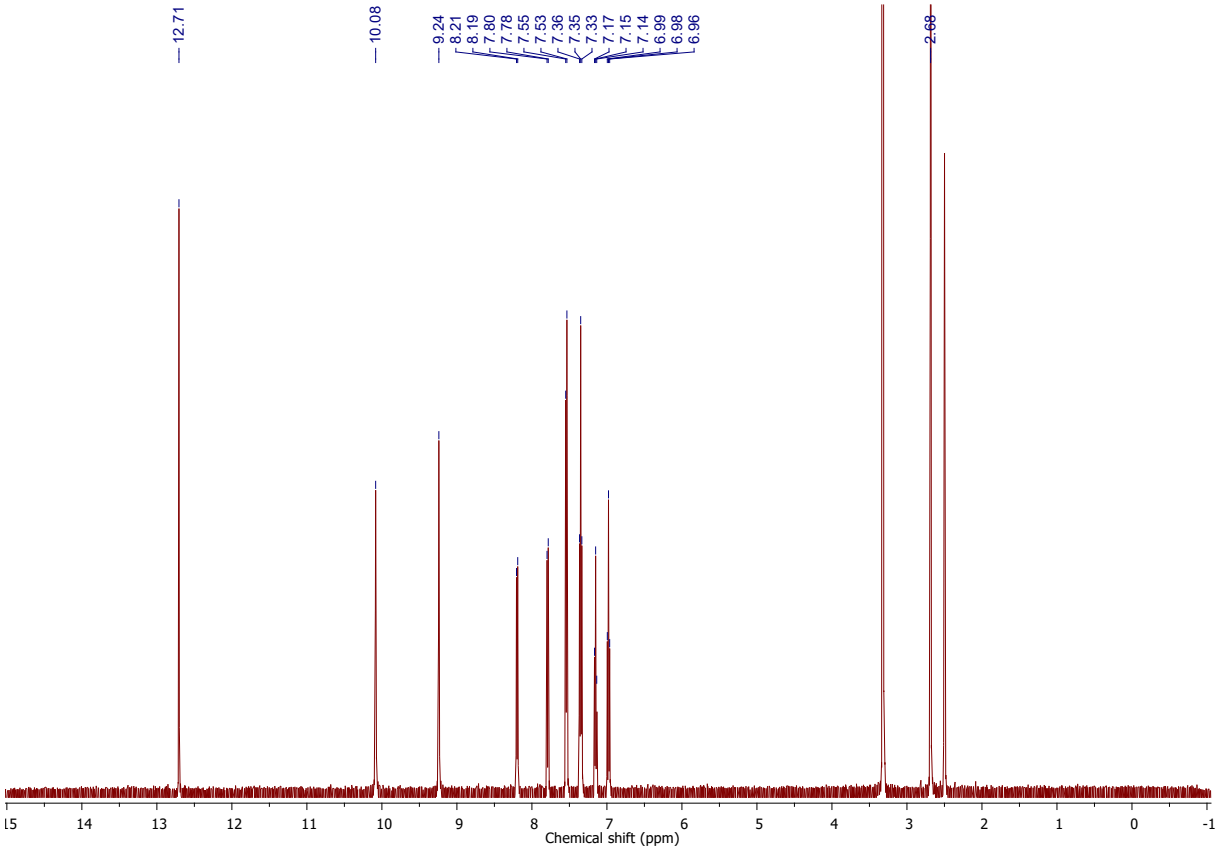

Figure S47. ^{1}H NMR (^{1}H = 498.557 MHz, 298.1 K, DMSO-d_6) spectrum of **HL$^{3\text{-S}}$**.

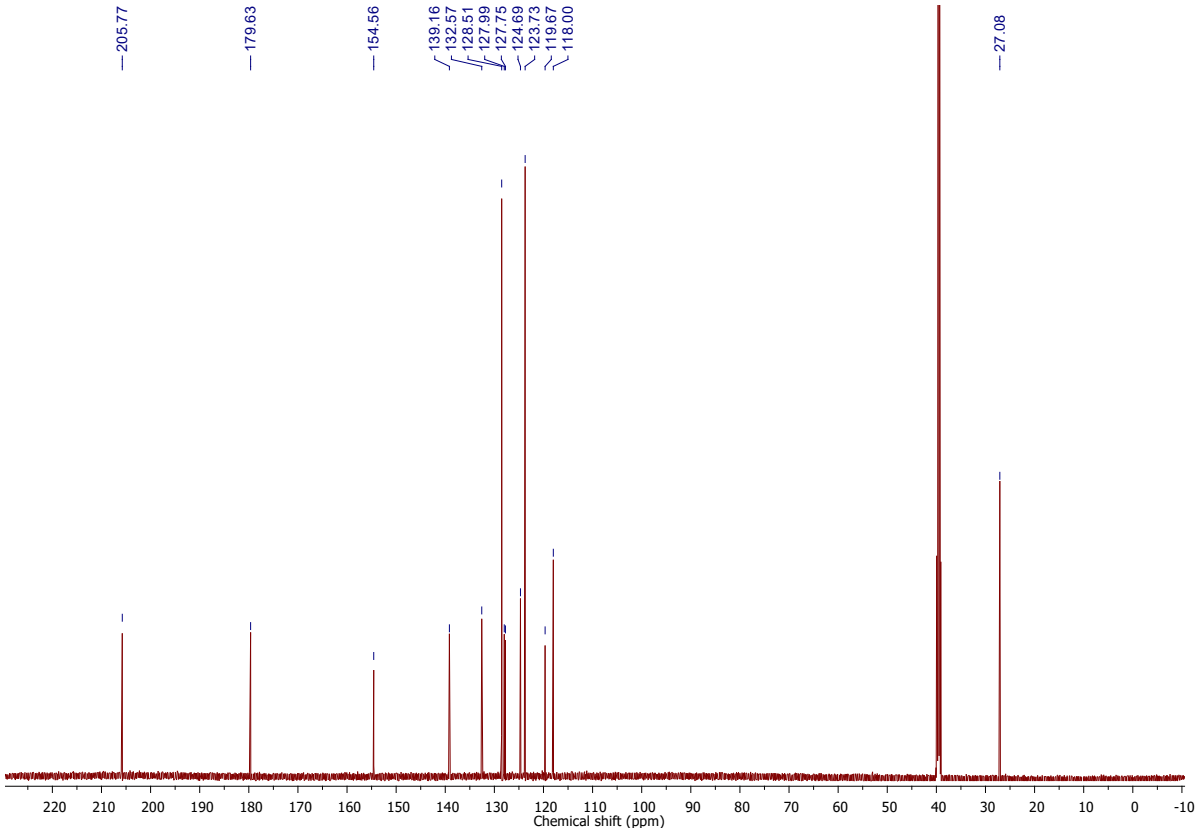

Figure S48. ^{13}C NMR (^{13}C{^{1}H} = 150.919 MHz, 298.0 K, DMSO-d_6) spectrum of **HL$^{3\text{-S}}$**.

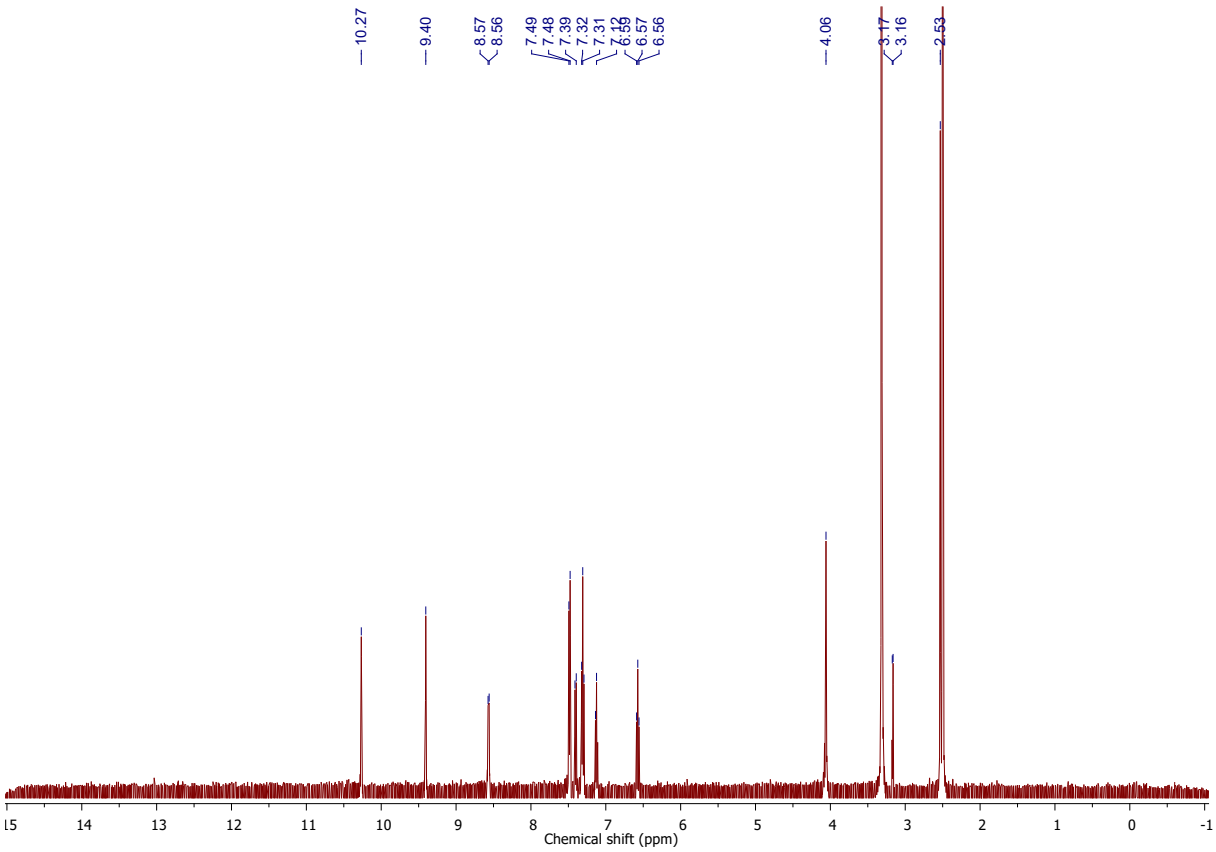

Figure S49. ^{1}H NMR (^{1}H = 498.557 MHz, 298.1 K, DMSO-d_6) spectrum of $\mathbf{H_2L^{3,3'\text{-}S}}$. A chemical shift present at 3.16 ppm (d, J = 5.5 Hz) is assigned to residual methanol.[15]

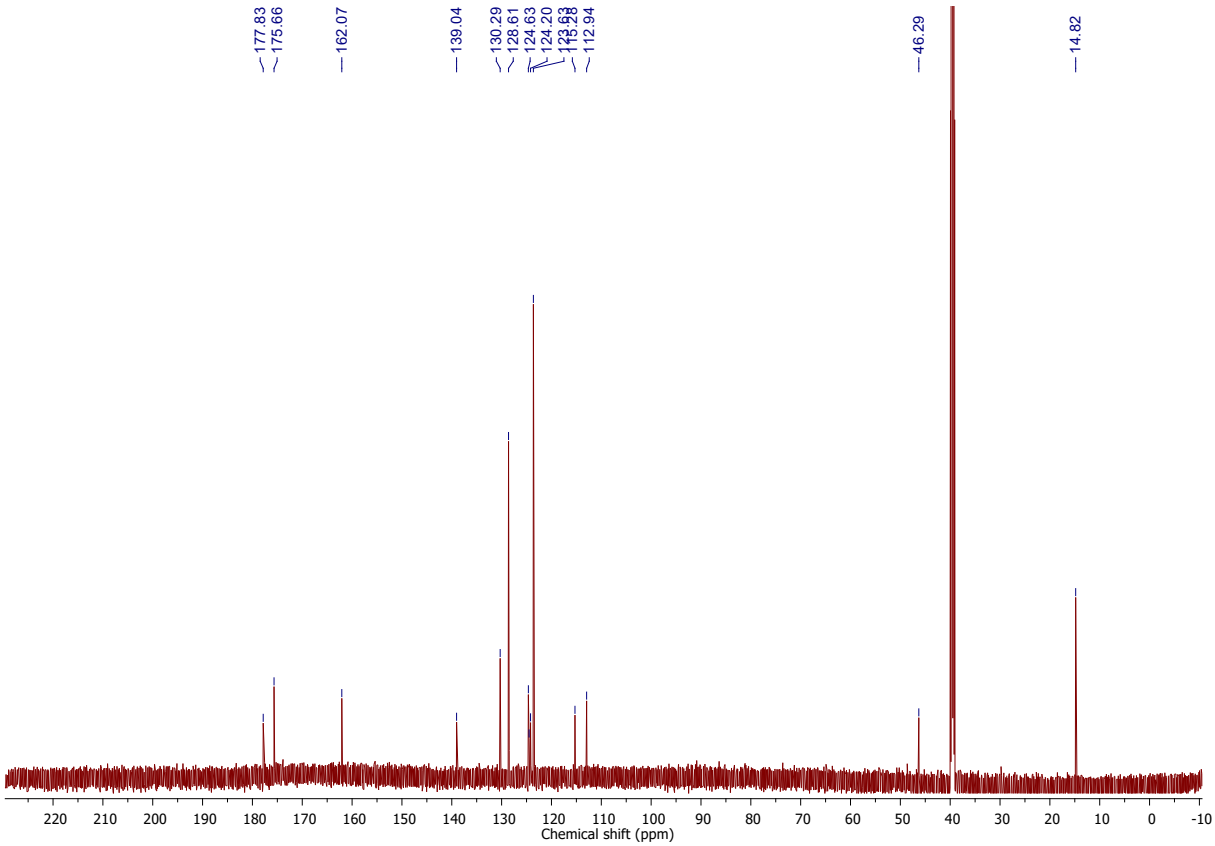

Figure S50. ^{13}C NMR (^{13}C{^{1}H} = 150.919 MHz, 298.0 K, DMSO-d_6) spectrum of $\mathbf{H_2L^{3,3'\text{-}S}}$.

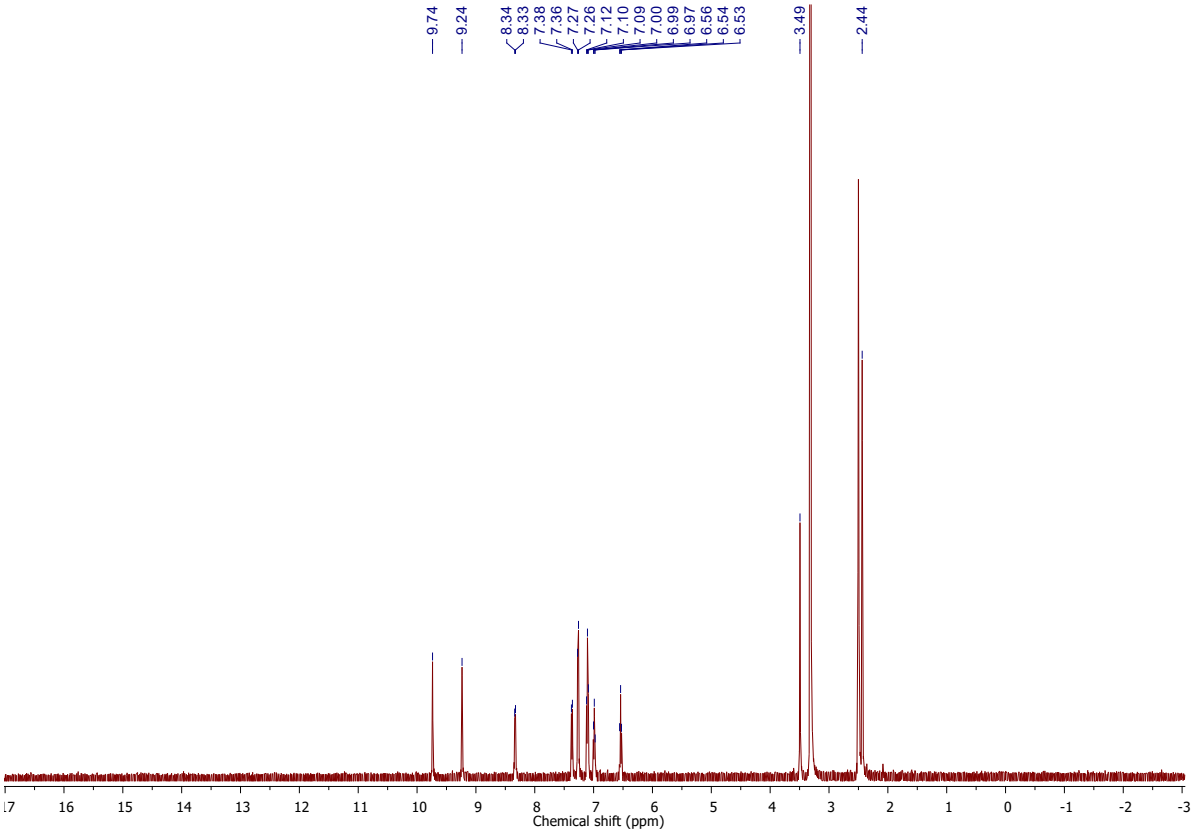

Figure S51. ^{1}H NMR (^{1}H = 498.557 MHz, 298.1 K, DMSO-d_6) spectrum of **NiL$^{3,3'\text{-S}}$**.

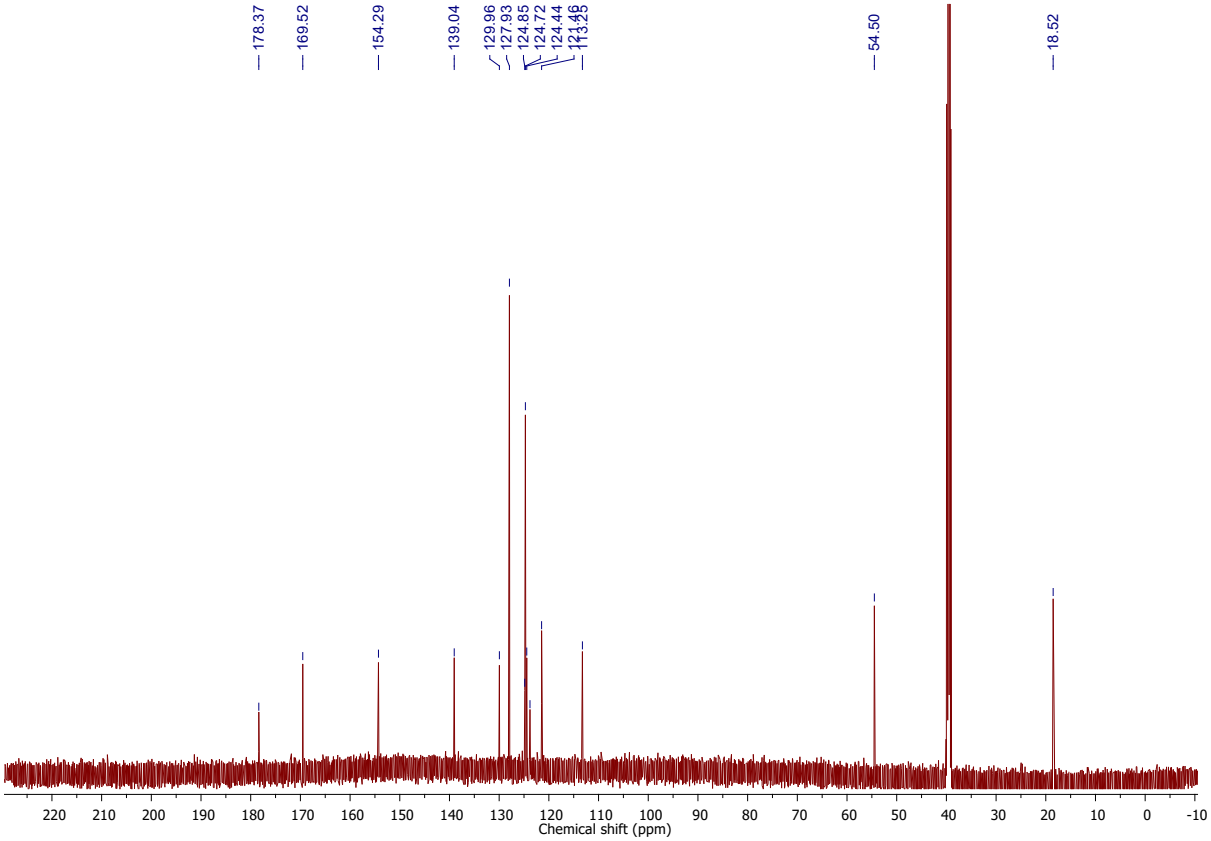

Figure S52. ^{13}C NMR (^{13}C{^{1}H} = 150.919 MHz, 298.0 K, DMSO-d_6) spectrum of **NiL$^{3,3'\text{-S}}$**.

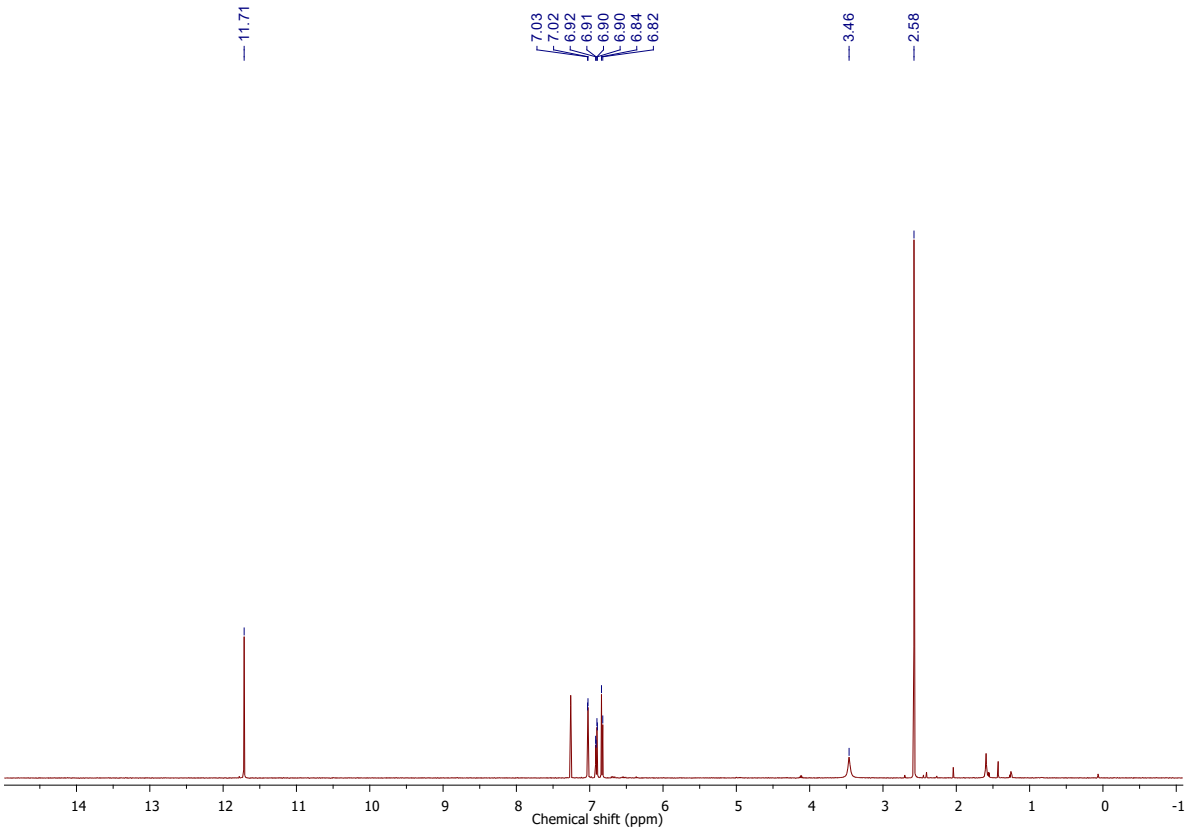

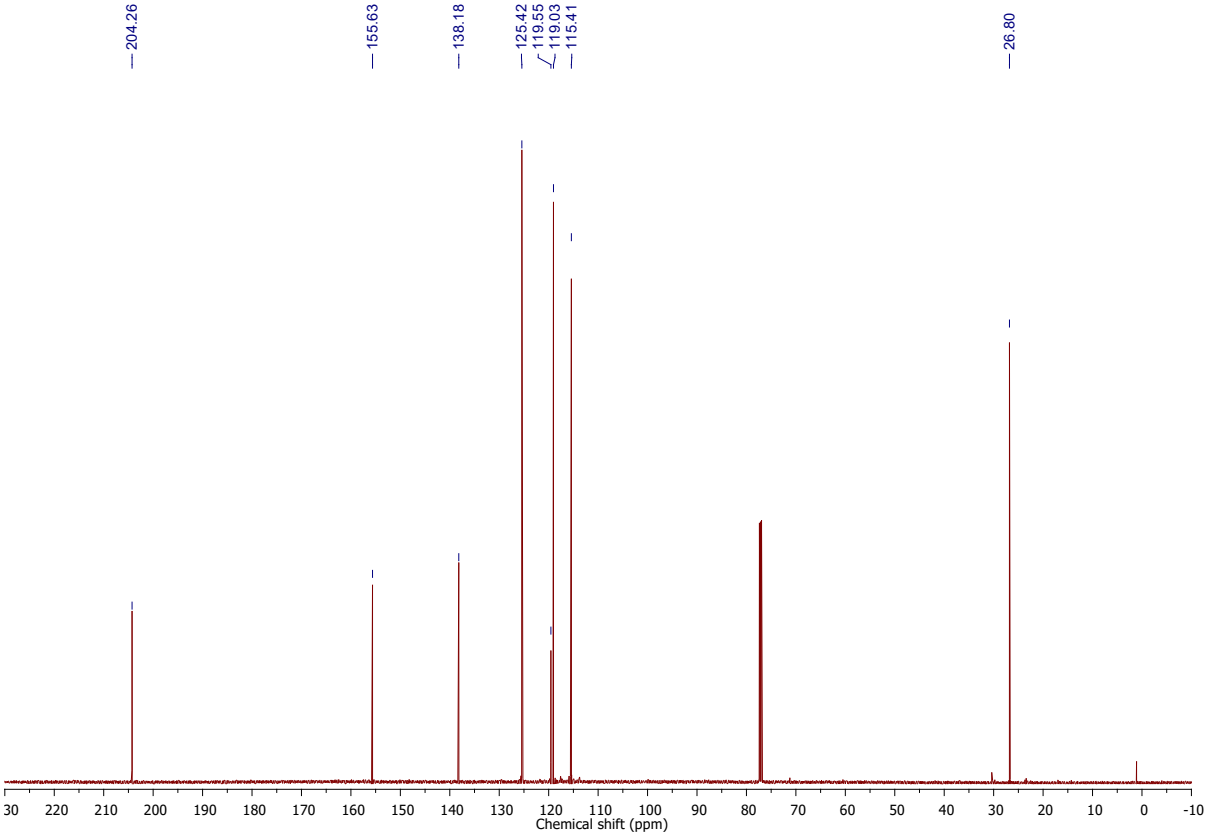

Figure S53. ^{1}H NMR (^{1}H = 498.557 MHz, 298.1 K, DMSO-d_6) spectrum of **5-NH$_2$**.

Figure S54. ^{13}C NMR (^{13}C{^{1}H} = 150.919 MHz, 298.0 K, $CDCl_3$) spectrum of **5-NH$_2$**.

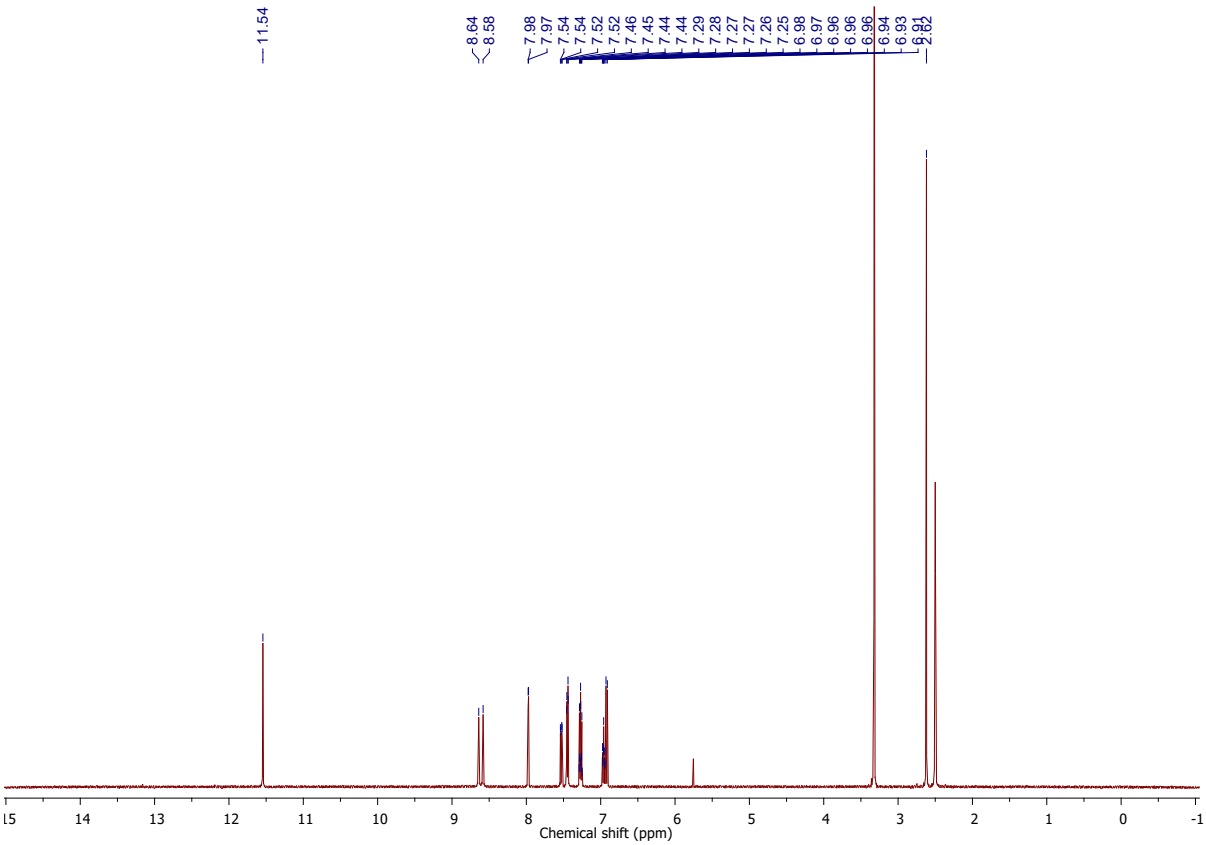

Figure S55. ^{1}H NMR (^{1}H = 498.557 MHz, 298.1 K, DMSO-d_6) spectrum of **HL$^{5\text{-O}}$**. A chemical shift present at 5.7 ppm (s) is assigned to residual dichloromethane.[15]

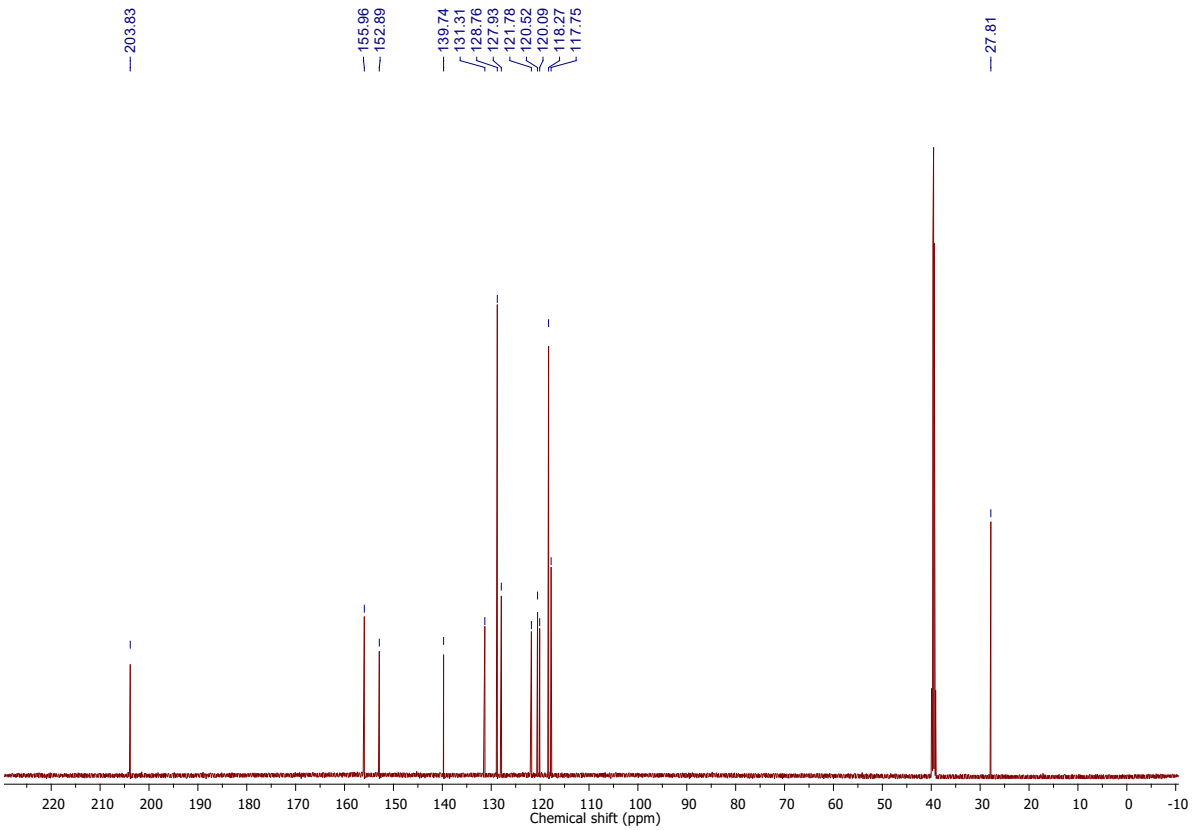

Figure S56. ^{13}C NMR (^{13}C{^{1}H} = 150.919 MHz, 298.0 K, DMSO-d_6) spectrum of **HL$^{5\text{-O}}$**.

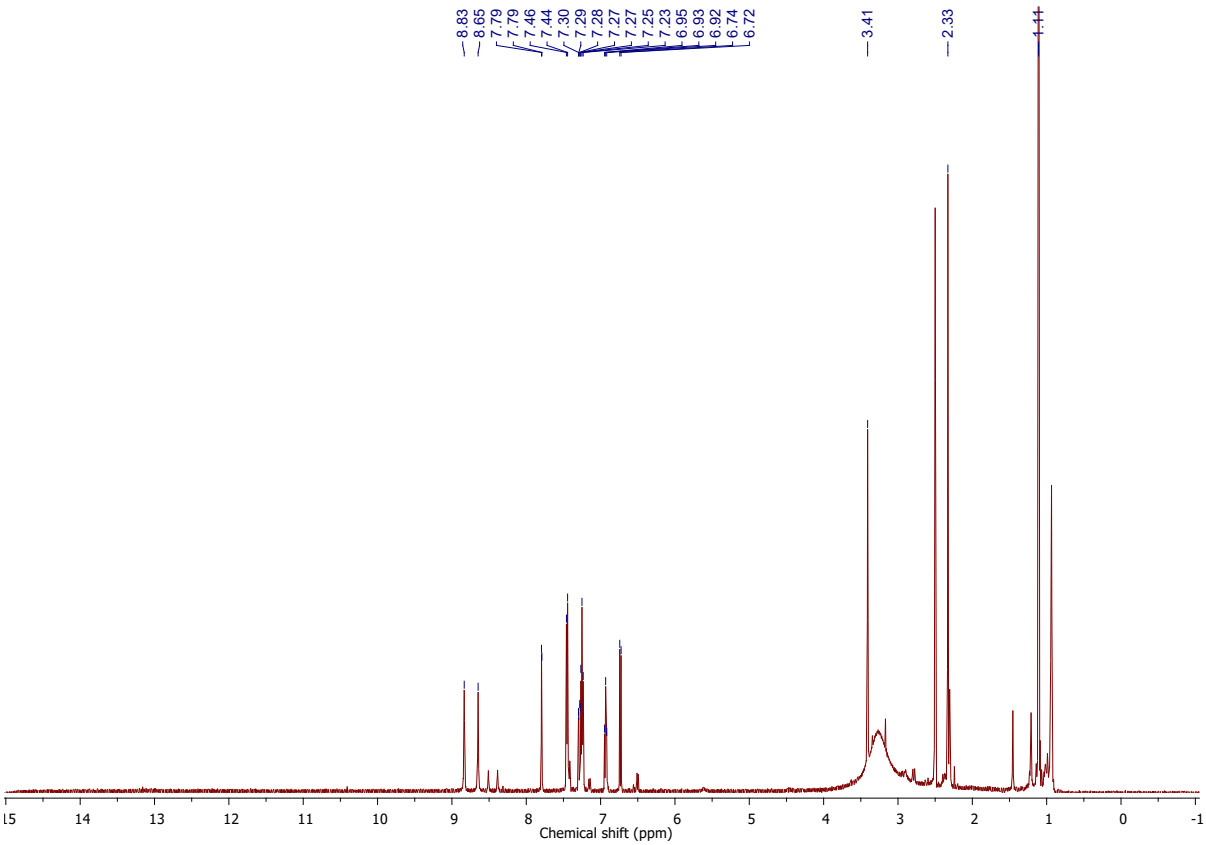

Figure S57. ^{1}H NMR (^{1}H = 498.557 MHz, 298.1 K, DMSO-d_6) spectrum of **HL$^{5\text{-O}}$NH$_2$**.

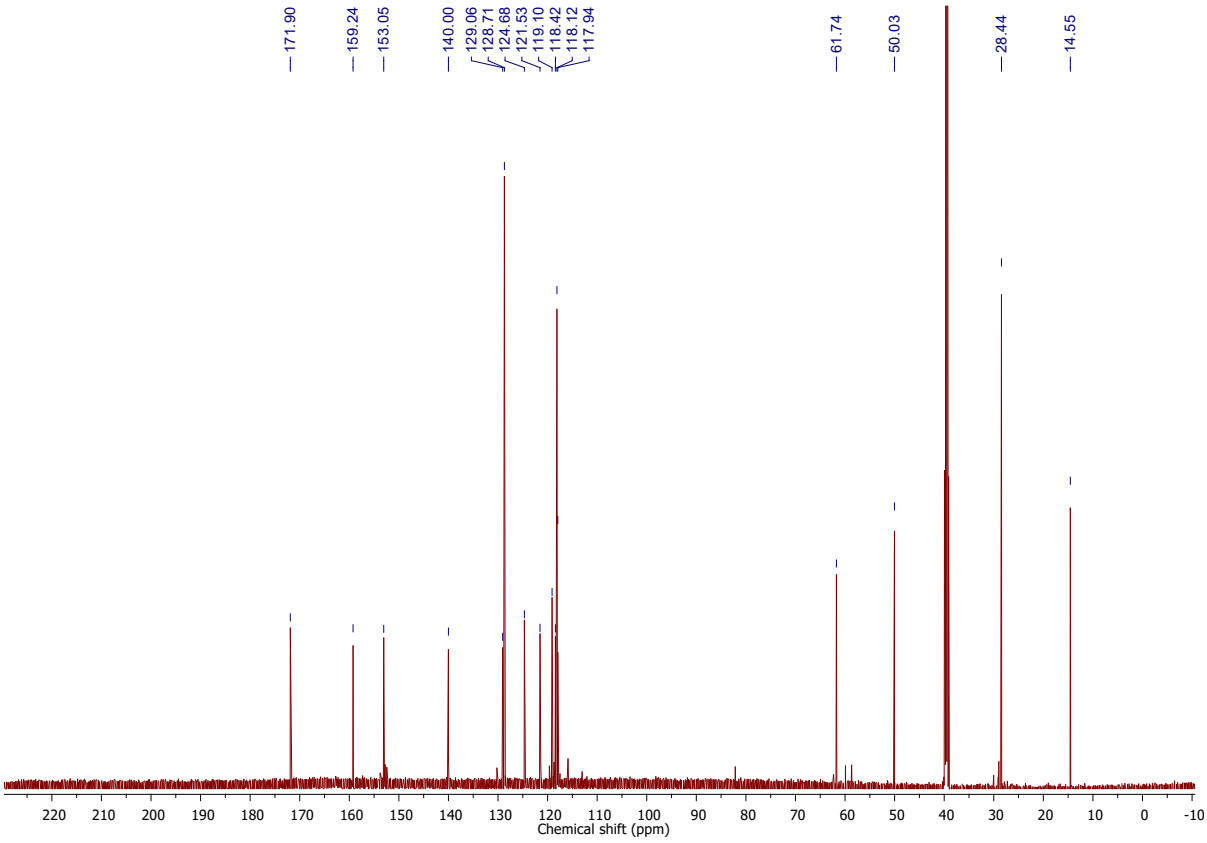

Figure S58. ^{13}C NMR (^{13}C{^{1}H} = 150.919 MHz, 298.0 K, DMSO-d_6) spectrum of **HL$^{5\text{-O}}$NH$_2$**.

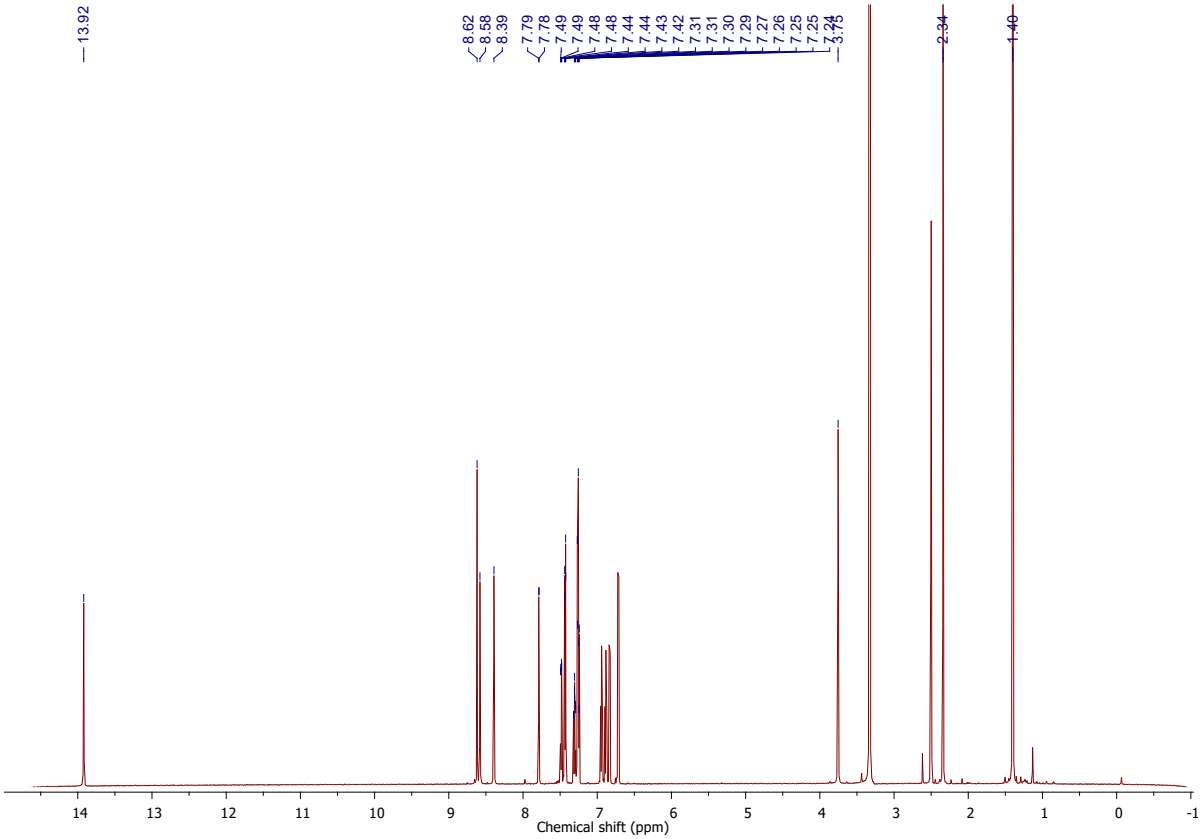

Figure S59. ^{1}H NMR (^{1}H = 600.124 MHz, 298.0 K, DMSO-d_6) spectrum of $\mathbf{H_2L^{5\text{-}O}}$.

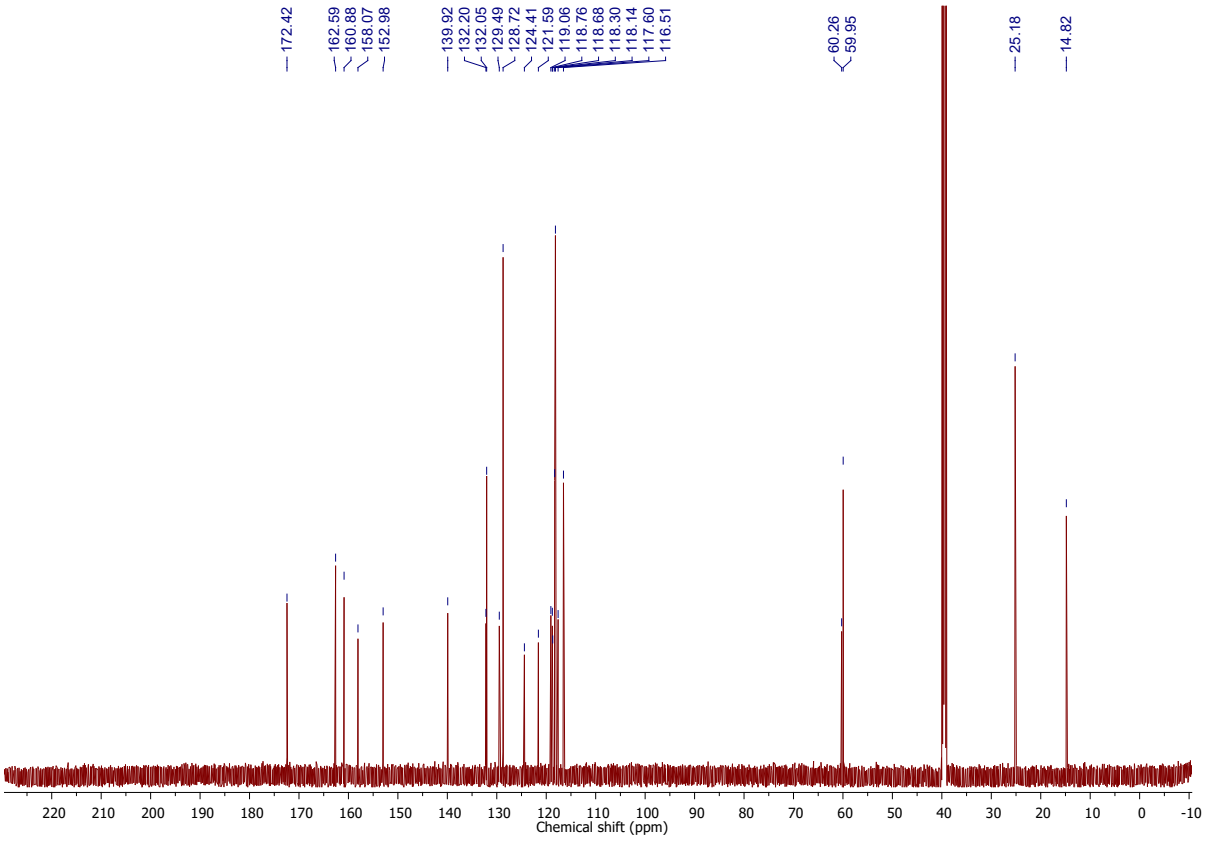

Figure S60. ^{13}C NMR (^{13}C{^{1}H} = 150.919 MHz, 298.0 K, DMSO-d_6) spectrum of $\mathbf{H_2L^{5\text{-}O}}$.

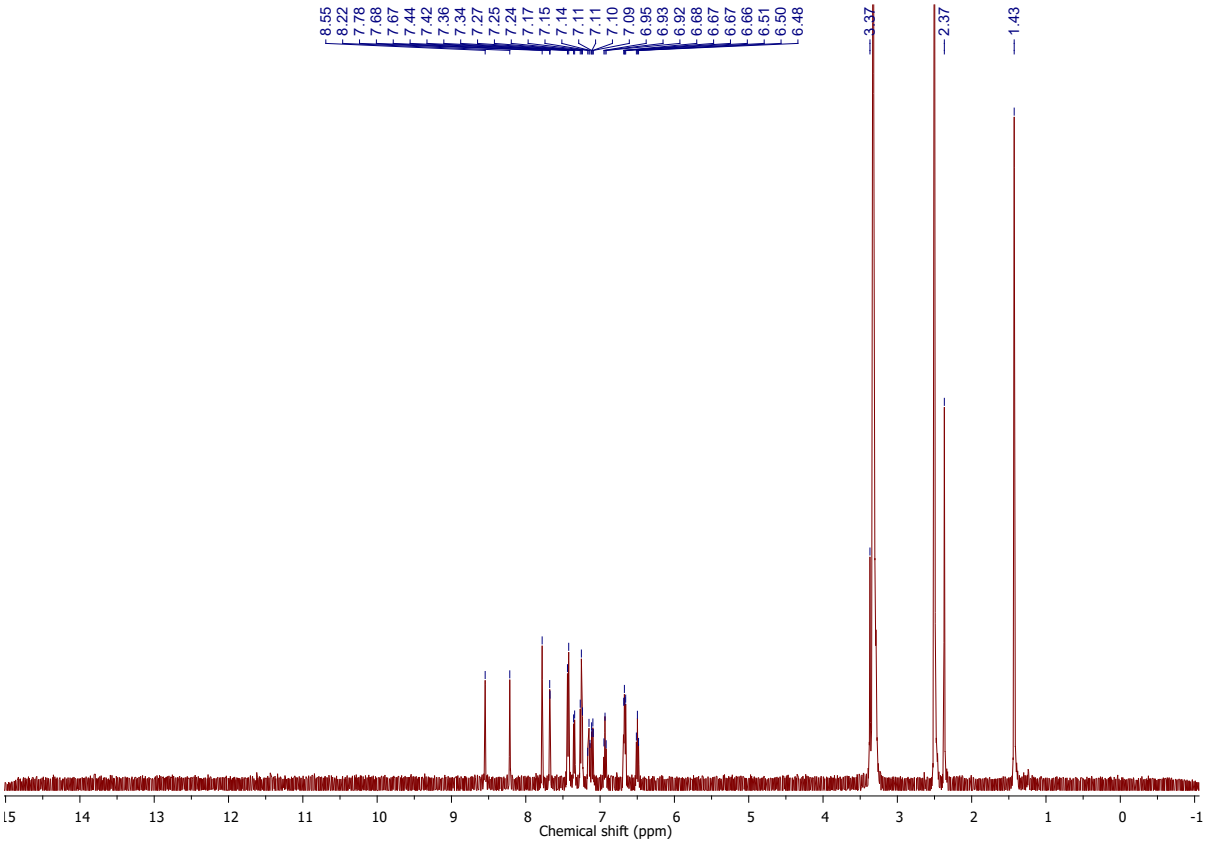

Figure S61. ^{1}H NMR (^{1}H = 498.557 MHz, 298.1 K, DMSO-d_6) spectrum of **NiL$^{5\text{-O}}$**.

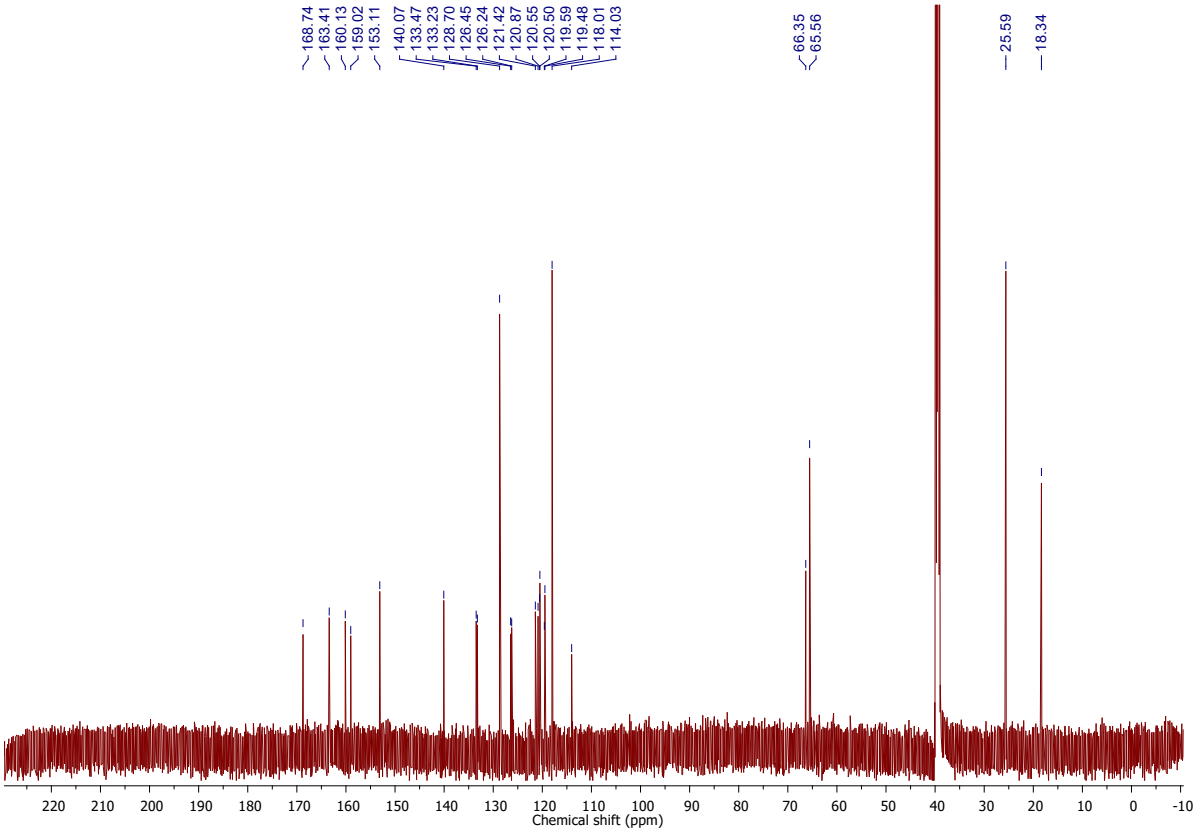

Figure S62. ^{13}C NMR (^{13}C{^{1}H} = 150.919 MHz, 298.0 K, DMSO-d_6) spectrum of **NiL$^{5\text{-O}}$**.

References

1 C. P. Rosenau, B. J. Jelier, A. D. Gossert and A. Togni, *Angew. Chem. Int. Ed.*, 2018, **57**, 9528–9533.

2 L. J. Farrugia, *J. Appl. Crystallogr.*, 1997, **30**, 565.

3 O. V Dolomanov, L. J. Bourhis, R. J. Gildea, J. A. K. Howard and H. Puschmann, *J. Appl. Crystallogr.*, 2009, **42**, 339–341.

4 M. Cushman, H. Zhu, R. L. Geahlen and A. J. Kraker, *J. Med. Chem.*, 1994, **37**, 3353–3362.

5 *APEX2*, Bruker AXS, Inc., Madison, WI, 2014.

6 *SAINT*, Bruker AXS, Inc., Madison, WI, 2013.

7 G. M. Sheldrick, *SADABS*, Bruker AXS, Inc., Madison, WI, 2014.

8 G. M. Sheldrick, *SHELXTL*, Bruker AXS, Inc., Madison, WI, 2014.

9 A. J. C. Wilson, Ed., *International Tables for Crystallography, Volume C*, Kluwer Academic Publishers, Dordrecht, 1st edn., 1992.

10 *APEX3*, Bruker AXS, Inc., Madison, WI, 2018.1–0., 2018.

11 A. L. Spek, *Acta Crystallogr. Sect. C*, 2015, **71**, 9–18.

12 A. L. Spek, *Acta Crystallogr. Sect. D*, 2009, **65**, 148–155.

13 G. M. Sheldrick, *CELL_NOW*, Bruker AXS, Inc., Madison, WI, 2008.

14 G. M. Sheldrick, *TWINABS*, Bruker AXS, Inc., Madison, WI, 2012.

15 G. R. Fulmer, A. J. M. Miller, N. H. Sherden, H. E. Gottlieb, A. Nudelman, B. M. Stoltz, J. E. Bercaw and K. I. Goldberg, *Organometallics*, 2010, **29**, 2176–2179.